High-Temperature Refrigerated Warehouse Operation under Real-Time Pricing of Electricity

by

Nitin Magoo

A thesis submitted in partial fulfillment

of the requirements for the degree of

Master of Science

(Mechanical Engineering)

At the

Solar Energy Laboratory

University of Wisconsin - Madison

2003

Academic Advisors:

Prof. Sanford A. Klein

Prof. Douglas T. Reindl

ABSTRACT

Refrigerated warehouses play an important link in the storage of food products throughout the year under conditions specially suited to prevent their decay. In doing so, refrigerated warehouses serve as an indispensable link in maintaining the availability of otherwise seasonal food products all year round. A proper humidity and temperature level has to be maintained in the warehouse at all times to make this possible.

The operation of the warehouse is an energy intensive process; however, under many electricity pricing tariffs, there are no cost benefits of adopting operating strategies that shift electrical usage to lower price (off-peak) periods, i.e., a demand-shifting strategy. But, with the deregulation of utility rate structures, there has been a gradual shift towards Real-Time Pricing (RTP), whereby the electricity price varies every hour. The RTP rate is a typical example of the demand-supply interaction. The RTP structure offers consumers the incentive of reducing their electricity bill if they can shift their loads from high price to low price periods. The benefit to the end-user is reduced utility operating costs (even with equal or slightly higher energy usage). The utilities benefit by being able to reduce their cost of electricity generation by stimulating stability in their aggregate demand of electricity through pricing signals.

It is with these thoughts in mind that this study investigates possible operating cost gains for high-temperature refrigerated warehouses by adopting operating strategies that shifts refrigeration system operation to lower price periods. By utilizing the thermal mass of the stored product, the warehouse refrigeration equipment can be operated in a way that would minimize the energy bill of the warehouse. Demand-shifting involves pre-cooling products stored in the warehouse to lower temperatures during low electricity price periods, and shutting off or operating the refrigerating equipment at reduced capacity during periods of high electricity prices. This strategy offers the possibility of shifting electrical usage from higher price to lower price periods resulting in the potential for realizing operating cost savings. A constraint in this process is the thermal risk to stored products. In all operating scenarios, stored product quality or food safety must not be compromised.

The warehouse being investigated in the current study is a high-temperature warehouse, or a "cooler", which means that the storage temperature in the warehouse is above the freezing point. Also, it is a distribution warehouse, which means that the stored products arrive "at-temperature", dwell in the warehouse for a short time and then ship to the market "at-temperature".

A computer simulation model for a warehouse located in Madison, WI was developed in TRNSYS. The simulation model includes the construction details of the warehouse as well as models for the refrigeration equipment needed to maintain desired storage temperatures. The infiltration exchange between the warehouse zones, and also between the warehouse and the ambient was modeled. The warehouse set-point temperature controller was developed to operate the refrigeration equipment depending on the time of the day and the maximum allowable product temperature. Two different models were developed for the stored products. The first assumed the product to behave as thermally lumped using a lumped capacitance model. The second discretized the product using a three-dimensional finite difference approach.

An economic analysis is performed for three different utility rate structures and the results indicate that following the demand-shifting strategy can lead to savings, without adversely affecting the quality of the stored product. The actual value of savings and the percentage savings depend on the utility rate structure in force.

ACKNOWLEDGEMENTS

IV

TABLE OF CONTENTS

VIII

LIST OF FIGURES

LIST OF TABLES

CHAPTER 1   INTRODUCTION

1.A   Overview of Cold Storage Warehouses

1.A.1   Cold Store

A cold store is a building or a group of buildings with thermal insulation and a refrigerating system in which perishable food products can be stored for various lengths of times in set conditions of temperature and humidity (IIR, 1993). Such storage under controlled conditions slows the deterioration and spoilage that would naturally occur in an uncontrolled natural environment. In addition to providing control of temperature and humidity, cold stores can also be designed to deliver controlled atmospheres by maintaining the requisite concentration of various gases that aid in the preservation of food products. Thus, cold storage warehouses play an important role in the storage of food products in the food delivery chain throughout the year under conditions specially suited to prevent their degradation. This function makes seasonal products available all year round.

The quality and nutritional value of food products is affected by the time and temperature of the storage. Large temperature fluctuations during storage, transportation, and handling accelerate the deteriorative effects to food products. Proper temperature and humidity levels have to be maintained in the warehouse at all times to maintain high quality, nutritious, and safe food products.

1.A.2   Trends in Storage Capacity

The construction and operation of refrigerated storage has been steadily growing in the US. At a national level, refrigerated storage capacity totaled 82 million m^3 (2.9 billion ft^3) on October 1, 1999, an increase of 6% since 1997 (USDA, 2000). While most of the increase in storage capacity was due to new construction, some was due to increased coverage of existing warehouses. The five states with the largest gross warehouse capacity (in million

cubic feet) were: California, Florida, Washington, Wisconsin and Texas. As can be observed, most refrigerated storage capacity exists in states where agriculture and dairy industry are well developed.

1.A.3   Cold Storage Classifications

The variable composition and structure of foods greatly affects their thermal properties. In addition, their chemical and physical properties change with time, temperature, and other ambient conditions. Even minor alterations and fluctuations in the condition of the food products might be undesirable if it compromises the food quality. ASHRAE Refrigeration Handbook (1998) specifies five categories for the classification of refrigerated storage warehouses for preservation of food quality, which are:

- Controlled atmosphere for long-term storage of fruits and vegetables
- Coolers at temperatures of 0 ^{o}C (32 ^{o}F) and above
- High-temperature freezers at –2 to –3 ^{o}C (28.4 to 26.6 ^{o}F)
- Low-temperature storage rooms for general frozen products, usually maintained at –23 to –29 ^{o}C (-9.4 to –20.2 ^{o}F)
- Low-temperature storages at –23 to –29 ^{o}C (-9.4 to –20.2 ^{o}F), with a surplus of refrigeration for freezing products received at temperatures above –18 ^{o}C (-0.4 ^{o}F)

The two main categories of storage facilities are (1) coolers that maintain products at temperatures usually above 0 ^{o}C (32 ^{o}F) and (2) low-temperature rooms (freezers) operating at temperatures less than 0 ^{o}C (32 ^{o}F). These classifications will be explained in more detail later in this chapter.

1.A.4   Stored Products

A variety of products are stored in these refrigerated warehouses, depending on the product characteristics and storage requirements. Some of the products that are stored at temperatures well below the freezing point are meat and fish products, poultry products, fruit juices, processed and canned foods, and ice cream. Some of the products that are

typically stored at temperatures around freezing include milk, dairy products like cheese and butter, eggs and egg products. Various fruits and vegetables are typically stored in a controlled atmosphere at temperatures much above freezing. ASHRAE Refrigeration Handbook (1998) specifies the individual storage temperatures for a wide variety of food products, while ASHRAE Fundamentals Handbook (1993) summarizes the thermal properties of food products.

1.A.5 Warehouse Zones

Most of the refrigerated warehouses typically have two zones or conditioned spaces. One zone is the shipping and receiving dock, which serves as a refrigerated anteroom to the other zone known as the cold storage area, or more commonly as the freezer or the cooler. For freezers, a dock is an absolute necessity in humid and warm climates due to a variety of reasons, some of which include:

- A reduced refrigeration load in the freezer, where energy demand and the energy cost per unit capacity of refrigeration is higher.
- Since the ambient air infiltrates first into the dock, undergoes moisture removal, and is then allowed to infiltrate into the freezer, there is less frost formation in the freezer.
- Ease of handling both the incoming and outgoing product.

The dock space has not only thermodynamic advantages, but is also favorable from a logistics viewpoint. Coolers may or may not have a conditioned dock. In this case, the dock provides a minimal thermodynamic advantage but still retains its logistical advantage.

1.A.6 Freezers

Freezer is the name typically given to refrigerated warehouses that maintain products at temperatures much below freezing, generally in the range of –23 to –29 ^{o}C (-9.4 to –20.2 ^{o}F), and not warmer than –18 ^{o}C (-0.4 ^{o}F). Freezers are optimally suited for long-term storage of seasonal agricultural crops, meat (beef, pork, poultry), fish, frozen dairy

products, and frozen fruit juices. As is evident from the low storage temperature, freezers have a high energy demand and high energy costs associated with their operation. The design and construction of freezers is a carefully planned exercise so as to provide the maximum insulation from the ambient conditions. Below is a range of thermal resistance values for freezer constructions, as recommended by ASHRAE (1998):

Floors: 4.8 to 5.6 m^2-K/W (27.26 to 31.8 ft^2-hr-F/Btu)

Walls: 6.2 to 7.0 m^2-K/W (35.21 to 39.75 ft^2-hr-F/Btu)

Roofs: 7.9 to 8.8 m^2-K/W (44.86 to 49.97 ft^2-hr-F/Btu)

Typically, the freezer walls comprise of a layer of insulation sandwiched between two layers of reinforced concrete (or other rigid material such as sheet metal). Commonly used insulation materials include polyurethane, polystyrene, and styrofoam.

1.A.6.1 Freezer Floor Construction

A very important aspect of freezer design is structural considerations, particularly floors. This is due to the fact that the freezers are maintained at such low temperatures and there is always some residual flow of heat from the ground below the freezer to the freezer floor, in spite of the insulation that has been installed. This heat flow reduces the ground temperature, and if the ground temperature drops below freezing, moisture in the surrounding soil freezes. As the moisture freezes, it will expand, resulting in a volume increase that causes the floor to heave. The dislocating floor has the potential of twisting the entire structure. This problem can become irreversible, and can even lead to eventual abandonment of the facility. The most effective prevention against this problem is to install a heating system beneath the slab, the choice of which depends on energy cost, reliability, and maintenance requirements. The most popular method of floor heating is to install a pipe grid system in the base concrete slab directly under the insulation. Hot air or glycol is circulated through this network of pipes and maintains the temperature of the slab base at above freezing. Floor heating does impose a parasitic load on the refrigeration equipment,

but this approach still remains the most effective way of overcoming the problem of freezer floor heave.

Frost heaving is actually attributed to two different phenomena (Rein and Burrous, 1987):

- Soil displacement associated with the expansion upon freezing, of water that was in the soil pore space prior to freezing. This is a closed-system phenomenon.
- Soil displacement that occurs as additional water is drawn to the freezing region from adjacent soil or other sources of water. This is an open-system phenomenon.

1.A.6.2 Freezer docks

The presence of a dock space is highly desirable and in almost all cases a necessity for freezers. The dock is typically maintained at temperatures just above freezing and is in direct contact with the surroundings. On account of thermodynamics, it is energy efficient to remove moisture from the humid ambient air infiltrating to the dock at the higher temperature of the dock itself rather than allowing ambient air to infiltrate directly into the freezer and then removing moisture from it at a much lower temperature. Logistically speaking too, the dock is very important for staging products during loading and unloading. It would not only impose a very high cooling load on the freezer if the product was directly brought in and taken out of the freezer, but would also be a logistics nightmare with all the personnel and equipment concentrated in the freezer.

1.A.7 Coolers

Cooler is the name typically given to refrigerated warehouses that maintain products at temperatures at or around freezing, generally in the range of -2 to 2 ^{o}C (28.4 to 35.6 ^{o}F), but are usually associated only with storage at temperatures above freezing as has been mentioned previously. Coolers are optimally suited for short-term storage of agricultural crops, milk, fresh meat, fresh vegetables, and dairy products. Coolers serve more as distribution or "in-transit" storage warehouses, having constant turnover of stored products. The energy requirement of a cooler is not as high as that of a freezer of

comparable size. Adequate precaution and care still has to be taken in the design of coolers to make them energy efficient and to reduce the operational costs as much as possible. Below is a range of ASHRAE (1998) recommended thermal resistance values for cooler constructions:

Floors: 3.5 m^2-K/W (19.87 ft^2-hr-F/Btu)
Walls: 4.2 to 5.6 m^2-K/W (23.85 to 31.8 ft^2-hr-F/Btu)
Roofs: 6.2 to 7.0 m^2-K/W (35.21 to 39.75 ft^2-hr-F/Btu)

1.A.7.1 Cooler walls/floor construction

As is the case for freezers, cooler walls are also made of a layer of insulation sandwiched between two layers of reinforced concrete. However, on account of the higher temperatures in a cooler, the relative thickness of these layers is less for coolers as compared to that for freezers. Since, most of the cooler applications are at temperatures above freezing, the dangers of floor heaving due to frost formation in the ground are significantly reduced. Coolers, therefore, do not require an elaborate floor heating system. A layer of insulation beneath the floor slab is still desirable to minimize heat gains from the surrounding soil.

1.A.7.2 Cooler docks

The dock space in a cooler is usually maintained at temperatures around 10 ^{o}C (50 ^{o}F). From a thermodynamic standpoint, presence of a dock connected to a cooler is not as essential as in freezers. This is due to the relatively higher temperatures maintained in a cooler. From a logistics perspective, the dock still serves essentially the same purpose in a cooler as in a freezer; staging inbound and outbound products.

1.B   Emerging Utility Rate Structures

1.B.1   General Considerations

Electricity is a form of energy that is not easily or cost-effectively stored. From a utility perspective, the demand for electrical energy is not constant over any given period of time; the demand can vary greatly depending on the time of the day, day of the week, and time of the year. In order to maintain a balance between supply and demand, while providing electricity at all times, the electricity generation capacity has to be properly controlled to meet the maximum load or the peak load that can occur. Electric utilities across the US have been studying ways to cost-effectively meet the peak electrical demand of their customers, while also trying to come up with viable alternatives to reduce the peak load.

One such alternative is to provide rate plans that include "interruptible" service options for the customers. In such a case, utilities suspend supply to their interruptible customers when aggregate electrical demand approaches the utilities' maximum available capacity. In exchange, the customer receives a lower overall electric rate. These periods of peak demand usually occur during the middle of hot summer days, when most residential and commercial air conditioners are in operation.

An important point to be understood is the way the aggregate electrical load profile varies over the day, the traditional ways in which the utilities try to meet that load, and the electricity pricing practices. Figure 1-1 shows an example load profile for a 24-hour period. Base-load is defined as the load that is relatively constant on the system most of the time. Intermediate-load is present on the system for most time of the day, and the peak load occurs only during a small fraction of time.
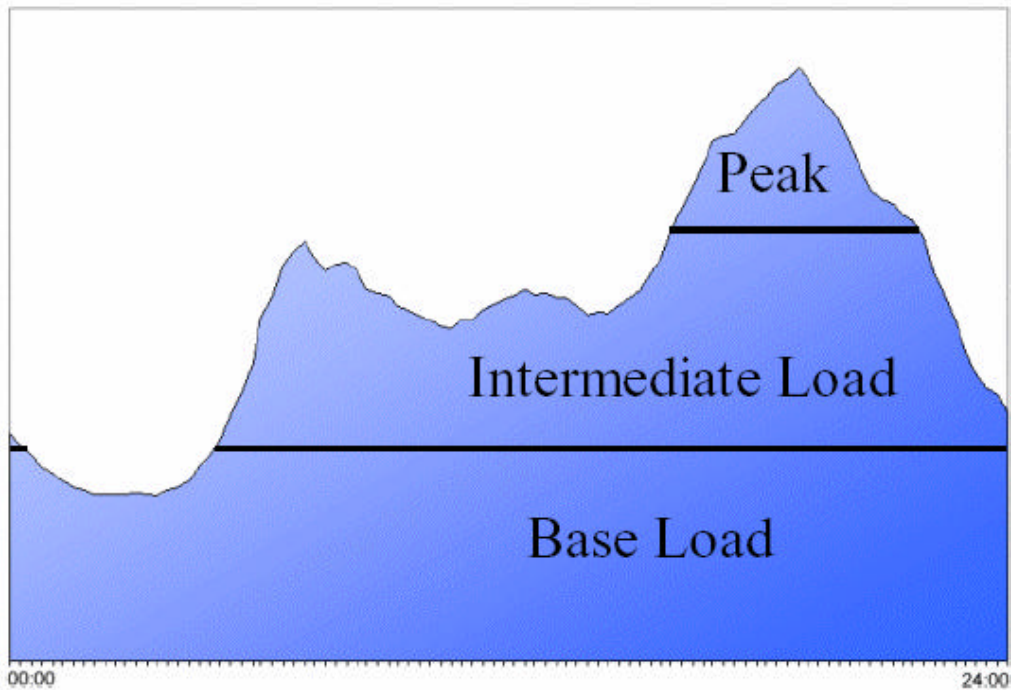
Figure 1-1: Example Load Profile

1.B.2   Electricity Generation

The methods of electricity generation are numerous, each having a different cost of generation. Traditionally, utilities have used different types of power plants to supply the different kinds of loads economically. For the base load, utilities will dispatch power plants with a low operating cost but a higher initial investment, e.g. nuclear power plants. Because of their capital, these plants are the most economically viable for baseline operation. Such plants are easily operated to maintain a continuous supply of electricity to provide a constant base load. For meeting the peak load, power plants having the least initial investment but substantially higher operating costs, e.g. gas turbine power plants, are the most viable. Such plants are also easy to start-up and shutdown, and are thus more suited towards meeting the peak demand at a short notice.

Keeping in mind the above considerations, it is obvious that the cost of generating electricity varies greatly. However, the price that customers historically pay for electricity is constant compared to the fluctuating production cost. The price is usually an average that covers the fixed cost, variable cost, and a reasonable profit for the utilities.

1.B.3   Real-Time Pricing (RTP)

With deregulation of the electricity markets over the past years, there has been a gradual shift away from "time-of-use" (TOU) price rate structures to emerging rate structures such as real-time pricing (RTP). The RTP pricing strategy is based on the idea that the electricity prices should, at all times, be reflective of the production cost of electricity. Under RTP, the electricity price varies hourly, depending on the projected electricity production cost made by the utility the day before. The customer is usually notified of the next day prices on the day before. An advantage that the customers can derive out of RTP is the possibility of reducing their electric bill if they can shift their loads from peak hours, when the electricity prices are high, to non-peak hours, when the prices are low. If the end-users shift their electricity usage, utilities benefit from improved load factors during the day and a more stable electricity demand.

A more detailed discussion about RTP, and the types of emerging rate structures, as well as the possible advantages and risks involved for cold storage warehouses' operation under RTP will be covered in the subsequent chapters.

1.C   Demand Shifting

1.C.1   General Concept

With deregulation of electricity markets in the US, more and more utilities have been modifying their electricity prices to match the cost of generation. The introduction of the concept of Real-Time Pricing (RTP) of electricity rates has led to the prices not being constant but dependent on the time of the day. The trend in prices reflects the economics of

a typical demand-supply interaction. This means that the prices are higher when the demand is high, i.e. during the peak hours, and the prices are low when the demand is low, i.e. during the off-peak hours.

Under standard electricity rates, cold storage warehouses are operated on an "as-needed" basis. The refrigeration system is operated continuously to keep the stored products within the permissible temperature range. However, the advent of RTP rate structures triggered the interest in the development of refrigeration system control strategies that would minimize the electricity bill for the warehouse, and which could also be beneficial to the utilities.

The RTP rate structure is inherently designed to provide an incentive to the customers to shift their electricity consumption from peak hours to off-peak hours. The customers can reduce their monthly bill, and utilities can benefit by having to cater to a more stable, constant electricity demand. This strategy would ensure a "win-win" situation for both the customers and the utilities. This research aims to investigate the feasibility of following the demand-shifting strategy by the cold storage warehouses, wherein, the stored products would be cooled to a temperature lower than the actual set point temperature when the prices are low, and the refrigeration equipment would be shut-off or operated at part-load, when the electricity prices are high.

1.C.2   Product Thermal Mass

An important concept to be understood in the operation of cold storage warehouses is the way the temperature of the products and the zone air is lowered. Since, the refrigeration equipment directly cools the air in the zone, it is the zone air temperature that reduces first. As the stored product has a higher thermal mass than the zone air, there is a time lag between when the air temperature is reduced and when the product temperature is reduced over time as heat is extracted. Alternatively, when the refrigeration equipment is shut-off, the air temperature shows a greater rise than the product temperature in the same time

interval. Thus, in effect, the demand-shifting strategy aims at utilizing the thermal mass of the stored product as a possible deterrent against the temperatures rising too high too fast.

As the most important consideration in a warehouse's operation is to not allow the product temperature to go outside the permissible safe range, it is sought to show that following the demand-shifting strategy could accomplish this even if the zone air temperature is higher. In the process, it would also be aimed at establishing whether this strategy can lead to cost savings for the warehouse, in spite of the fact that the total electricity consumption could possibly increase while following the demand-shifting strategy.

1.C.3   Possible Limitations

Though, the demand-shifting strategy has its advantages for both the warehouse operators and the utilities, there might be possible disadvantages in terms of risk to the product quality, shelf life, and nutrient content (Van Arsdel, 1957). The storage life of fresh perishable foods such as meats, fish, vegetables, and fruits can be extended by several days by storing them at temperatures just above freezing, usually between 1 ^{o}C and 4 ^{o}C (Cengel and Boles, 1998). ASHRAE (1998) recommends that the best temperature to slow down deterioration of food products is the lowest temperature that can safely be maintained without freezing the commodity, which is 0.5 to 1 K above the freezing point of the commodity. No direct investigation of the effect of temperature fluctuations on the quality and nutritional value of the food products was conducted during the course of this project, but an extensive literature search revealed numerous related studies in this field. The observations and conclusions of some of the previous studies are summarized in the following paragraphs.

Quality of food products is defined as the composite of characteristics that differentiate individual units and have significance in determining the degree of acceptability of the unit by the user (Kramer and Twigg, 1968). The overall quality of a food product may be expressed by component characteristics, each of which may be measured, and possibly controlled independently.

12

It is well known that there is an exponential negative relationship between storage temperatures and maintenance of sensory and nutritional quality of refrigerated foods (Kramer, et al., 1979). A study done on pallet lots of frozen foods concluded that net energy saving can be gained without serious damage to the quality of frozen foods by maintaining 12-hour periods of high and low temperature levels in freezer storage rooms (Bailey, et al., 1979). It was further stated that the exact amount of energy saved would depend largely on the characteristics of the individual storage facility; e.g., type and thickness of insulation, percentage of storage volume used, size of refrigeration equipment, and number of door openings.

1.D   References

Altwies, J. (1998). Electrical Demand Reduction in Refrigerated Warehouses. Solar Energy Laboratory. Madison, WI, University of Wisconsin – Madison.

American Society of Heating, Refrigerating, and Air-Conditioning Engineers (ASHRAE) (1993), 1993 ASHRAE Handbook – Fundamentals.

American Society of Heating, Refrigerating, and Air-Conditioning Engineers (ASHRAE) (1998), 1998 ASHRAE Handbook – Refrigeration.

Bailey W. A., A. H. Bennett, W. Moleeratanond, B. H. Ashby, and A. Kramer, "Energy Savings and Quality Deterioration from Holding Frozen Foods at Two Daily Temperature Levels." *Transactions of the ASAE,* (1979): 938-943.

Cengel, Y. A., and M. A. Boles. Thermodynamics: An Engineering Approach. 3rd Ed. Mc-Graw Hill, 1998.

International Institute of Refrigeration (IIR), Cold Store Guide, 3rd edition, 1993.

Kramer, A., and B. A. Twigg, "Measure of Frozen Food Quality and Quality Changes." *The Freezing Preservation of Foods*, 4th Ed., Vol. 2 (1968). Quoted from Singh R. P., and C. Y. Wang, "Quality of Frozen Foods – A Review." *Journal of Food Process Engineering 1,* (1977): 97-127.

Kramer, A., W. A. Bailey, B. H. Ashby, A. H. Bennett, and W. Moleeratanond, "Effect of Temperature Fluctuations on Energy Consumption and Quality Changes of Palletized Foods in Frozen Storage." *ASHRAE Transactions,* (1979): 56-65.

Rein, R. G., and C. M. Burrous, "Basic Concepts of Frost Heaving." *ASHRAE Transactions,* 1987 (2): 1087-1094.

Stoeckle, R. (2001). Refrigerated Warehouse Operation Under Real-Time Pricing. Solar Energy Laboratory. Madison, WI, University of Wisconsin – Madison.

USDA (2000). Refrigerated Storage Capacity, 1999 Summary, United States Department of Agriculture. Website: http://www.nass.usda.gov/ny/pressreleases.htm

Van Arsdel, W. B. (1957), Time-temperature tolerance of frozen foods. I. Introduction/the problem and the attack. *Food Technol.* II(1):28-33. Quoted from Ashby B. H., W. A. Bailey, A. H. Bennett, W. Moleeratanond, and A. Kramer, "Energy Savings and Quality Deterioration from Holding Frozen Foods at Two Daily Temperature Levels." *Transactions of the ASAE,* (1979): 938-943.

CHAPTER 2   COOLER MODELING

The entire warehouse modeling, for the purpose of this project, was done using the software package TRNSYS (SEL, 2000), Transient System Simulation Program. This chapter describes the various existing TRNSYS components used for modeling the warehouse, including the new components that were developed for this project, and their specific design and usage. The development of new component models was pursued by first creating and testing it using Engineering Equation Solver (EES, 2000). Once the model's working was validated in EES, it was converted to Fortran for implementation into TRNSYS.

IISIBAT (Intelligent Interface for the Simulation of Buildings, 2000) and PREBID (2000), an interface for creating the building description files used by TRNSYS Type 56 building model, were the primary programs used for carrying out the TRNSYS simulations. IISIBAT is a general simulation environment program with a graphical user interface that can be used for representing the connections between the various components of the simulation. The building construction is modeled external to TRNSYS in the PREBID program developed by TRANSSOLAR. PREBID serves as an easy-to-use tool for creating the building description file (*.BLD), and the ASHRAE wall transfer function file (*.TRN), both of which are then accessed by TRNSYS for running the simulation.

2.A   Load Estimation

2.A.1   Warehouse Description

The warehouse has 2 distinct zones, maintained at different temperatures, and providing different functions. The zone where the actual product is stored (for either long or short term storage periods) is referred to as the "cooler". The "dock" is a separate zone that serves as the staging area for incoming and outgoing products. Under normal operating conditions, the cooler is at a lower temperature than the dock. The dock temperature is maintained around 10 ^{o}C (50 ^{o}F), while different set-point temperatures have been

investigated for the cooler depending on the optimum storage temperature for the various food products considered during the course of the project.

A prototype cooler was considered in this analysis based on the warehouse model developed by Stoeckle (2001). The cooler floor plan is a square with an area of 9,204 m^2 (100,000 ft^2), with each sidewall of length 95.94 m (314.8 ft). The height of the cooler walls is 9.6 m (31.5 ft), leading to a cooler volume of 88,368 m^3 (3,121,000 ft^3). The dock adjoins the entire length of the cooler's north wall. Therefore, the long side of the dock is 95.94 m (314.8 ft), parallel to the cooler, and the short sides of the dock are 19.19 m (62.96 ft) long. These dimensions result in a dock floor-area of 1,841 m^2 (20,000 ft^2), and with the height of the dock walls being 3.66 m (12.01 ft), the dock volume is 6,733 m^3 (237,773 ft^3). Figure 2.1 shows the floor plan of the warehouse.
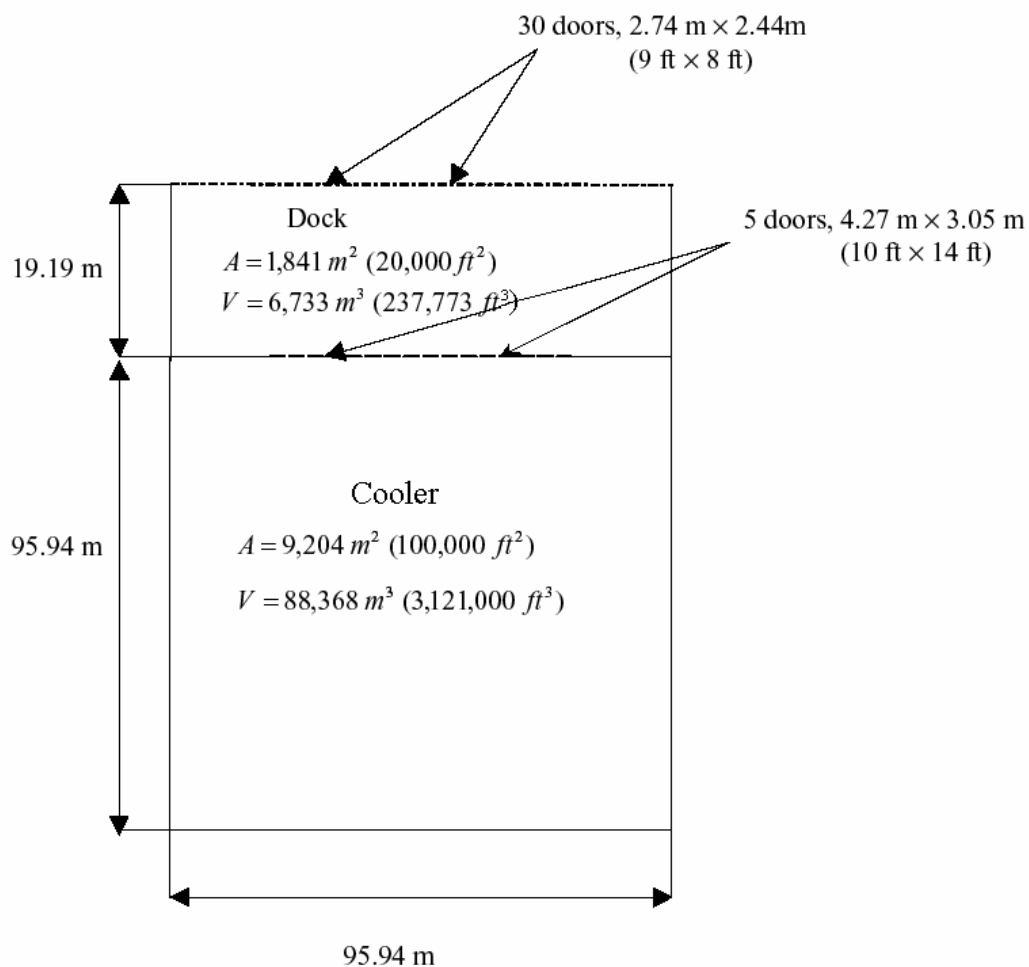
Figure 2.1: Plan view of the warehouse

The walls of the warehouse are modeled as a layer of insulation between two layers of concrete. The insulation thickness is different for the cooler and the dock. For the cooler wall, three different values of insulation thicknesses were studied, resulting in different U-values for each wall. The different insulation U-values studied are:

a) 0.203 W/m^2-K (0.0358 Btu/hr-ft^2-F) for an insulation thickness of 14.5 cm (5.71 in)
b) 0.268 W/m^2-K (0.0472 Btu/hr-ft^2-F) for an insulation thickness of 10.9 cm (4.29 in)
c) 0.228 W/m^2-K (0.0402 Btu/hr-ft^2-F) for an insulation thickness of 12.9 cm (5.08 in)

The first value corresponds to the ASHRAE (1998) recommended value for insulation material resistance or R-value for cooler walls, for coolers maintained in the –4 to 2 ^{o}C (25 to 36 ^{o}F) temperature range. The second value corresponds to the value used by Stoeckle (2001). The last value corresponds to the R-value recommended by ASHRAE (1998) for coolers maintained in the 4 to 10 ^{o}C (39 to 50 ^{o}F) temperature range.

The insulation material has a layer of concrete on either side; 5.1 cm (2 in) of concrete thickness facing towards the external surroundings, and 15.2 (5.98 in) cm of concrete thickness facing into the conditioned space or the cooler.

The dock wall is built of three layers, from outside to inside: 5.1 cm (2 in) of concrete, 4.7 cm (1.85 in) of insulation, and 15.2 cm (5.98 in) of concrete. The total thickness of the dock walls is 25 cm (9.84 in), with an overall U-value of 0.554 W/m^2-K (0.09756 Btu/hr-ft^2-F). This value corresponds to the recommendations from ASHRAE (1998) for minimum insulation for a dock (Jekel, 2000).

The roof of the dock and the cooler is assumed to have the same construction as the zone walls. The floor construction for the warehouse is common for both the dock and the cooler space. The floor has two layers, from outside to inside: 30 cm (11.8 in) of concrete, and 3.5 cm (1.38 in) of insulation, resulting in a floor with a total thickness of 33.5 cm (13.19 in), and a U-value of 0.686 W/m^2-K (0.1208 Btu/hr-ft^2-F). The value is based on the value from Stoeckle (2001), and Jekel (2000). Since, the zone temperature for both the

zones is above freezing, there is no danger of frost heaving of the warehouse floor. Consequently, no allowance for under-floor heating has been made. The other side of the floor slab is in direct contact with soil, and the soil temperature has been assumed constant at 10 ^{o}C (50 ^{o}F).

The cooler is connected to the dock by five doors, each 4.27 m (10 ft) wide and 3.05 m (14ft) high. The dock has 30 truck doors, 2.74 m (9 ft) wide and 2.44 m (8 ft) high each, connecting it to the surroundings. The detailed modeling of infiltration through these doors is explained later in the chapter.

The analysis assumes that on an average, 60% of the cooler floor area is covered with pallets of stored product. The warehouse is assumed to be a distribution type where product is constantly shipped from and received in the warehouse. Also, the product is assumed to arrive "at-temperature", which means that there are no additional thermal gains or losses to the zone on account of the shipped and received product.

2.A.2   Infiltration

The exchange of warm and cold air masses through doorways due to natural convection is a well-known phenomenon observed in the operation of cold store rooms, and it has been studied in detail by numerous researchers. Hendrix, et al. (1989) pointed out that the impact of infiltration on refrigerated warehouse operating costs is always significant and must be accounted for in the design process. The major considerations include: 1) warm air that enters the refrigerated room increases energy costs for the facility, 2) the temperature integrity of the cold room may be affected adversely, resulting in product damage, and 3) moisture in the warm air may result in moisture (in the form of water for coolers or ice for freezers) accumulation on floors and other inside surfaces including walls, and product pallets.

A new component was created for TRNSYS to separately model the infiltration loads for each zone, namely the dock and cooler. The model is referred to as Type 202, and the

modeling is based on the fact that infiltration between zones most commonly occurs because of air density differences between the zones (ASHRAE, 1998). Gosney and Olama (1975) developed the air exchange equation for fully established flow, and it is the equation recommended by ASHRAE (1998) to calculate infiltration heat gains between zones. The same equation has been used in the infiltration model developed for the purpose of this research, and is given below:

$$Q_{inf} = 0.221 * A * (h_{out} - h_{zone}) * r_{zone} * \sqrt{1 - {r_{out}}/{r_{zone}}} * F_m * \sqrt{g * H} \qquad (2.1)$$

$$F_m = \left[\frac{2}{1 + \sqrt[3]{\left({r_{zone}}/{r_{out}} \right)}} \right]^{1.5} \qquad (2.2)$$

where, Q_{inf} = Infiltration load (kW)

A = Doorway area (m^2)

h_{out} = Enthalpy of surrounding air (kJ/kg)

h_{zone} = Enthalpy of zone air (kJ/kg)

ρ_{out} = Density of surrounding air (kg/m^3)

ρ_{zone} = Density of zone air (kg/m^3)

g = Acceleration due to gravity (m/s^2)

H = Doorway height (m)

F_m = Density factor

The heat gain through doorways from air exchange is then expressed as follows:

$$Q_t = Q_{inf} * D_t * D_f * (1 - E) * N \qquad (2.3)$$

$$D_t = \frac{P * (t_p + t_o)}{3600 * t_d} \qquad (2.4)$$

$$\dot{m} = \frac{Q_t}{\left(h_{out} - h_{zone}\right)} \tag{2.5}$$

where, Q_t = Average heat gain (kW)

$\quad\quad D_t$ = Doorway open-time factor

$\quad\quad D_f$ = Doorway flow factor

$\quad\quad E$ = Effectiveness of doorway protective device

$\quad\quad N$ = Number of doors between the zones

$\quad\quad P$ = Number of passages per door per hour

$\quad\quad t_p$ = Door open-close time (s)

$\quad\quad t_o$ = Time door stands open (s)

$\quad\quad t_d$ = Time period (hr)

$\quad\quad \dot{m}$ = Infiltration air mass (kg/s)

The doorway flow factor D_f is the ratio of actual air exchange to that which would occur for fully established flow. Fully established flow occurs only in the unusual case of an unused doorway standing open between the zones, and where the air flow is not impeded by obstructions like stored pallets; D_f in such a case is 1.0. Hendrix, et al. (1989) found that a flow factor D_f of 0.8 is conservative for a 16 K temperature difference. Tests by Downing and Meffert (1993) at temperature differences of 7 K and 10 K found a flow factor of 1.1. Based on these results, ASHRAE (1998) recommends a flow factor of 1.1 for temperature differentials less than 11 $^{\circ}$C, and a value of 0.8 for higher differentials. A value of 0.8 has been assumed for D_f for the purpose of this investigation.

ASHRAE (1998) recommends a value of 0.95 for the effectiveness E of doorway protective devices for newly installed strip doors. However, depending on the traffic level and door maintenance, E may quickly drop to 0.8 for cooler doors. A more conservative value of 0.8 for the effectiveness has been assumed for the purpose of this investigation.

The TRNSYS component configuration for the infiltration model is explained in Appendix A.1.

2.A.2.1 Dock-ambient doors

The dock-ambient doors are the truck bays in the warehouse through which the food products are either brought into the warehouse or taken away from the warehouse to be sold in the market. These doors will henceforth be simply referred to as the dock doors. In a typical warehouse, there are a large number of dock doors, though it is obvious that not all of them would be in operation at the same time. The dock doors are the source of infiltration of warm and humid ambient air into the warehouse.

The model created for the purpose of this investigation has 30 dock doors, each 2.74 m (9 ft) wide and 2.44 m (8 ft) high. In the simulation, it has been assumed that each dock door is open 30 s per passage, and also that the door open-close time is 30 s per passage through the door. The total door open time, therefore, is 60 s per passage. Furthermore, there is one passage through each door every hour. Although, these figures seem to be too small for a single-door operation, the fact that they account for the operation of each of the 30 doors in an hour, gives an overall value of D_t, the doorway open-time factor, which is representative of the actual operation.

The doorway flow factor, D_f, and the effectiveness of the doorway protective device, E, has been fixed at 0.8, as per ASHRAE recommendations (1998).

An important consideration in the modeling of dock doors is that in winter, there are situations when the ambient temperature is lower than the dock temperature, which is maintained around 10 $^{\circ}$C (50 $^{\circ}$F). In such a situation, the dock does not gain heat from the ambient on account of infiltration, but rather loses heat to the ambient. This situation translates into a heating load requirement for the dock. Mathematically speaking, since the infiltration model is air density based, the density factor, F_m, and the infiltration load, Q_{inf}, must be altered under such conditions. To overcome this problem, the model treats the ambient as the refrigerated space, and the dock as the surroundings; and, calculates the infiltration cooling load for the ambient, based on the same equations. The heating load for the dock is then the negative of the cooling load for the ambient, and is subtracted from the dock cooling load requirement.

Figure 2.2 shows the cooling load on the dock because of infiltration from the ambient. An average January day's psychrometric data was generated using Extremes weather sequence generation software (1998) and the simulation was run for a month. The plot is the result for the last 1-week period; any initial effects are, therefore, negligible. Since the dock air is at a higher temperature than the ambient air, the infiltration load is less than zero because of the reason discussed in the preceding paragraph.
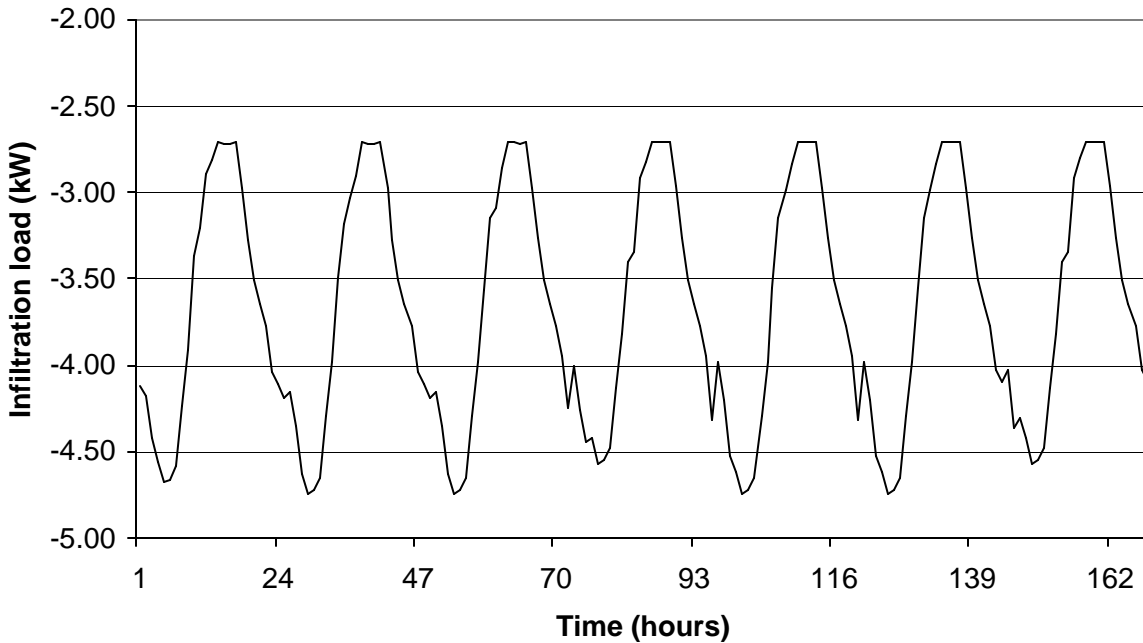
Figure 2.2: Dock-ambient infiltration load during one week in January

Though, the above discussion explains the modeling of the dock doors, the dock zone has another source of infiltration, which is the cooler. The modeling of the cooler-dock doors is discussed in the following section.

2.A.2.2 Cooler-dock doors

The cooler-dock doors serve as a passage for incoming products to be brought into the cooler from the dock for long-term storage, or for removal of products to the dock from whereon to be distributed in the market. These doors will henceforth be simply referred to

as the cooler doors. These doors are the source of infiltration exchange between the two warehouse zones, namely the dock and the cooler. The number of cooler doors in a warehouse is typically much less than the number of dock doors, although the rate of traffic movement through cooler doors is much higher due to multiple passages through each door per hour.

Five cooler doors have been modeled for the purpose of this investigation, each 4.27 m (10 ft) wide and 3.05 m (14 ft) high. In actual warehouses, it is a normal practice to keep the dock-cooler doors open at all times, if the temperature difference between the two zones is not very high. Since, this investigation models such a situation, where the temperature difference between the dock and the cooler is less than 10 $^{\circ}$C (50 $^{\circ}$F), it has been assumed that the cooler doors are open all the time. Such an assumption leads to a doorway open-time factor, D_t, of 1.0 for the purpose of this simulation. The value, however, is not fixed and can be modified in order to model a different situation. As with dock doors, the doorway flow factor, D_f, and also the effectiveness of the doorway protective device, E, have been assumed to be 0.8 each.

Since the dock is always maintained at a higher temperature than the cooler, it is safe to assume that the infiltration air always imposes a cooling load on the cooler. However, the dock also has the same mass of low-temperature air from the cooler infiltrating into it, which thereby imposes an effective heating load on the dock. The infiltration load calculated (Equation 2.3) is, therefore, an addition to the cooling load for the cooler, and at the same time also a subtraction from the cooling load for the dock.

Figure 2.3 shows the cooling load on the cooler because of infiltration from the dock. An average January day's psychrometric data was generated using Extremes weather sequence generation software (1998) and the simulation was run for a month. The plot is the result for the last 1-week period; any initial effects are, therefore, negligible. The cooler being at a lower temperature than the dock, the infiltration air always imposes a positive cooling load on the cooler.
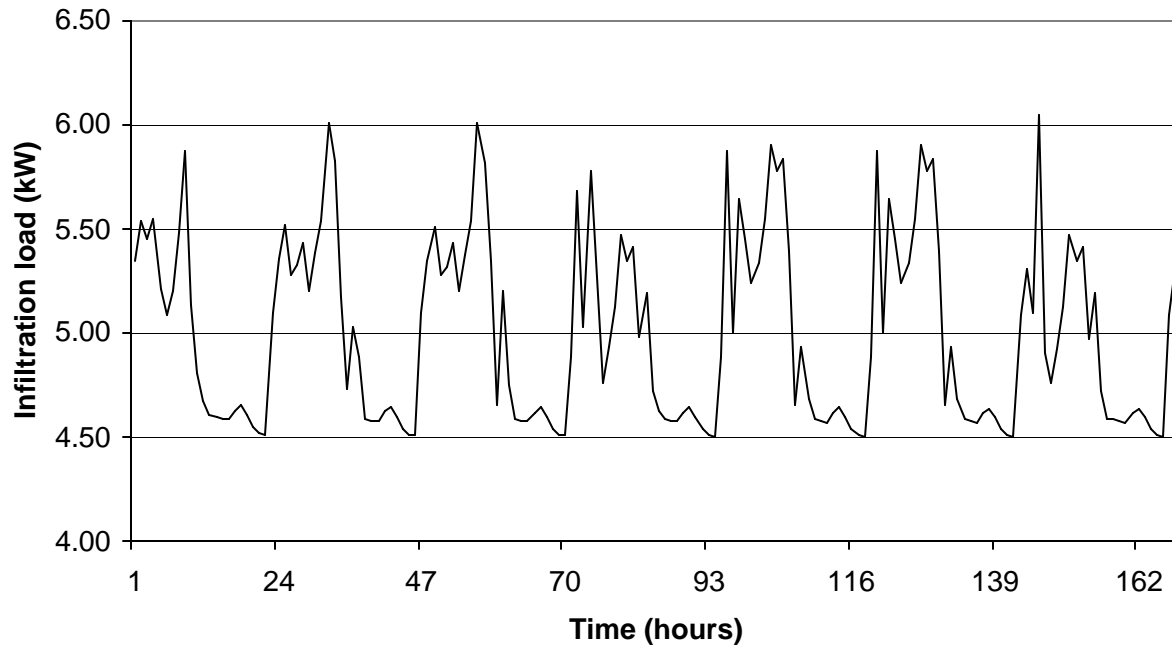
Figure 2.3: Cooler-dock infiltration load during one week in January

2.A.3 Internal Loads

Lights, people, and fork trucks contribute to the internal loads in the warehouse. The assumptions made for the estimation of these loads are based on the warehouse model developed by Stoeckle (2001). The loads are specified as gains to the cooler and dock zones within the PREBID model.

2.A.3.1 Lights

For the cooler, a power density of 4.84 W/m^2 (0.45 W/ft^2) is assumed, which corresponds to an additional load of 44.5 kW (12.65 tons) for the 9,204 m^2 (100,000 ft^2) cooler. It is assumed that 70% of the power is a radiative heat gain, and the rest is convective heat gain. Stoecker (1998) recommends a value of 5 W/m^2 (0.46 W/ft^2) for general-purpose illumination in food storage warehouses. For the dock, the power density is higher, and a

value of 26.91 W/m² (2.5 W/ft²) is assumed. With a dock area of 1,841 m² (20,000 ft²), the total power from dock lights is 49.54 kW (14.1 tons). The break-up between the radiative and convective parts of the power gain is the same as that for the cooler.

2.A.3.2 People

The people working in the warehouse also contribute to the heat gain within the refrigerated space, although, their contribution to the load, as compared to other internal gains, is rather small. ASHRAE (1998) specifies the heat load from a person in a refrigerated space in the form of Equation (2.6).

$$q_p = 272 - 6 * t \tag{2.6}$$

where, q_p: Heat load per person (W)

t: Temperature of the refrigerated space (°C)

For the dock, an average temperature of 10 °C (50 °F) has been assumed for applying the above equation, and an average temperature of 1 °C (34 °F) has been assumed for the cooler. It has been further assumed that there are 7 people in the dock and 3 in the cooler, at all times. For the cooler, the total gain from people is then calculated to be 0.798 kW (0.227 tons), and for the dock it is calculated to be 1.484 kW (0.422 tons). The radiative part of this gain is 60 %, and the rest is convective heat gain, for both the cooler and the dock.

2.A.3.3 Fork trucks

Fork trucks are used for the transportation of the stored product between the cooler and the dock, and also for transportation between the dock and the trucks. For the cooler, the total gain from fork trucks is assumed to be 54.3 kW (15.44 tons), and for the dock it is assumed to be 9.6 kW (2.73 tons). The radiative part of this gain is 70%, and the rest is convective heat gain, for both the cooler and the dock.

2.B   Refrigeration System Simulation

The refrigeration system model designs for the operation of evaporator, compressor, and condenser for both the zones, i.e., the cooler and the dock. The TRNSYS type developed to model the refrigeration system for the dock is referred to as Type 204, while that for the cooler is referred to as Type 206. The design and operation of the refrigeration system is same for both the dock and the cooler; the difference being in the fact that the dock has a fixed set point temperature throughout the simulation, while the cooler set point temperature is explicitly controlled by a separate controller (Type 208), modeled to take real-time price (RTP) of electricity into account.

The Type 56 warehouse model allows two different modes of operation: "Temperature level" control, and "Energy rate" control. The temperature level control allows for a user specified temperature set point for the zone, and calculates the required cooling load to maintain that set point. The energy rate control allows for a cooling load input to the zone, and determines the resultant temperature of the zone. Since the refrigeration system has been modeled external to the warehouse model, it was necessary to use the energy rate control strategy for the purpose of this simulation. The refrigeration system so designed is subject to certain controls on the basis of which the available cooling power to the zone is calculated as an output. The available cooling power is then supplied as an input to Type 56, and the resultant zone temperature is then determined by PREBID.

2.B.1   Compressor Description

Manufacturer's compressor performance data was taken from the Vilter Manufacturing Corporation for the compressor model VSS-451, and this compressor model was used for the purpose of the investigation. The data provides the refrigeration capacity and the electrical power requirement of the compressor for different values of the Saturated Suction Temperature (SST) and the Saturated Discharge Temperature (SDT). SST is the saturation temperature of the refrigerant vapor entering the compressor at suction pressure, and SDT is the refrigerant temperature at the discharge from the compressor and

corresponds to the refrigerant discharge pressure. The data points were plotted in Engineering Equation Solver (EES) and regression analysis was performed to obtain second order polynomial representations for the cooling capacity and electrical power as functions of SST and SDT. It has been previously shown by Brownell (1998) that a second order polynomial with cross term fits the manufacturer's data quite well. Equations (2.7) and (2.8) show the resulting relations for the cooling capacity and the electrical power requirement, respectively. Table 2.1 shows the values of the regression coefficients.

$$CAP = C_1 + C_2 * SST + C_3 * SST^2 + C_4 * SDT + C_5 * SDT^2 + C_6 * SST * SDT \quad (2.7)$$

$$BHP = P_1 + P_2 * SST + P_3 * SST^2 + P_4 * SDT + P_5 * SDT^2 + P_6 * SST * SDT \quad (2.8)$$

where, CAP: Available cooling capacity (tons)

BHP: Electrical power requirement (hp)

C_1, C_6: Regression coefficients for cooling capacity

P_1, P_6: Regression coefficients for electrical power

SST: Saturated Suction Temperature (F)

SDT: Saturated Discharge Temperature (F)

n	1	2	3	4	5	6
C_n	135.07	3.4549	0.025544	-0.19667	-0.0014444	-0.006755
P_n	-7.1422	-1.2347	-0.0075143	1.7382	0.00058333	0.024345

Table 2.1: Regression coefficients for compressor data polynomial representation

Plotting the dependent variable of Equations (2.7) and (2.8) against the SST for different values of SDT results in a plot commonly referred to as a compressor map. Figure 2.4 shows an example of a compressor map displaying the cooling capacity (in tons) as a function of SST and SDT. Figure 2.5 shows another compressor map displaying the electrical power requirement (in bhp) as a function of SST and SDT.
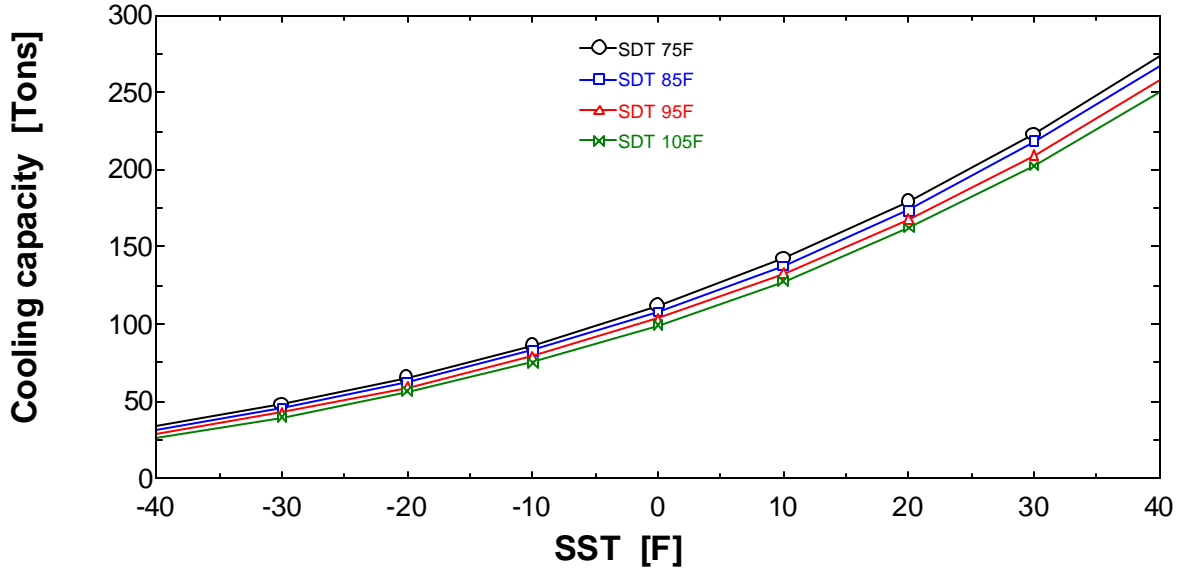
Figure 2.4: Available cooling capacity as a function of SST and SDT
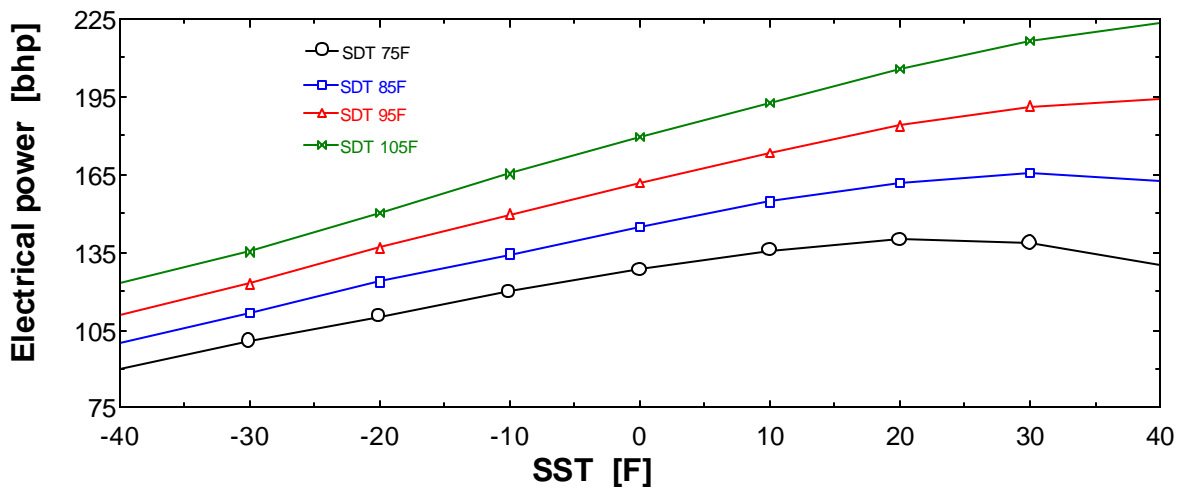
Figure 2.5: Electrical power requirement as a function of SST and SDT

2.B.2   Refrigeration System Design

At the first call of the TRNSYS simulation, the "refrigeration system" type designs the refrigeration equipment, i.e., compressor, evaporator, and condenser, to meet the cooling loads in the warehouse throughout the simulation. The design is based on a set of user-specified parameters, such as the ambient and zone design psychrometric conditions, and expected value of zone peak cooling load. The design of the refrigeration system is

necessary to ensure proper sizing of the evaporator and condenser fans, and also the compressor. The system design is such that the peak cooling load can be met by the equipment at all times during the simulation.

2.B.2.1 Compressor Selection

The compressor selection is based on a user specified zone set point temperature and design cooling load. The refrigerant SST is set to be 8.3 ^{o}C (15 ^{o}F) less than the design zone temperature, and the refrigerant SDT is also a design parameter set by the user. For the purpose of this simulation, the refrigerant SDT has been set equal to 35 ^{o}C (95 ^{o}F). On the basis of these values, a scaling factor is calculated for the VSS 451 compressor model. This scaling factor is used as a means of adjusting the time-average compressor capacity as per the design parameters. The cooling capacity and the electrical power requirement of the compressor, as calculated from the SST and SDT dependent polynomial representations, are then multiplied by this scaling factor throughout the simulation. This scaling factor is a constant value calculated only at the start of the simulation. Basically, the scaling factor represents the number of compressors required to meet the peak warehouse load.

2.B.2.2 Evaporator design

The evaporator is designed so as to meet the design cooling load under the specified design zone conditions. An important user specified design parameter is the evaporator effectiveness. Both the design and the operation of the evaporators during the simulation is based on the effectiveness model. The effectiveness approach has been previously used by Manske (1999). Effectiveness for an evaporator is defined in Equation (2.9), and shown in psychrometric coordinates in Figure 2.6.

$$Effectiven\,ess = \frac{CoilCapacity}{MaxCoilCapacity} = \frac{m_{air} * (h_{air,in} - h_{air,out}\,|_{T,air,out})}{m_{air} * (h_{air,in} - h_{air,out}\,|_{T,refrigerant})} \quad (2.9)$$

The numerator of the above equation corresponds to the actual heat transfer occurring across the evaporator coils, while the denominator corresponds to the maximum or the

ideal heat transfer that would take place if the inlet air temperature were reduced to the refrigerant SST, at the evaporator outlet. Figure 2.4 shows an example psychrometric evaporator effectiveness chart.
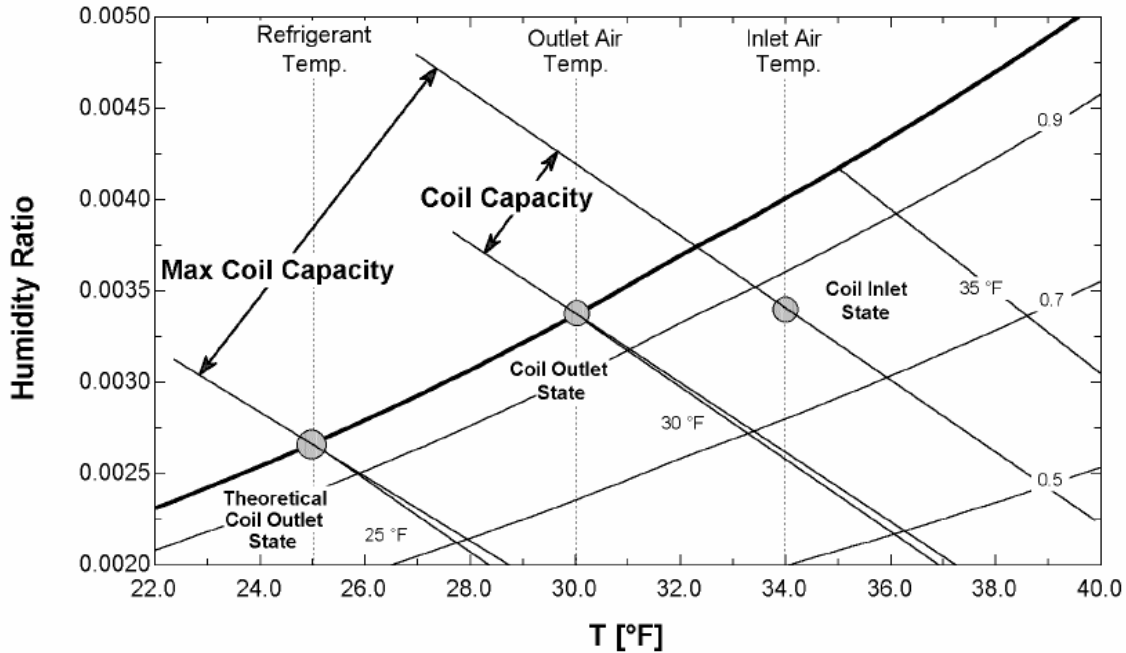
Figure 2.6: Psychrometric Evaporator Effectiveness (Manske, 1999)

At the design step for the evaporator, the unknown variable in Equation (2.9) is the air mass flow rate, m_{air}. The numerator is equivalent to the design cooling load. The value of air mass flow rate calculated is then used as the maximum allowable flow rate of air through the evaporators during the simulation.

2.B.2.3 Condenser design

Applying the principles of thermodynamics to the refrigeration cycle, assuming the compressor is adiabatic, it is inferred that the heat rejection capacity of the condenser must equal the sum of the cooling load on the evaporator and the electrical power requirement of the compressor. The relationship is expressed in Equation (2.10).

$$Q_{Condenser} = Q_{Cooling,Evaporator} + W_{Compressor} \qquad (2.10)$$

The condenser design is also based on the effectiveness approach previously discussed for the evaporator. Effectiveness for a condenser is defined in Equation (2.11).

$$Effectiveness = \frac{Cond.Capacity}{MaxCondCapacity} = \frac{m_{air} * (h_{air,out} |_{T,air,out,Sat} - h_{air,in})}{m_{air} * (h_{air,out} |_{T,refrigerant,Sat} - h_{air,in})} \quad (2.11)$$

The maximum condenser capacity, the denominator of Equation (2.11), is the difference between the maximum possible outlet specific enthalpy and the specific enthalpy of the inlet air, multiplied with the mass flow rate of air. The maximum possible specific enthalpy would occur if the outlet air stream were unit saturated at a dry bulb temperature equal to the refrigerant SDT. The numerator of Equation (2.11) is the actual condenser capacity, expressed as the difference in enthalpy between the outlet and inlet air streams, times the mass flow rate of air.

At the design step for the condenser, the unknown variable in Equation (2.11) is the air mass flow rate, m_{air}. The numerator is equivalent to the condenser heat rejection capacity as calculated from Equation (2.10). The value of air mass flow rate so calculated is then used as the maximum allowable flow rate of air through the condenser during the simulation.

2.B.3 Refrigeration System Operation

The design of the refrigeration system explained in the previous section is established once at the first step of the simulation. After the system is designed, the actual simulation starts. The basic principle for the operation of the equipment remains the same as that for design, but a few changes are introduced in the approach used for obtaining a convergent solution to the equations that describe the refrigeration system. The methodology used for the evaporator, compressor, and condenser operation is discussed in the following sections.

2.B.3.1 Evaporator operation

When the cooling load is less than the design value, which is most of the time, the refrigeration capacity delivered by the evaporators is reduced. Manske (1999) discusses various strategies for modeling the part-load operation of the evaporators. For the purpose of this simulation, a ten-step controller on evaporators has been used in the warehouse. For each load step, the model adjusts the air mass flow rate and refrigerant flow through the evaporators. It is, therefore, assumed that the evaporator fans operate on or off to deliver air mass flow rate between 10% and 100% of the maximum allowable flow rate as calculated in the design step. In actual operation, using ten different evaporator fans that operate on an on-off basis would attain the adjustment in the mass flow rate. The control level is actually dependent on the difference in the zone temperature and the zone set point temperature, and is set as a parameter in the simulation. The control strategy used for the purpose of this simulation is outlined in Table 2.2.

Coil Operating Strategy	$T_{zone} - T_{set\ point}$	Level of Operation	Number of Evaporators Operating
1.	Less than Equal to 0	0%	0
2.	Less than 0.05 °C	10%	1
3.	Between 0.05 and 0.10 °C	20%	2
4.	Between 0.10 and 0.15 °C	30%	3
5.	Between 0.15 and 0.20 °C	40%	4
6.	Between 0.20 and 0.25 °C	50%	5
7.	Between 0.25 and 0.30 °C	60%	6
8.	Between 0.30 and 0.35 °C	70%	7
9.	Between 0.35 and 0.40 °C	80%	8
10.	Between 0.40 and 0.45 °C	90%	9
11.	Greater than 0.45 °C	100%	10

Table 2.2: Evaporator part-load behavior control strategy

However, the change in air mass flow rate affects the evaporator effectiveness (Incropera and DeWitt, 1996). The evaporator model takes the change into account, and calculates the effectiveness value corresponding to the air mass flow rate. The relationship between two different air mass flow rates, m_1 and m_2, and the corresponding evaporator effectiveness', E_1 and E_2, is shown in Equation (2.12).

$$E_2 = 1 - \exp\left[\frac{m_1}{m_2} * \log_e (1 - E_1)\right] \qquad (2.12)$$

The zone set point temperature is an input to the refrigeration model from the controller, and the zone temperature is an input from the Type 56 warehouse model. The refrigerant SST is set to be 8.3 $^\circ$C (15 $^\circ$F) less than the zone temperature, which gives the minimum possible evaporator outlet air enthalpy. The cooling load that the evaporator coils can meet is then calculated as shown in Equation (2.13). The evaporator outlet air temperature is determined from the outlet air enthalpy, calculated using the evaporator cooling load as shown in Equation (2.14).

$$Q_{Evaporator} = m_{air,evap} * E_{evap} * (h_{air,in,evap} - h_{air,out,refrigerant SST}) \qquad (2.13)$$

$$h_{air,out,evap} = h_{air,in,evap} - \frac{Q_{Evaporator}}{m_{air,evap}} \qquad (2.14)$$

2.B.3.2 Compressor operation

The operation of the compressor is dependent on that of the evaporator and the condenser. The compressor has to meet the evaporator cooling load, if possible, and also ensure that the condenser has the required heat rejection capacity. During most times of normal equipment operation the cooling load is less than the maximum available cooling capacity and the compressor is operated at part-load. This part-load operation of the compressor is expressed by the Part Load Ratio (PLR), and is defined in Equation (2.15).

$$PLR = \frac{Q_{Evaporator\,,load}}{Q_{Compressor\,,capacity}}$$

(2.15)

As observed in the compressor map for electrical power requirement, at a fixed value of SST the compressor electrical power requirement increases with SDT. However, as will be explained in the next section, the condenser fan power requirement decreases with increase in refrigerant SDT. The system model, therefore, uses an iterative method to find the value of SDT at which the sum of compressor power and condenser fan power is the minimum. The range of SDT values between which iterations are performed is specified by the user, and is same as the range of SDT values in the manufacturer's compressor data.

2.B.3.3 Condenser operation

The condenser operation principles are the same as that for the design step; the heat rejection capacity of the condenser being equal to the sum of evaporator cooling load and compressor work requirement. The effectiveness approach for the condenser operation is same as that for the evaporator. The expression used for calculating the condenser heat rejection capacity is shown in Equation (2.16).

$$Q_{Condenser} = m_{air,condenser} * E_{condenser} * (h_{air,SDT,Sat} - h_{air,ambient})$$

(2.16)

The air mass flow rate through the condenser cannot exceed the maximum value calculated at the design step, and it is assumed that the condenser also has a Variable Frequency Drive (VFD) motor. The strategy followed to calculate the required air flow rate through the condenser is to compare the required condenser heat rejection with the possible heat rejection at maximum air flow rate and the possible heat rejection at half the maximum flow rate. The method of bisection and linear interpolation is then used to calculate the required mass flow rate. The mathematical expression for this is shown in Equations (2.17) and (2.18).

$$\Delta Q = \frac{Q_{required} - Q_2}{Q_1 - Q_2} \tag{2.17}$$

$$m_{required} = \left[(m_1 - m_2) * \Delta Q\right] + m_2 \tag{2.18}$$

where, subscripts 1 and 2 denote values at maximum flow rate and half the maximum flow rate, respectively.

The fan speed of the condenser fans is directly proportional to the air flow rate, and the electric power consumption of the condenser fans is proportional to the cube of the fan speed. Therefore, the electrical power consumption of the condenser fans can be said to be proportional to the cube of the air flow rate. Equation (2.19) expresses the relation between the rated fan power, W_{rated}, at maximum air mass flow rate, m_{rated}, and the actual power consumption, W_{actual}, at the actual air mass flow rate, m_{actual}.

$$W_{actual} = W_{rated} * \left(\frac{m_{actual}}{m_{rated}}\right)^3 \tag{2.19}$$

It can be seen from the above equation that as the mass flow rate decreases, the fan power consumption also decreases. From Equation (2.16), for the same amount of condenser heat rejection, as the refrigerant SDT increases, the enthalpy difference increases, and consequently the required mass flow rate decreases. Combining both the statements implies that an increase in refrigerant SDT reduces the condenser fan power consumption. However, as was previously pointed out, an increase in refrigerant SDT leads to an increase in compressor power consumption. Therefore, iterations are performed to find the value of SDT that leads to the least total electrical power consumption.

36

Figure 2.7 shows an example SDT profile for a 1-week period during the simulation, with no demand-shifting. Figure 2.8 shows an example SDT profile for the same period during the simulation, with demand-shifting. The points where no SDT value is displayed correspond to the time intervals during which the refrigeration equipment is shut off. The weather data corresponds to an average July day; initial affects are, therefore, negligible.
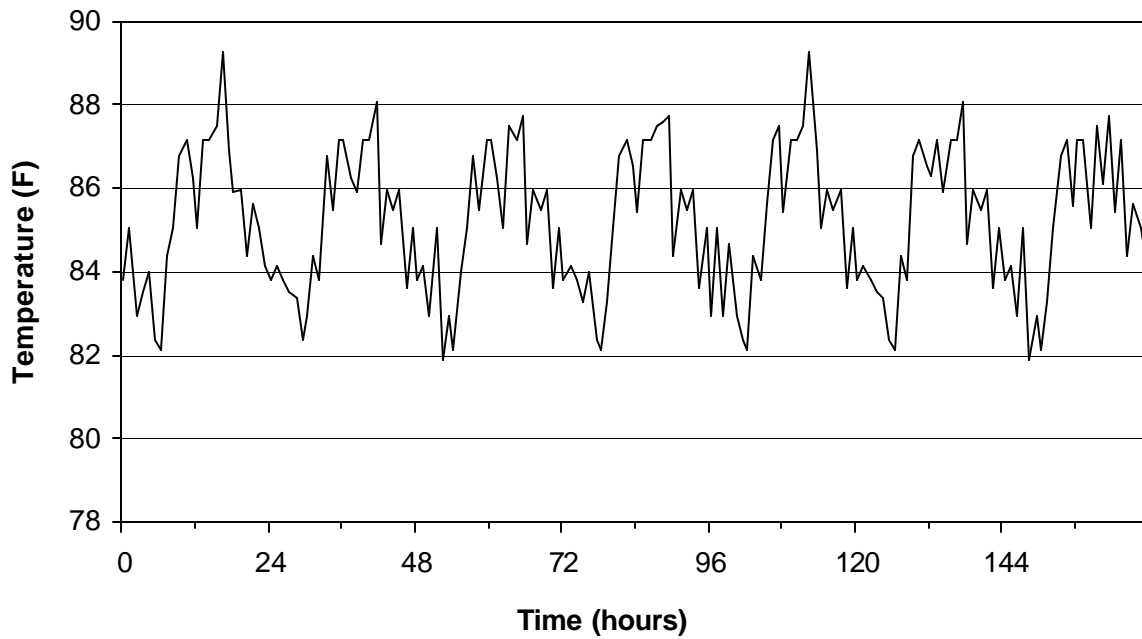
Figure 2.7: Saturated Discharge Temperature (SDT) profile with no demand-shifting
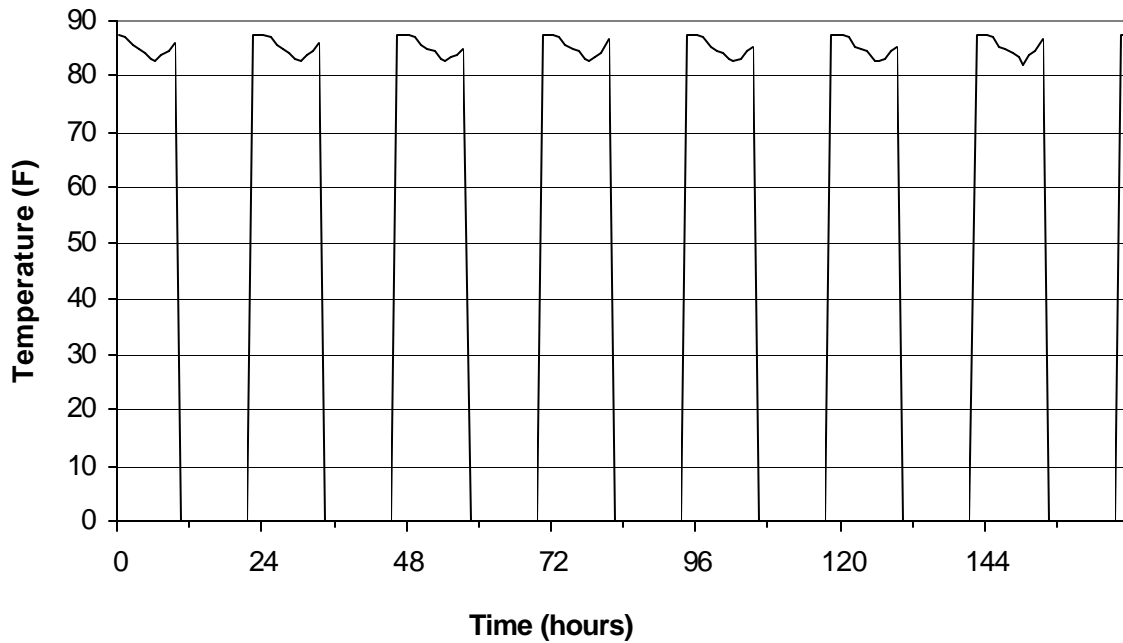
Figure 2.8: Saturated Discharge Temperature (SDT) profile with demand-shifting

Figure 2.9 shows an example cooling load profile for a 1-week period during the simulation, with no demand-shifting. Figure 2.10 shows an example cooling load profile for the same period during the simulation, with demand-shifting. The points show the instantaneous value of the cooling load at the end of each hour. The points where no value is displayed correspond to the time intervals during which the refrigeration equipment is shut off. The weather data corresponds to an average July day; initial affects are, therefore, negligible.
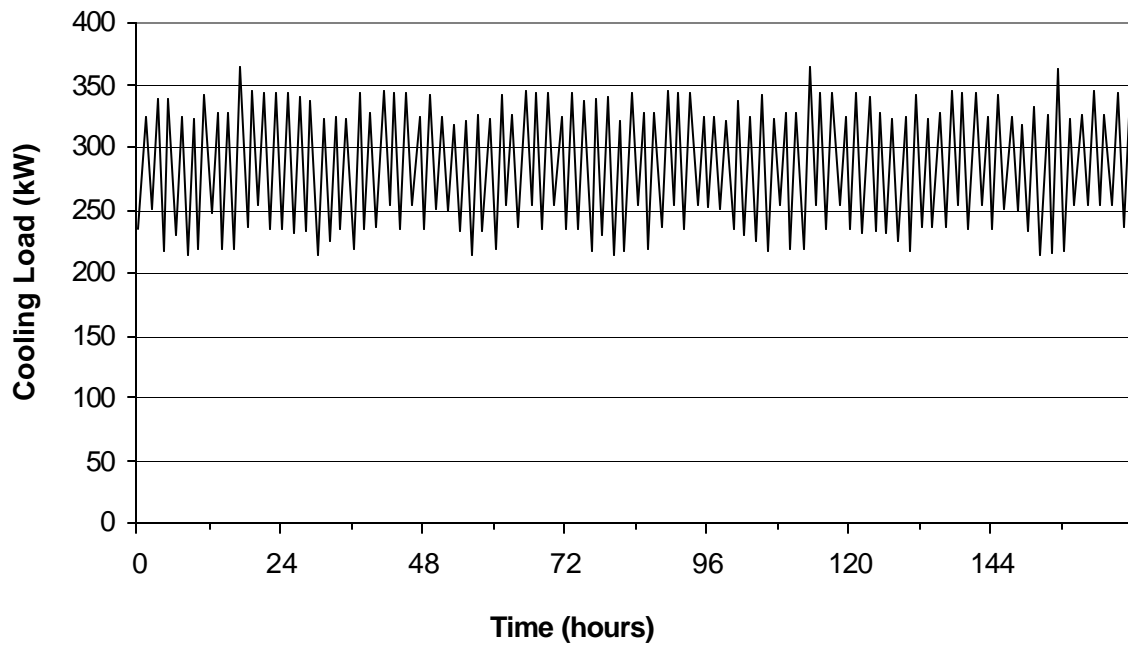
Figure 2.9: Cooling load sample profile with no demand-shifting
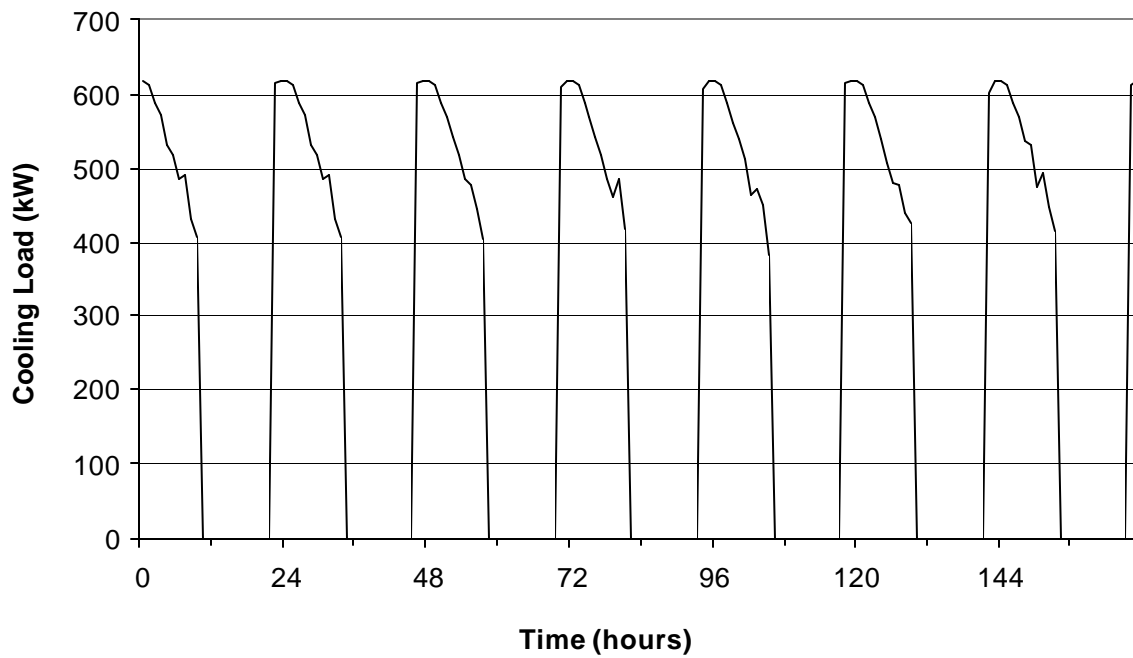
Figure 2.10: Cooling load sample profile with demand-shifting

The TRNSYS component configuration for the refrigeration system model is explained in Appendix A.2.

2.C   Stored Product Modeling

The product stored in the warehouse is the most important component to be considered in the warehouse. The simulation and the demand control strategies developed are constrained only by the fact that under no circumstances should the temperature of the stored product go outside the permissible temperature range for safe storage. The thermophysical properties of food items change drastically as they freeze, and therefore it is important that during the storage of food products, the commodity temperature must be kept above its initial freezing point to avoid freezing damage. In addition, there is a close thermal interaction between the product and its surroundings, namely the cooler air. As long as a constant temperature is maintained in the cooler and the product is brought into the cooler at the cooler temperature, there would be no heat exchange between the product and the surrounding air. However, in following the demand-shifting strategy, wherein the cooler is pre-cooled during certain times and the equipment is shut-off at other times, the cooler temperature varies. This temperature differential between the stored product and the cooler air leads to heat flow into or out of the product.

It will be shown later that this stored product – cooler air thermal interaction is a process that is happening at all times during the simulation; at times, the product being at a lower temperature than the cooler air and the resultant heat flow being from the cooler air to the stored product, and at times, the product being at a higher temperature than the cooler air and the resultant heat flow being from the stored product to the cooler.

The total heat flow from the entire product block to the zone air is calculated and supplied to the Type 56 warehouse model as a heat input to the zone. A positive heat flow would,

therefore, add to the cooling load requirement of the zone, while a negative heat flow would effectively decrease the zone cooling load.

Three different approaches were followed to model the stored product, and a new TRNSYS type was developed based on each approach:

- Lumped capacitance model of the product, Type 201.
- Three-dimensional finite difference model, Type 210.
- Two-dimensional finite difference model, Type 209.

The following sections explain the methodology and construction of the product model based on the above approaches.

2.C.1   Lumped Capacitance Model

The lumped capacitance model assumes that the temperature of the stored product is spatially uniform at any instant of time. This assumption implies that temperature gradients within the stored product are negligible, that is, the stored product is assumed to have infinite thermal conductivity due to which the temperature at all points within the stored product is same. Although, such a situation is clearly not possible in reality, it can be closely approximated for a fully-mixed fluid in which temperature gradients at any point within the fluid would be negated as a result of convective mass flow between the points of differing temperature.

The thermal interaction between such a stored product and its surroundings is modeled as a convective heat exchange. The transient temperature response is determined by performing an overall energy balance on the product, relating the rate of heat loss at the surface to the rate of change of internal energy of the product. The product temperature, T_{final}, at any time, t, is determined according to Equation (2.20). The heat transfer, Q, from the stored product to the zone air, over a time period, is expressed by Equation (2.21).

$$T_{final} = T_{zone} + (T_i - T_{zone}) * \exp\left[-\left(\frac{h \cdot A_s}{r \cdot V \cdot c}\right) \cdot t\right]$$

(2.20)

$$Q = (r \cdot V \cdot c) * (T_i - T_{zone}) * \left[1 - \exp\left(\frac{-h \cdot A_s \cdot t}{r \cdot V \cdot c}\right)\right]$$

(2.21)

where, T_{final} = Final product temperature (C)

Q = Heat transfer from product to zone (J)

T_{zone} = Zone air temperature (C)

T_i = Initial product temperature (C)

h = Convection heat transfer coefficient (W/m^2-C)

A_s = Heat transfer surface area (m^2)

r = Product density (kg/m^3)

V = Product volume (m^3)

c = Product specific heat (J/kg-C)

t = Time elapsed (s)

For the purpose of this simulation, the lumped capacitance approach was applied assuming milk as the stored product. ASHRAE (1998) recommends a safe storage temperature range for milk as between 0.6 and 4.4 ^{o}C (33.1 and 39.9 ^{o}F). The convective heat transfer coefficient was set equal to 4.26 W/m^2-C (0.75 Btu/hr-ft^2-F), the value recommended by Altwies (1998). The thermodynamic properties for milk were taken from ASHRAE (1998), and are listed below:

Specific Heat: 3894 J/kg-C (0.9301 Btu/lbm-F)
Density: 1050 kg/m^3 (65.55 lbm/ft^3)

The TRNSYS component configuration for the lumped capacitance model of the product is explained in Appendix A.3.

Figure 2.11 and Figure 2.12 show the zone air temperature and the product temperature, respectively, for the case of a constant set point temperature for the zone at all times, and no pre-cooling or floating durations. The zone air set point temperature was kept at 2 $^{\circ}$C (36 $^{\circ}$F), and milk was modeled as the stored product. An average July day's psychrometric data was generated using Extremes weather sequence generation software (1998) and the simulation was run for a month. The plots are the results for the last 1-week period; any initial effects are, therefore, negligible.
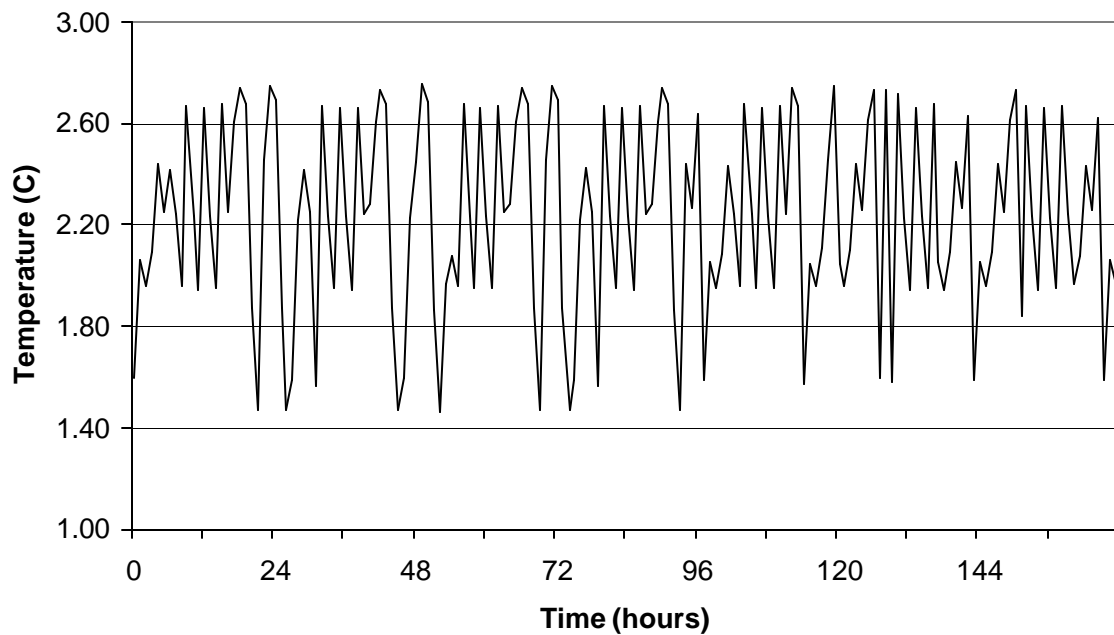
Figure 2.11: Zone air temperature for no demand-shifting
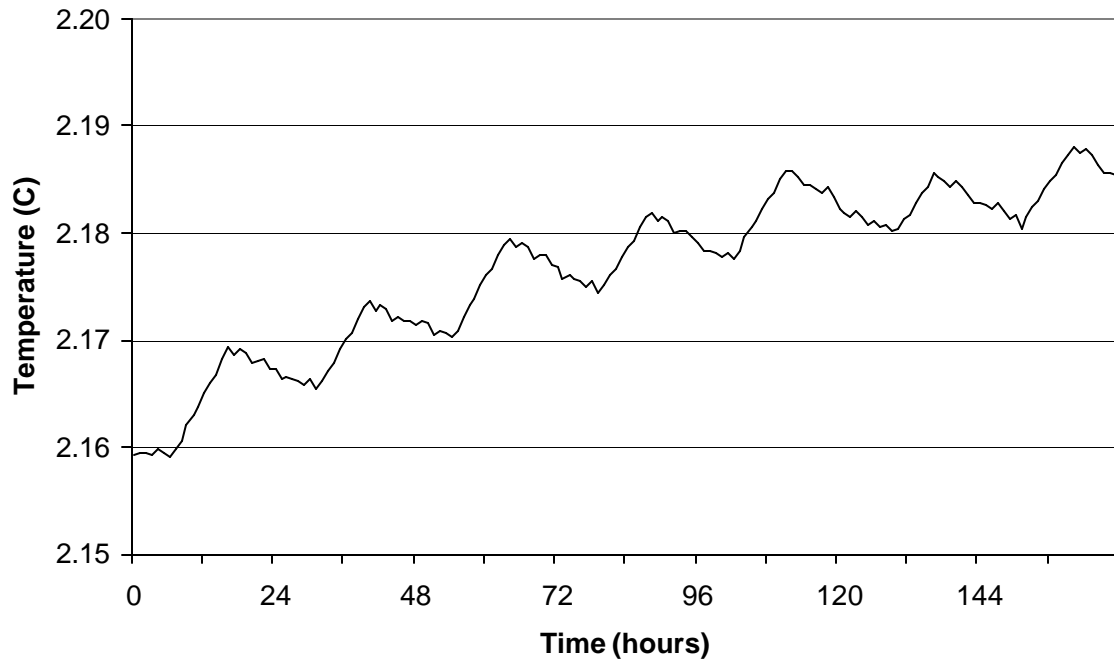
Figure 2.12: Product temperature for no demand-shifting

Figure 2.13 and Figure 2.14 show the zone air temperature and the product temperature, respectively, for the case with demand-shifting. The zone air set point temperature during pre-cooling was kept at 2 ^{o}C (36 ^{o}F), and milk was modeled as the stored product. The floating duration was 10 hours, from 11 A.M. to 9 P.M. The weather data used is the same as that for the case with no demand-shifting.
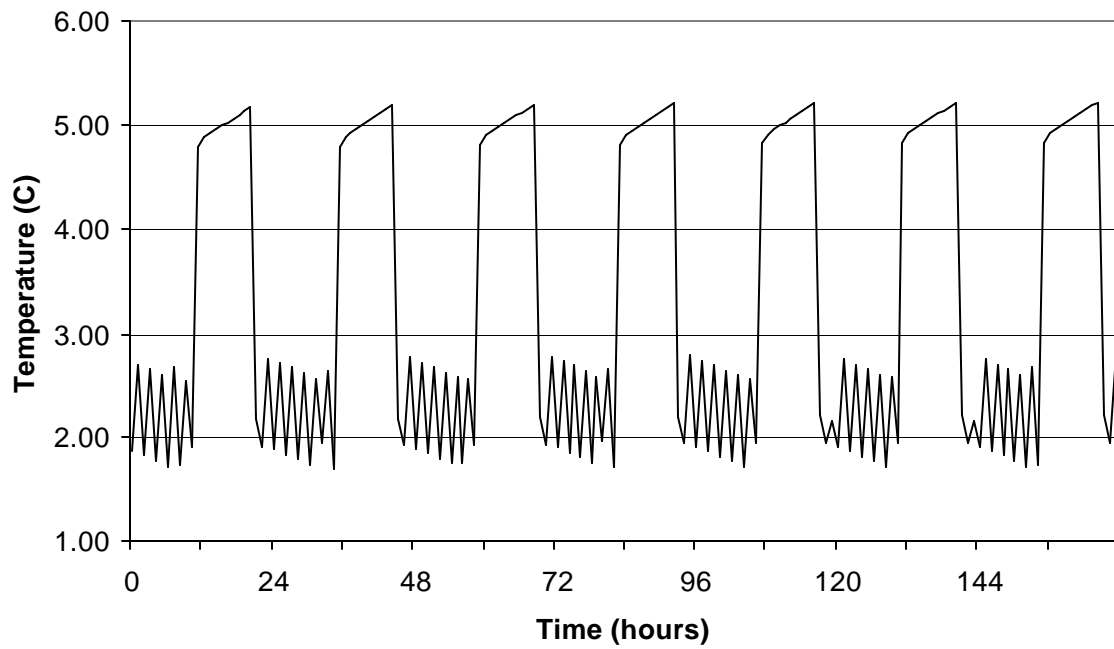
Figure 2.13: Zone air temperature with demand-shifting
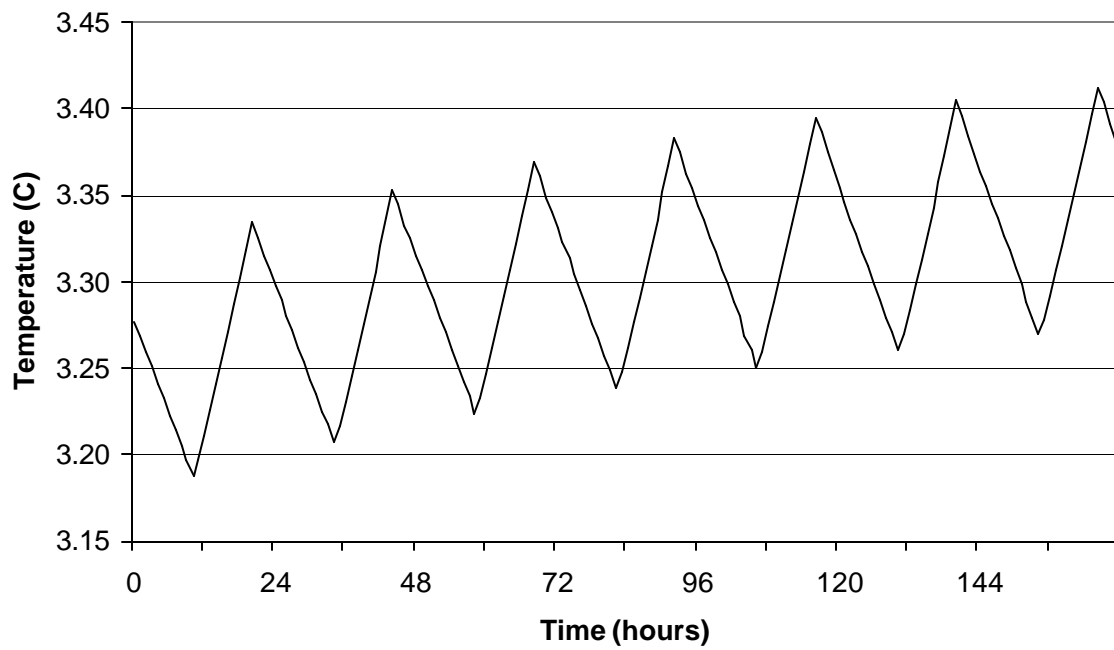
Figure 2.14: Product temperature with demand-shifting

2.C.2 3-D Finite Difference Model

The three dimensional finite-difference model of the product is a more precise model for determining the temperature gradients within the stored product. The entire product block is divided into a number of small regions, and a reference point is assigned at the center of each region. The reference point is referred to as a nodal point, or simply, as a node, and the aggregate of all points is referred to as the nodal network or the grid. In the three spatial dimensions, each node is identified by its X-, Y-, and Z-coordinates.

Having divided the product block into nodes, it is then sought to determine the temperature of each node at every time step of the simulation. The modes of heat transfer considered at each node are: conduction from the surrounding nodes and convection from the zone air. An energy balance equation is written for a control volume around each node, and for convenience it is assumed that all heat flow is into the node. This assumption, though impossible, if applied consistently for all nodes, gives the correct values for temperature of each node. Equation (2.22) is a simple representation of the energy balance equation for a single node.

$$\Delta U = m \cdot C_p \cdot \frac{dT}{dt} = \sum \left(\dot{Q}_{conduction,in} + \dot{Q}_{convection,in} \right) \qquad (2.22)$$

The energy balance Equation (2.22) is actually the mathematical expression for stating that the change in the internal energy of a node over a certain period of time is equal to the sum of all heat flows into the node, during the time period being considered. Knowing the temperature of each node at a previous time step, and applying Equation (2.22), the temperature of each node at each subsequent time step is calculated. At the beginning of the simulation, initial conditions are specified for the temperature of each node, and those conditions serve as the starting point for the subsequent calculations.

The total heat transfer between the zone and the product block is estimated as the sum of convective heat transfers between the zone air and each node that is in direct thermal contact with the zone air. The change in internal energy of each node is also calculated at

each time step, over the previous time step. The integrated value of total heat transfer and the change in internal energy is compared at each time step, and by the first law of thermodynamics, both must be equal in the absence of any work. Equations (2.23) and (2.24) respectively express the formulae for calculating the heat transfer, $\dot{Q}_{conv}$, and the change in internal energy, ΔU. The superscripts, t and (t+1), of the temperature variable, T, denote the time step.

$$\dot{Q}_{conv} = \sum_{Nodes} \left[\bar{h}_{conv} \cdot A_{node} \cdot \left(T_{zone} - T_{node} \right) \right] \tag{2.23}$$

$$\Delta U = \sum_{Nodes} \left[m_{node} \cdot C_p \cdot \left(T_{node}^{t+1} - T_{node}^{t} \right) \right] \tag{2.24}$$

The value recommended by Altwies (1998) has been used for the convective heat transfer coefficient, $\bar{h}_{conv}$, and is equal to 4.26 W/m^2-C (0.75 Btu/hr-ft^2-F). This value takes into account the thermal resistance of the product packaging, and is the average of the coefficient for increased forced convection due to the evaporator fans running, and the coefficient for reduced forced convection with the evaporator fans off.

The bottom of the product block is on a wooden pallet, and a corresponding thermal resistance, between the zone floor and the product block, is used to represent it. The value of the resistance is based on the value used by Stoeckle (2000), and is equal to 0.1656 m^2-C/W (0.9403 ft^2-F-hr/Btu).

2.C.2.1 Nodal Heat Transfer Description

The product block is modeled assuming a line of symmetry in the middle of the X- (width) and Z- (depth) dimensions. The Y- dimension represents the height of the block, the top being in contact with zone air, and the bottom being on the wooden pallet. In order to explain the modes of heat transfer along the six faces of a node consider Figure 2.15, which represents a node with coordinates (X,Y,Z).
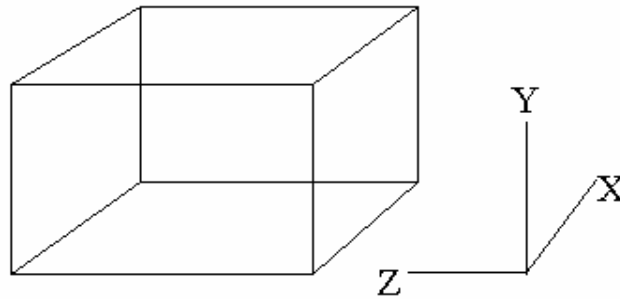
Figure 2.15: Node configuration in X-, Y-, and Z- directions

Following is a description of the modes of heat transfer considered for each face of the node:

Face X-Y along Z-1: If the node is on the front face of the block, there will be convective heat transfer between the zone air and this face. If the node is not on the front face of the block, then it is an interior node in the Z-direction, and is in direct contact with another node of the stored product in the Z-1 direction. In that case, there is conductive heat transfer between the faces of the two nodes in contact.

Face X-Y along Z+1: The node is always in direct thermal contact with the corresponding face of another node in the Z+1 direction, and there is conductive heat transfer between the nodes. However, due to the assumption of symmetry along the middle of the block depth, the node in the center of the block along Z- direction will be adiabatic on this face.

Face X-Z along Y-1: If the node is on the bottom face of the block, it will be in contact with the wooden pallet, and the conductive heat transfer between the floor and the node face is represented using the thermal resistance of the pallet. If the node is in the interior of the block along the Y- direction, then it will be in contact with another node of the product,

along this face. There will be conductive heat transfer between the two nodes along this face.

Face X-Z along Y+1: If the node is on the top face of the block, then it will be in contact with the zone air, and there will be convective heat transfer between the zone air and the node face. If the node is in the interior of the block along the Y- direction, then it will be in contact with another node of the product, along this face, and there will be conductive heat transfer between the two nodes along this face.

Face Y-Z along X+1: The node is always in direct thermal contact with the corresponding face of another node in the X+1 direction, and there is conductive heat transfer between the nodes. However, due to the assumption of symmetry along the middle of the block width, the node in the center of the block along X- direction will be adiabatic on this face.

Face Y-Z along X-1: If the node is on the side face of the block, it will be in contact with the zone air along this face, and there will be convective heat transfer between the zone air and the node along this face. However, if the node is in the interior along the X- direction, it will be in contact with another node of the stored product in the X-1 direction, and there will be conductive heat transfer between the two nodes along this face.

For each node of the product block, the equation for the heat flow on each face is written, and the sum of heat flows on all faces is equal to the change in internal energy of that node, over a time step. The generalized expression for any node is then expressed by Equation (2.25).

$$dx \cdot dy \cdot dz \cdot r \cdot C_p \cdot \left(T_{x,y,z}^{t+1} - T_{x,y,z}^{t}\right) = \Delta t \cdot \left(q_{z-1} + q_{z+1} + q_{y-1} + q_{y+1} + q_{x-1} + q_{x+1}\right) \quad (2.25)$$

where, dx, dy, and dz: Node dimensions in X-, Y-, and Z- direction, respectively (m).

ρ: Density of stored product (kg/m^3)

C_p: Specific heat of stored product (J/kg-C)

$T_{x,y,z}^{t+1}$: Temperature of node at next time step (C)

$T_{x,y,z}^{t}$: Temperature of node at previous time step (C)

Δt: Time interval (s)

q: Rate of heat flow into the node (J/s). The subscripts denote the direction of heat flow.

Equation (2.26), Equation (2.27), and Equation (2.28) contain the expression for the final temperature of an internal node, at the end of a time step, for the corner most face, inner faces, and the center face, respectively.

$$T_{x,y,1}^{+} = T_{x,y,1} + \Delta t \cdot \frac{h}{\boldsymbol{r} \cdot C_p \cdot dz} \cdot \left(T_{zone} - T_{x,y,1}\right) + \boldsymbol{a} \cdot \Delta t \cdot \frac{T_{x+1,y,1} - T_{x,y,1}}{dx^2} + \boldsymbol{a} \cdot \Delta t \cdot \frac{T_{x-1,y,1} - T_{x,y,1}}{dx^2} +$$

$$\boldsymbol{a} \cdot \Delta t \cdot \frac{T_{x,y-1,1} - T_{x,y,1}}{dy^2} + \boldsymbol{a} \cdot \Delta t \cdot \frac{T_{x,y+1,1} - T_{x,y,1}}{dy^2} + \boldsymbol{a} \cdot \Delta t \cdot \frac{T_{x,y,2} - T_{x,y,1}}{dz^2} \qquad (2.26)$$

$$T_{x,y,z}^{+} = T_{x,y,z} + \boldsymbol{a} \cdot \Delta t \cdot \frac{T_{x+1,y,z} - T_{x,y,z}}{dx^2} + \boldsymbol{a} \cdot \Delta t \cdot \frac{T_{x-1,y,z} - T_{x,y,z}}{dx^2} + \boldsymbol{a} \cdot \Delta t \cdot \frac{T_{x,y-1,z} - T_{x,y,z}}{dy^2} +$$

$$\boldsymbol{a} \cdot \Delta t \cdot \frac{T_{x,y+1,z} - T_{x,y,z}}{dy^2} + \boldsymbol{a} \cdot \Delta t \cdot \frac{T_{x,y,z+1} - T_{x,y,z}}{dz^2} + \boldsymbol{a} \cdot \Delta t \cdot \frac{T_{x,y,z-1} - T_{x,y,z}}{dz^2} \qquad (2.27)$$

$$T_{x,y,z\max}^{+} = T_{x,y,z\max} + \boldsymbol{a} \cdot \Delta t \cdot \frac{T_{x+1,y,z\max} - T_{x,y,z\max}}{dx^2} + \boldsymbol{a} \cdot \Delta t \cdot \frac{T_{x-1,y,z\max} - T_{x,y,z\max}}{dx^2} +$$

$$\boldsymbol{a} \cdot \Delta t \cdot \frac{T_{x,y-1,z\max} - T_{x,y,z\max}}{dy^2} + \boldsymbol{a} \cdot \Delta t \cdot \frac{T_{x,y+1,z\max} - T_{x,y,z\max}}{dy^2} + \boldsymbol{a} \cdot \Delta t \cdot \frac{T_{x,y,z\max-1} - T_{x,y,z\max}}{dz^2}$$

$$(2.28)$$

Equation (2.29), Equation (2.30), and Equation (2.31) contain the expression for the final temperature of a node in the top row, at the end of a time step, for the corner most face, inner faces, and the center face, respectively. The expression for a node in the bottom row

is same with the only difference being that instead of convection from the zone air on the top face, there would be a conductive heat transfer term from the zone floor on the bottom face, and the pallet is represented as an effective resistance.

$$T_{x,y\max,1}^{+} = T_{x,y\max,1} + \Delta t \cdot \frac{h}{r \cdot C_p \cdot dz} \cdot \left(T_{zone} - T_{x,y\max,1}\right) + a \cdot \Delta t \cdot \frac{T_{x+1,y\max,1} - T_{x,y\max,1}}{dx^2} +$$

$$a \cdot \Delta t \cdot \frac{T_{x-1,y\max,1} - T_{x,y\max,1}}{dx^2} + a \cdot \Delta t \cdot \frac{T_{x,y\max-1,1} - T_{x,y\max,1}}{dy^2} + a \cdot \Delta t \cdot \frac{T_{x,y\max,2} - T_{x,y\max,1}}{dz^2} +$$

$$\Delta t \cdot \frac{h}{r \cdot C_p \cdot dy} \cdot \left(T_{zone} - T_{x,y\max,1}\right)$$

(2.29)

$$T_{x,y\max z}^{+} = T_{x,y\max z} + a \cdot \Delta t \cdot \frac{T_{x+1,y\max z} - T_{x,y\max z}}{dx^2} + a \cdot \Delta t \cdot \frac{T_{x-1,y\max z} - T_{x,y\max z}}{dx^2} +$$

$$a \cdot \Delta t \cdot \frac{T_{x,y\max-1,z} - T_{x,y\max z}}{dy^2} + a \cdot \Delta t \cdot \frac{T_{x,y\max z+1} - T_{x,y\max z}}{dz^2} + a \cdot \Delta t \cdot \frac{T_{x,y\max z-1} - T_{x,y\max z}}{dz^2} +$$

$$\Delta t \cdot \frac{h}{r \cdot C_p \cdot dy} \cdot \left(T_{zone} - T_{x,y\max z}\right)$$

(2.30)

$$T_{x,y\max,z\max}^{+} = T_{x,y\max,z\max} + a \cdot \Delta t \cdot \frac{T_{x+1,y\max,z\max} - T_{x,y\max,z\max}}{dx^2} + a \cdot \Delta t \cdot \frac{T_{x-1,y\max,z\max} - T_{x,y\max,z\max}}{dx^2} +$$

$$a \cdot \Delta t \cdot \frac{T_{x,y\max-1,z\max} - T_{x,y\max,z\max}}{dy^2} + a \cdot \Delta t \cdot \frac{T_{x,y\max,z\max-1} - T_{x,y\max,z\max}}{dz^2} +$$

$$\Delta t \cdot \frac{h}{r \cdot C_p \cdot dy} \cdot \left(T_{zone} - T_{x,y\max,z\max}\right)$$

(2.31)

Equation (2.32), Equation (2.33), and Equation (2.34) contain the expression for the final temperature of a node in the front row, at the end of a time step, for the corner most face, inner faces, and the center face, respectively.

$$T_{2,y,1}^{+} = T_{2,y,1} + \Delta t \cdot \frac{h}{\boldsymbol{r} \cdot C_p \cdot dz} \cdot \left(T_{zone} - T_{2,y,1}\right) + \boldsymbol{a} \cdot \Delta t \cdot \frac{T_{3,y,1} - T_{2,y,1}}{dx^2} + \boldsymbol{a} \cdot \Delta t \cdot \frac{T_{2,y,2} - T_{2,y,1}}{dz^2} +$$

$$\boldsymbol{a} \cdot \Delta t \cdot \frac{T_{2,y-1,1} - T_{2,y,1}}{dy^2} + \boldsymbol{a} \cdot \Delta t \cdot \frac{T_{2,y+1,1} - T_{2,y,1}}{dy^2} + \Delta t \cdot \frac{h}{\boldsymbol{r} \cdot C_p \cdot dx} \cdot \left(T_{zone} - T_{2,y,1}\right)$$

$$(2.32)$$

$$T_{2,y,z}^{+} = T_{2,y,z} + \boldsymbol{a} \cdot \Delta t \cdot \frac{T_{3,y,z} - T_{2,y,z}}{dx^2} + \boldsymbol{a} \cdot \Delta t \cdot \frac{T_{2,y,z+1} - T_{2,y,z}}{dz^2} + \boldsymbol{a} \cdot \Delta t \cdot \frac{T_{2,y-1,z} - T_{2,y,z}}{dy^2} +$$

$$\boldsymbol{a} \cdot \Delta t \cdot \frac{T_{2,y+1,z} - T_{2,y,z}}{dy^2} + \boldsymbol{a} \cdot \Delta t \cdot \frac{T_{2,y,z-1} - T_{2,y,z}}{dz^2} + \Delta t \cdot \frac{h}{\boldsymbol{r} \cdot C_p \cdot dx} \cdot \left(T_{zone} - T_{2,y,z}\right)$$

$$(2.33)$$

$$T_{2,y,z\max}^{+} = T_{2,y,z\max} + \boldsymbol{a} \cdot \Delta t \cdot \frac{T_{3,y,z\max} - T_{2,y,z\max}}{dx^2} + \boldsymbol{a} \cdot \Delta t \cdot \frac{T_{2,y,z\max-1} - T_{2,y,z\max}}{dz^2} +$$

$$\boldsymbol{a} \cdot \Delta t \cdot \frac{T_{2,y-1,z\max} - T_{2,y,z\max}}{dy^2} + \boldsymbol{a} \cdot \Delta t \cdot \frac{T_{2,y+1,z\max} - T_{2,y,z\max}}{dy^2} + \Delta t \cdot \frac{h}{\boldsymbol{r} \cdot C_p \cdot dx} \cdot \left(T_{zone} - T_{2,y,z\max}\right)$$

$$(2.34)$$

Equation (2.35), Equation (2.36), and Equation (2.37) contain the expression for the final temperature of a node at the bottom corner, at the end of a time step, for the corner most face, inner faces, and the center face, respectively. The expression for the node at the top corner is similar; the difference being that a convective heat transfer from the zone air on the top face replaces the conductive heat transfer from the zone floor.

$$T_{2,2,1}^{+} = T_{2,2,1} + \Delta t \cdot \frac{h}{\boldsymbol{r} \cdot C_p \cdot dz} \cdot \left(T_{zone} - T_{2,2,1} \right) + \Delta t \cdot \frac{h}{\boldsymbol{r} \cdot C_p \cdot dx} \cdot \left(T_{zone} - T_{2,2,1} \right) +$$

$$\Delta t \cdot \frac{\left(T_{floor} - T_{2,2,1} \right)}{R_{floor} \cdot \boldsymbol{r} \cdot C_p \cdot dy} + \boldsymbol{a} \cdot \Delta t \cdot \frac{T_{3,2,1} - T_{2,2,1}}{dx^2} + \boldsymbol{a} \cdot \Delta t \cdot \frac{T_{2,2,2} - T_{2,2,1}}{dz^2} + \boldsymbol{a} \cdot \Delta t \cdot \frac{T_{2,3,1} - T_{2,2,1}}{dy^2}$$

$$(2.35)$$

$$T_{2,2,z}^{+} = T_{2,2,z} + \Delta t \cdot \frac{h}{\boldsymbol{r} \cdot C_p \cdot dx} \cdot \left(T_{zone} - T_{2,2,z} \right) + \Delta t \cdot \frac{T_{floor} - T_{2,2,z}}{R_{floor} \cdot \boldsymbol{r} \cdot C_p \cdot dy} + \boldsymbol{a} \cdot \Delta t \cdot \frac{T_{3,2,z} - T_{2,2,z}}{dx^2} +$$

$$\boldsymbol{a} \cdot \Delta t \cdot \frac{T_{2,2,z+1} - T_{2,2,z}}{dz^2} + \boldsymbol{a} \cdot \Delta t \cdot \frac{T_{2,3,z} - T_{2,2,z}}{dy^2} + \boldsymbol{a} \cdot \Delta t \cdot \frac{T_{2,2,z-1} - T_{2,2,z}}{dz^2}$$

$$(2.36)$$

$$T_{2,2,z\max}^{+} = T_{2,2,z\max} + \Delta t \cdot \frac{h}{\boldsymbol{r} \cdot C_p \cdot dx} \cdot \left(T_{zone} - T_{2,2,z\max} \right) + \Delta t \cdot \frac{T_{floor} - T_{2,2,z\max}}{R_{floor} \cdot \boldsymbol{r} \cdot C_p \cdot dy} +$$

$$\boldsymbol{a} \cdot \Delta t \cdot \frac{T_{3,2,z\max} - T_{2,2,z\max}}{dx^2} + \boldsymbol{a} \cdot \Delta t \cdot \frac{T_{2,2,z\max-1} - T_{2,2,z\max}}{dz^2} + \boldsymbol{a} \cdot \Delta t \cdot \frac{T_{2,3,z\max} - T_{2,2,z\max}}{dy^2}$$

$$(2.37)$$

2.C.2.2 Product Model Simulation Description

For the purpose of this simulation, the thermal properties of cheese have been used to represent the stored product. The following values recommended by Zehr (1997) have been used:

Conductivity: 0.31 W/m-C (0.1791 Btu/hr-ft-F)
Density: 1090 kg/m^3 (68.05 lbm/ft^3)
Specific heat: 2102 J/kg-C (0.502 Btu/lbm-F)

Zehr (1997) conducted a study on two cheese plants in Wisconsin. The product storage details of one of those plants, located in Marshfield, have been used for this study. A single cheese block weighs 21.85 kg (48.17 lb), and measures 0.2985 m (11.75 in) in width, 0.1778 m (7 in) in height, and 0.3778 m (14.875 in) in depth. 54 such blocks are placed onto each pallet; the boxes stacked six high and arranged "chimney style" to allow for circulation of air through the pallet to expedite cooling. The dimensions of a single pallet of cheese are then 0.8955 m (35.25 in) in width, 1.0668 m (42 in) in height, and 1.1334 m (44.625 in) in depth. However, the symmetry criterion implies that the node analysis is done for only half-width and half-depth.

The analysis has been done for different number of nodes, ranging from $10*10*10$ nodes up to $35*35*35$ nodes. The product corner temperatures are analyzed for, because the corner-most points of the product block are the points in direct contact with the zone air, and these points show the extreme temperatures. The product corner is the most sensitive to changes in the cooler temperature. If the cooler temperature increases, it is most likely that the corner has the highest temperature in the whole block. Therefore, the corner temperature is monitored as an indicator of whether the product temperature is outside the permissible safe temperature range for storage.

At the start of the simulation, the temperature of each node, and hence the temperature of the entire block is set to an initial value. From then on, the TRNSYS type calculates the heat exchange between the product block and the zone air, and also the temperature of each node of the product block. The boundary conditions specified are as following: a) Both the side faces are in contact with zone air, b) Both the front faces are in contact with zone air, c) The top face is in contact with zone air, and d) The bottom face is on the wooden pallet.

Figure 2.16, Figure 2.17, and Figure 2.18 show the product block top corner temperature, product block center face temperature, and the zone air temperature, respectively, for a different number of nodes, ranging from $10*10*10$ nodes up to $30*30*30$ nodes. A

constant set point temperature for the zone, equal to 0 $^{\circ}$C (32 $^{\circ}$F), was used, and no demand-shifting was followed. Cheese was modeled as the stored product. An average July day's psychrometric data was generated using Extremes weather sequence generation software (1998) and the simulation was run for a month. The plots are the results for the last 1-week period; any initial effects are, therefore, negligible.
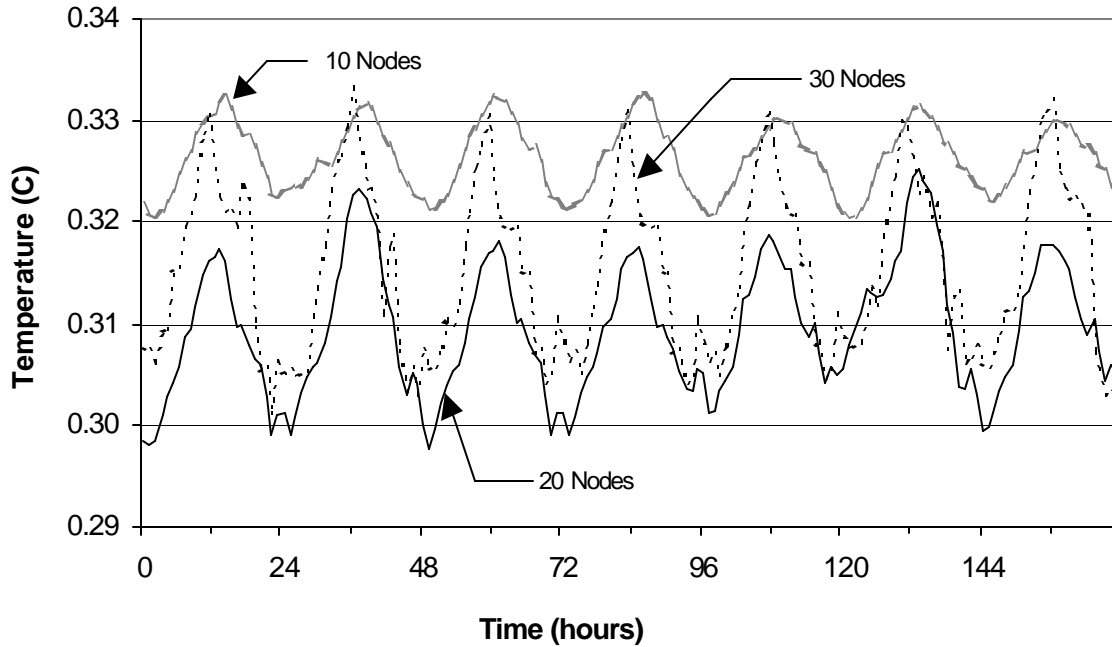
Figure 2.16: Product top corner temperature with no demand-shifting
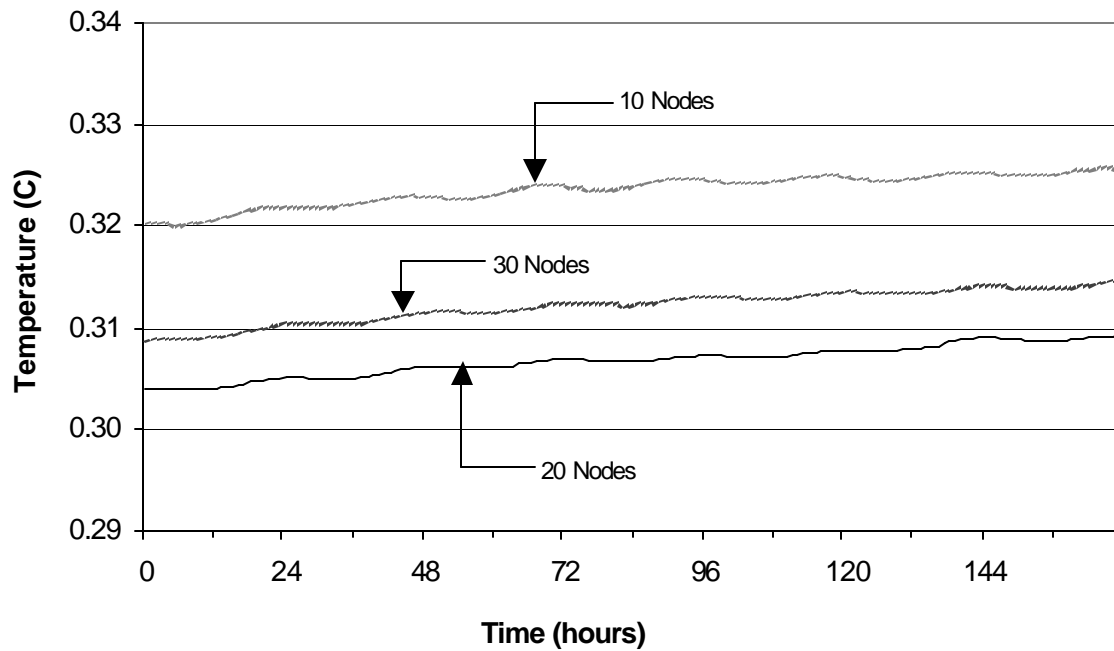
Figure 2.17: Product center temperature with no demand-shifting
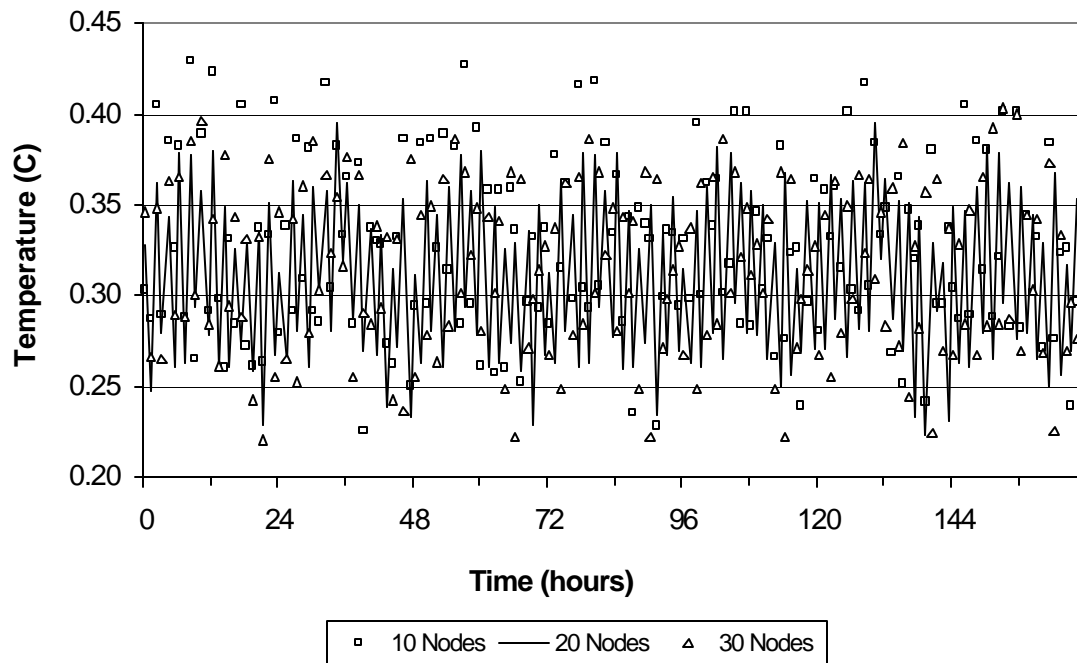
Figure 2.18: Zone air temperature with no demand-shifting

Figure 2.19, Figure 2.20, and Figure 2.21 show the product block top corner temperature, product block center face temperature, and the zone air temperature, respectively, for a different number of nodes, ranging from $10*10*10$ nodes up to $30*30*30$ nodes. The pre-cooling set point temperature for the zone was fixed equal to 0 $^{\circ}$C (32 $^{\circ}$F), and a floating duration of 12 hours, centered around 4 P.M. was followed. Cheese was modeled as the stored product. An average July day's psychrometric data was generated using Extremes weather sequence generation software (1998) and the simulation was run for a month. The plots are the results for the last 1-week period; any initial effects are, therefore, negligible.
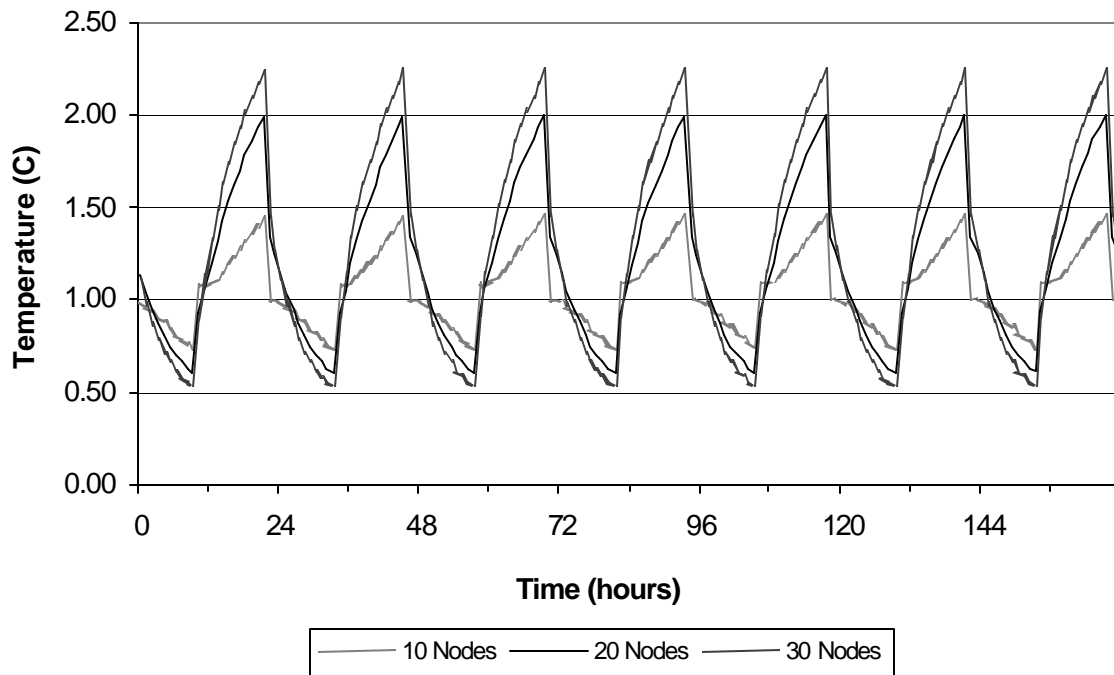
Figure 2.19: Product top corner temperature with demand-shifting
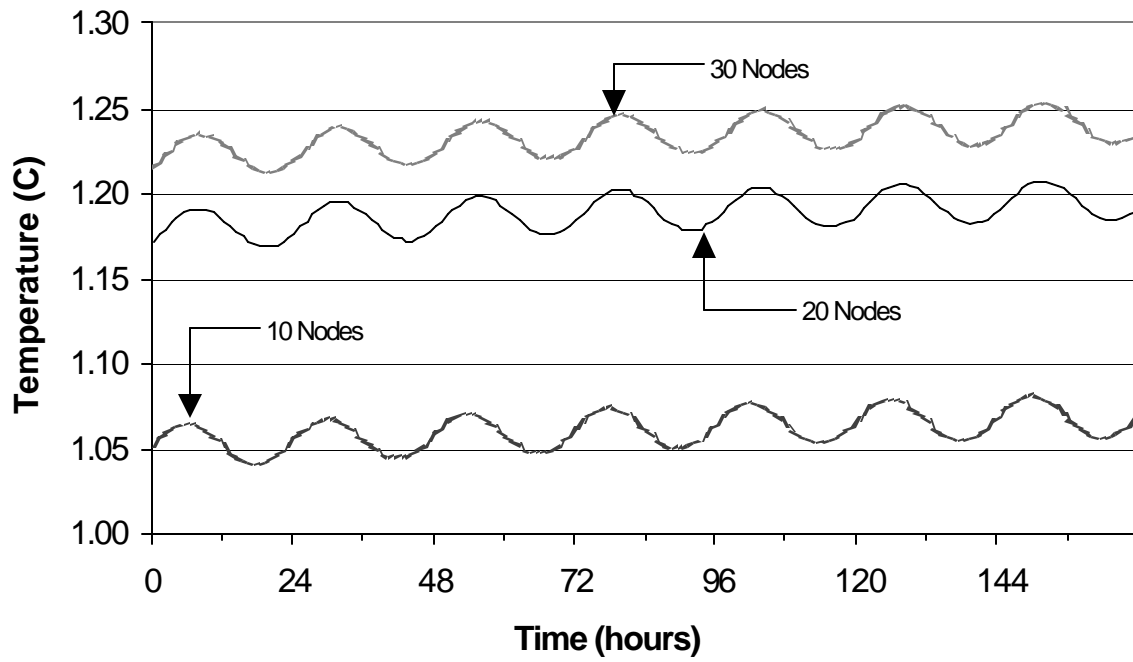
Figure 2.20: Product center temperature with demand-shifting
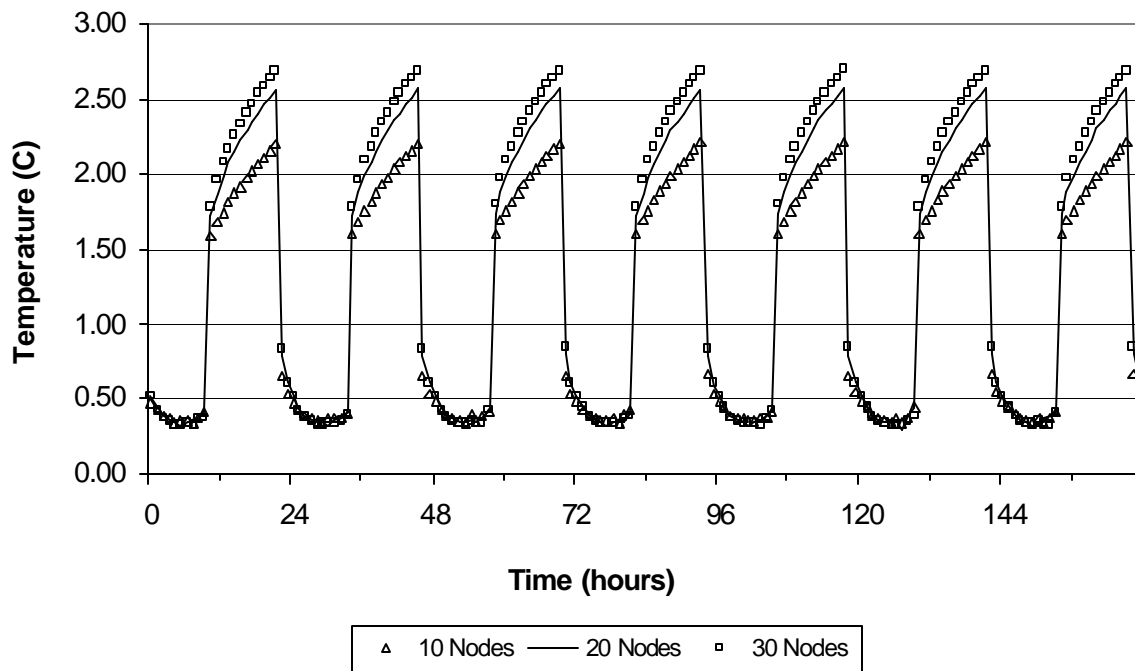
Figure 2.21: Zone air temperature with demand-shifting

The TRNSYS component configuration for the three-dimensional finite difference product model is explained in Appendix A.4.

2.C.3   2-D Finite Difference Model

The two-dimensional finite difference model to represent a block of the stored product is based on a similar model developed by Stoeckle (2001). Although, the 2-D model is not used for the present analysis, a few results were obtained with this model, as it is the "stepping stone" for the 3-D model. The difference between the two models is in the fact that the 2-D model does not have any nodes along the product block depth, or the Z-direction.

The heat flow is calculated for the 2-D model per unit of depth, and multiplication with the product depth gives the heat flow into the bottom, front, and the top of the product block. The 3-D heat flow is finally obtained by assuming the same heat flow per unit area into the sides of the product than through the front. The boundary conditions and the mathematical expressions for calculating the node temperatures are the same as that for the 3-D model, and are thus not discussed in detail as part of this section.

On the basis of the value used by Stoeckle (2001), it was assumed that the product block measures 7.62 m (25 ft) in height, 7.62 m (25 ft) in depth, and 6.10 m (20 ft) in width, and there are 85 such blocks in the zone.

Figure 2.22 and Figure 2.23 show the product block top corner temperature, and the zone air temperature, respectively, for a different number of nodes, ranging from 10∗10 nodes up to 30∗30 nodes. A constant set point temperature for the zone, equal to 0 $^{\circ}$C (32 $^{\circ}$F), was used, and no demand-shifting was followed. Cheese was modeled as the stored product. An average July day's psychrometric data was generated using Extremes weather sequence generation software (1998) and the simulation was run for a month. The plots are the results for the last 1-week period; any initial effects are, therefore, negligible.
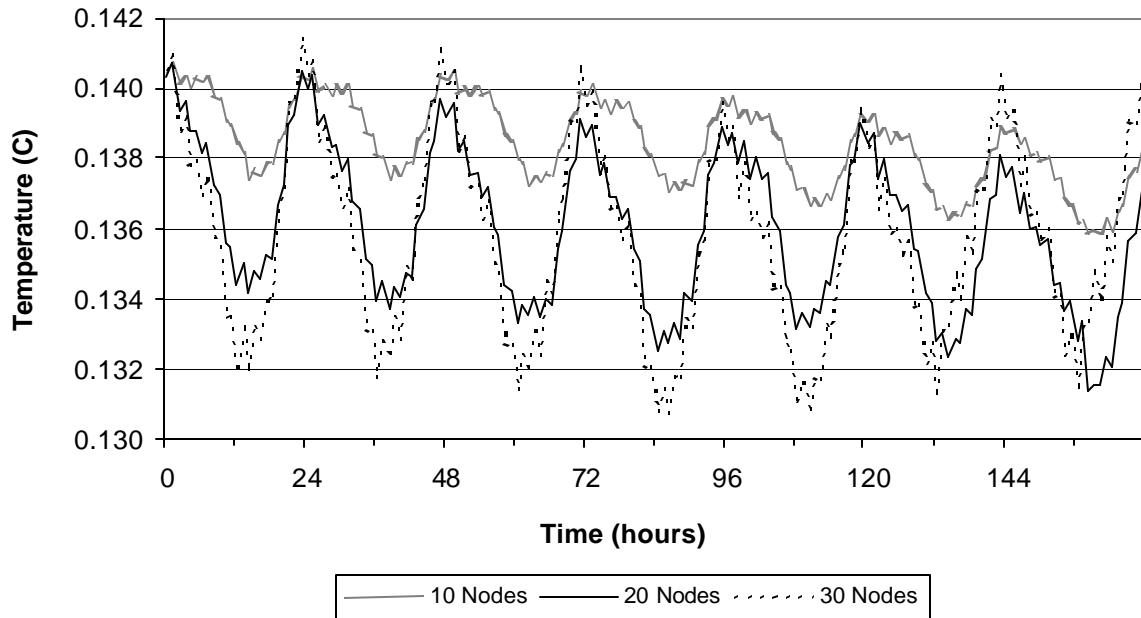
Figure 2.22: Product top corner temperature with no demand-shifting
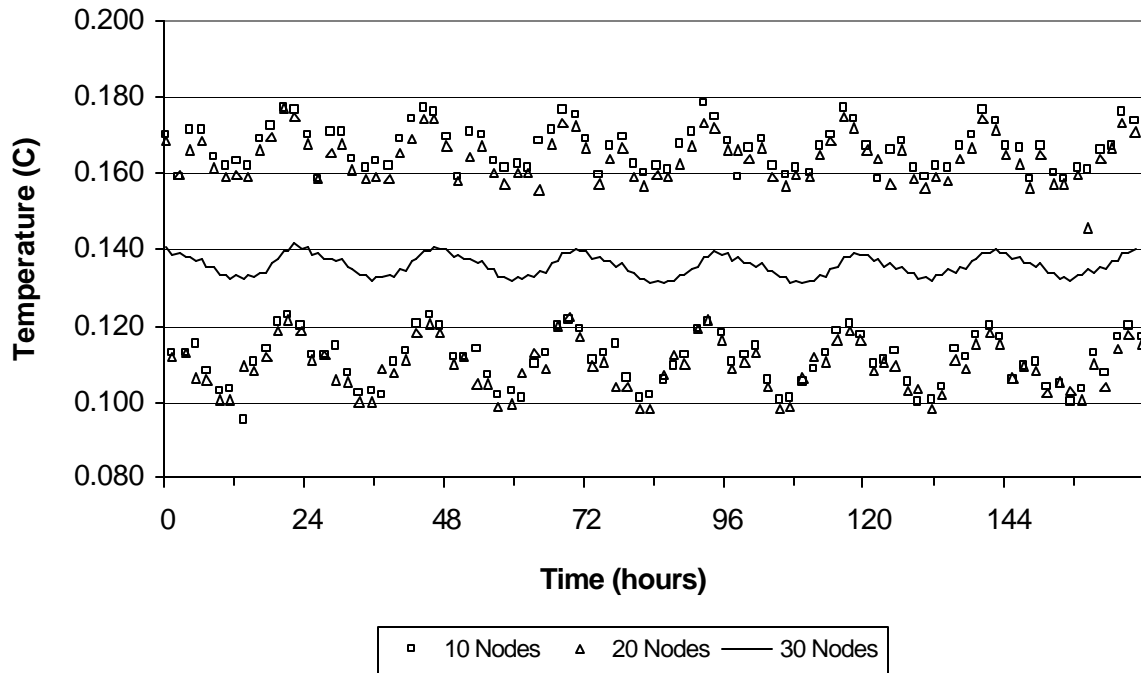
Figure 2.23: Zone air temperature with no demand-shifting

Figure 2.24, and Figure 2.25 show the product block top corner temperature, and the zone air temperature, respectively, for a different number of nodes, ranging from 10∗10 nodes up to 30∗30 nodes. The pre-cooling set point temperature for the zone was fixed equal to 0 ^{o}C (32 ^{o}F), and a floating duration of 12 hours, œntered around 4 P.M. was followed. Cheese was modeled as the stored product. An average July day's psychrometric data was generated using Extremes weather sequence generation software (1998) and the simulation was run for a month. The plots are the results for the last 1-week period; any initial effects are, therefore, negligible.
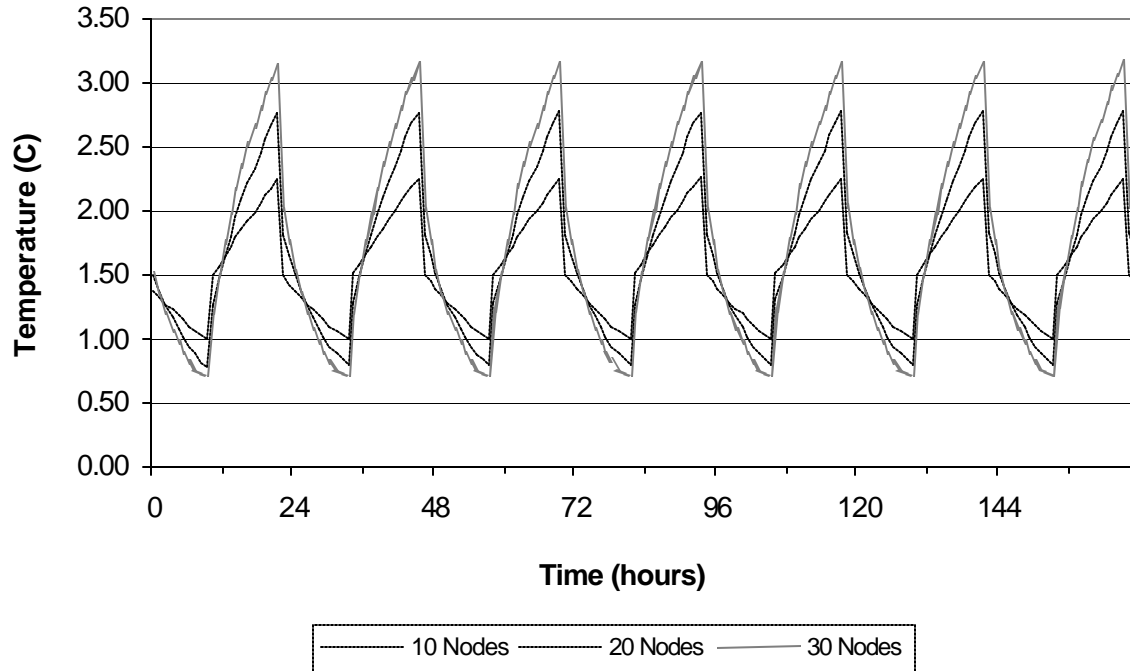
Figure 2.24: Product top corner temperature with demand-shifting

Figure 2.25: Zone air temperature with demand-shifting

2.D Zone Temperature Set-point Controller

In order to facilitate operation under the demand-shifting strategy, it is imperative to have different set point temperatures for the zone during the pre-cooling and floating durations. At any point during the simulation, the set point temperature is dependent on the time of the day. During on-peak hours of the day, in the afternoon, the equipment is shut-off, as it corresponds to the floating duration. During off-peak hours, during night, the equipment is operated at a pre-cooling set point temperature.

The new TRNSYS type's function is basically to determine the 'time of the day' at any point of the simulation, and is referred to as Type 208. The user has to specify the floating duration for the refrigeration equipment, centered around 4 P.M., and also the pre-cooling set point temperature, as parameters. Type 208 determines the value of the set point temperature corresponding to the time of the day. The output set point temperature is

passed on to the refrigeration equipment as an input. Equation (2.38) expresses the time-dependence of the zone temperature set point, in the form of an If-Then-Else statement.

$$If\left(Floating_{start} \leq Time \leq Floating_{end}\right)$$

$$Then \Rightarrow T_{setpoint} = T_{floating}\left(\cong Effectives\,hutoff\right)$$

(2.38)

$$Else \Rightarrow T_{setpoint} = T_{precooling}$$

In order to safeguard against the stored product getting spoiled due to high temperatures, a maximum value for the zone temperature is also specified as a parameter for Type 208. In case, the zone temperature exceeds this maximum value, the controller sets the zone set point temperature to the pre-cooling set point value even if the time of the day corresponds to the floating duration. This safety action switches on the refrigeration equipment so that the zone temperature is brought down to a safe level. It is for this reason that the zone temperature is an input to the controller at every step of the simulation.

The TRNSYS component configuration for the zone temperature set point controller is explained in Appendix A.5.

2.E   References

Altwies, J. (1998). Electrical Demand Reduction in Refrigerated Warehouses. Solar Energy Laboratory. Madison, WI, University of Wisconsin – Madison.

American Society of Heating, Refrigerating, and Air-conditioning Engineers (ASHRAE) (1998), 1998 ASHRAE Handbook – Refrigeration.

Brownell, K. A. (1998). Investigation of the Field Performance for Industrial Refrigeration Systems. Solar Energy Laboratory. Madison, WI, University of Wisconsin – Madison.

Downing, C. C., and W. A. Meffert (1993). "Effectiveness of cold-storage door infiltration protective devices." *ASHRAE Transactions,* 99(2).

Gosney, W. B., and H. A. L. Olama (1975). "Heat and Enthalpy Gains through Cold Room Doorways." Paper presented before *the Institute of Refrigeration at the Faculty of Environmental Science and Technology*, The Polytechnic of the South Bank, London (December). Quoted from ASHRAE (1998) Refrigeration Handboook.

Hendrix, W. A., D. R. Henderson, and H. Z. Jackson (1989). "Infiltration heat gains through cold storage room doorways." *ASHRAE Transactions,* 95(2).

Incropera, F. P., and D. P. DeWitt. Introduction to Heat Transfer. 3rd Ed. John Wiley & Sons, 1996.

Jekel, T. B., and D. T. Reindl (2000). Energy efficiency operations at Supervalu. Madison, WI, University of Wisconsin, HVAC&R Center. Quoted from Stoeckle, R. (2001). Refrigerated Warehouse Operation under Real-Time Pricing. Solar Energy Laboratory. Madison, WI, University of Wisconsin – Madison.

Manske, K. A. (1999). Performance Optimization of Industrial Refrigeration Systems. Solar Energy Laboratory. Madison, WI, University of Wisconsin – Madison.

Mitchell, J. W., and J. E. Braun (1998). Design, Analysis, and Control of Space Conditioning Equipment and Systems. University of Wisconsin – Madison.

Klein, S. A., D. D. Schmitt, and D. T. Reindl (1998). Automated Generation of Hourly Design Sequences. Extremes Weather Sequence Generator. ASHRAE Project 962.

Klein, S. A., and F. L. Alvarado (2000). Engineering Equation Solver. Middleton, WI, F-chart software.

SEL (2000). IISIBAT – An Intelligent Interface for the Simulation of Buildings. Madison, WI, Solar Energy Laboratory.

SEL (2000). PREBID – Building Description Software. Madison, WI, Solar Energy Laboratory.

SEL (2000). TRNSYS – A Transient System Simulation Program. Madison, WI, Solar Energy Laboratory.

Stoecker, W. F. Industrial Refrigeration Handbook. Mc-Graw Hill, 1998.

Stoeckle, R. (2001). Refrigerated Warehouse Operation under Real-Time Pricing. Solar Energy Laboratory. Madison, WI, University of Wisconsin – Madison.

Zehr, S. E. (1997). Process Energy Efficiency Improvement in Wisconsin Cheese Plants. Solar Energy Laboratory. Madison, WI, University of Wisconsin – Madison.

CHAPTER 3   OBSERVATIONS AND RESULTS

This chapter presents the results of a cooler operating with the product modeled assuming both lumped capacitance and distributed (with a three-dimensional finite difference model) models. The primary objective here is to compare alternative operating strategies for coolers under Real-Time Pricing (RTP) rate structures. To accomplish this objective, a base case was developed for each product model type and its comparison with a strategy that shifts energy usage to lower cost pricing periods is presented. In the base case, the zone refrigeration equipment is operated continuously to meet the loads as they occur, and maintain the desired zone set point temperature. Alternative cases for load shifting are then compared with the base case. A constraint imposed on the load shifting cases limits the worst-case product temperature (usually the product corner temperature) rise from exceeding a predetermined maximum permissible value for safe storage. Yearly simulations using the Madison weather data were run to establish the base case and the alternate cases.

Also included in this Chapter are the results of an investigation to assess the impact of the zone wall conductance (or U-values), and the zone temperature on annual energy use and cost. As outlined in Section 2.A.1, three different wall constructions have been modeled for the cooler. The wall constructions are reflective of a range of alternatives used in industrial coolers. A different base case operation was established for each construction, and the demand-shifting results have been evaluated against each base case.

The products in the warehouse can be safely stored over a range of temperature, and, for many products there is no single value for the optimum storage temperature. Therefore, the study also investigates the operation of the refrigeration equipment, both for the base case and the demand-shifting strategy, at different set point temperatures for the cooler. A constraint maintained in the simulations is that the product temperature is always maintained within the permissible safe temperature range to prevent spoilage.

To study the refrigeration equipment operation under the demand-shifting strategy, different pre-cooling zone set point temperatures have been investigated, and for each set point temperature, the maximum possible floating duration has been determined. The longer the floating duration, the higher is the rise in product and zone temperatures. However, a longer floating duration can, possibly, lead to greater operational cost savings. The floating duration has been centered around 4 P.M.

Altwies (1998) investigated three strategies for operation under time-of-use pricing. The first option was "full demand-shifting", which means that the refrigeration equipment was completely shut down during the on-peak window and operated at maximum capacity during the off-peak periods. The second strategy was "load leveling" in which the refrigeration equipment was operated at a constant level 24 hours a day. The operating level chosen for this strategy was such that the average warehouse load was met and the product temperature stayed within the permissible range. The third option was a combination of the first two options: operating at a lower capacity level during the on-peak and a higher capacity level during the off-peak period. Altwies concluded that maximum savings could be realized with the first option of full demand-shifting. In addition to evaluating RTP rate scenarios, this Chapter presents results of Time-of-Use (TOU) pricing with a full demand-shifting operational strategy.

3.A   Utility Rate Data

The electric rates used in the analysis of warehouse operation are taken from four different sources, as explained in the following sections.

3.A.1   Data Based on Price Ratios

This data has been adapted from the Madison Gas & Electric (MG&E) Company's time-of-use rates as they apply to commercial and industrial customers. The costs do not represent the dollar value of electricity, but are ratios of on-peak and off-peak rates on

which the actual costs are based. Table 3.1 gives the duration of each season in the year, for rate determination.

Season	Duration
Summer	June 15$^{\text{th}}$ – October 15$^{\text{th}}$
Winter	October 16$^{\text{th}}$ – June 14$^{\text{th}}$

Table 3.1: Seasonal Durations adapted from MG&E rate data

The definition for on-peak and off-peak hours is as follows:

On-peak rates: Monday – Friday, 10 A.M. to 10 P.M.

Off-peak rates: Monday – Friday, 10 P.M. to 10 A.M., and Weekends.

Table 3.2 gives the seasonal price ratios for both on-peak and off-peak hours.

Hour	Summer ratio	Winter ratio
On-peak hours	2.0	1.5
Off-peak hours	1.0	1.0

Table 3.2: Seasonal price ratios adapted from MG&E rate data

Based on the above considerations, a TRNSYS-readable data file was made, containing the price ratio corresponding to each hour of the year-long simulation. This electric rate structure will be henceforth referred to as "Case I" when warehouse operating costs are discussed.

3.A.2   MG&E Time-of-Use Rate

These data represent the Time-of-Use prices charged by MG&E to a major industrial account in its service territory that utilizes significant refrigeration in its operation. The duration of summer and winter season in a year is same as that given in Table 3.1. The weekly definition for on-peak and off-peak hours is same as that discussed for Case I, in Section 3.A.1.

Table 3.3 gives the seasonal energy prices (in $ per kWh) for both on-peak and off-peak hours.

Hour	*Summer rates ($/kWh)*	*Winter rates ($/kWh)*
On-peak hours	0.044	0.0405
Off-peak hours	0.02836	0.02836

Table 3.3: Large industrial rates for MG&E

Based on the above considerations, a TRNSYS-readable data file was made, containing the electric prices corresponding to each hour of the year-long simulation. This electric rate structure will be henceforth referred to as "Case II" when operating costs are discussed.

3.A.3   PG&E Real-Time Pricing Rate Structure

Pacific Gas and Electric (PG&E) Corporation serves northern California, and one of its pricing structures is based on real-time prices (RTP). In the RTP rate structure, the price of electricity changes every hour of the day. The data used for this study are the same as those used by Stoeckle (2001), and correspond to PG&E prices for the year 1998. The PG&E pricing structure has, by far, the biggest differences in prices between daytime and nighttime period (analogous to "on-peak" and "off-peak" periods). Therefore, this pricing

structure may offer the maximum possible savings for demand-shifting as compared to the base case operation. Figure 3.1 shows the hour-by-hour prices for the entire year in 1998. This electric rate structure and its associated prices will be henceforth referred to as "Case III" when operating costs are discussed.
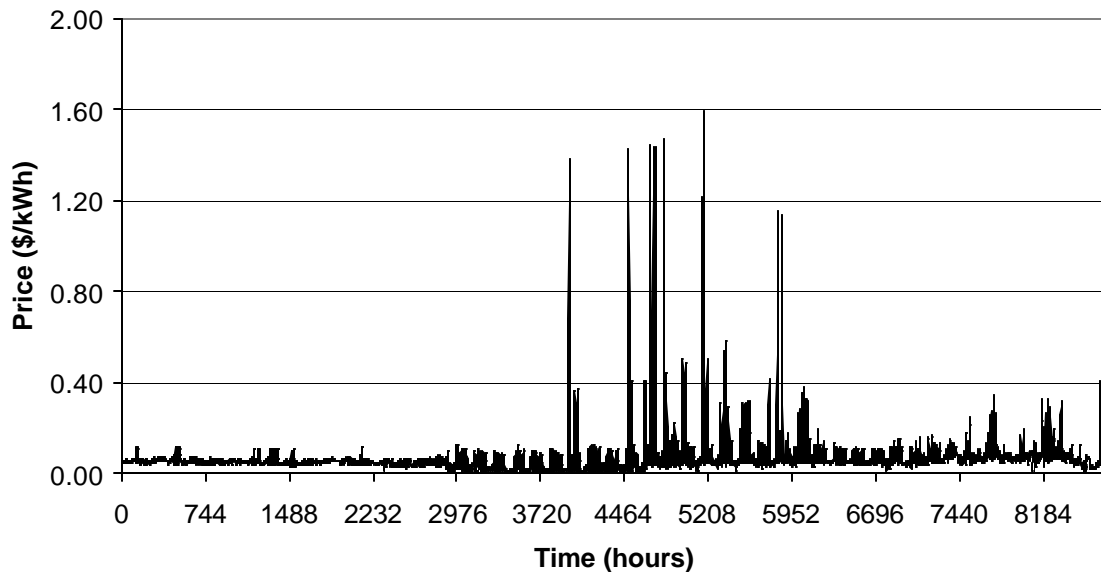
Figure 3.1: PG&E pricing data for the entire 1998 calendar year

3.A.4   Southern Company Real-Time Pricing Structure

The Southern Company provides power to the state of Alabama, and its pricing structure is also based on real-time prices, wherein, the price of electricity changes every hour. The data used for this study are the same as those used by Stoeckle (2001), and correspond to Southern Company's prices for the year 1998. In contrast to PG&E's prices, the Southern Company prices are not nearly as volatile. Figure 3.2 shows the hourly price for the entire year. This electric utility rate structure and associated prices will be henceforth referred to as "Case IV" when operating costs are discussed.
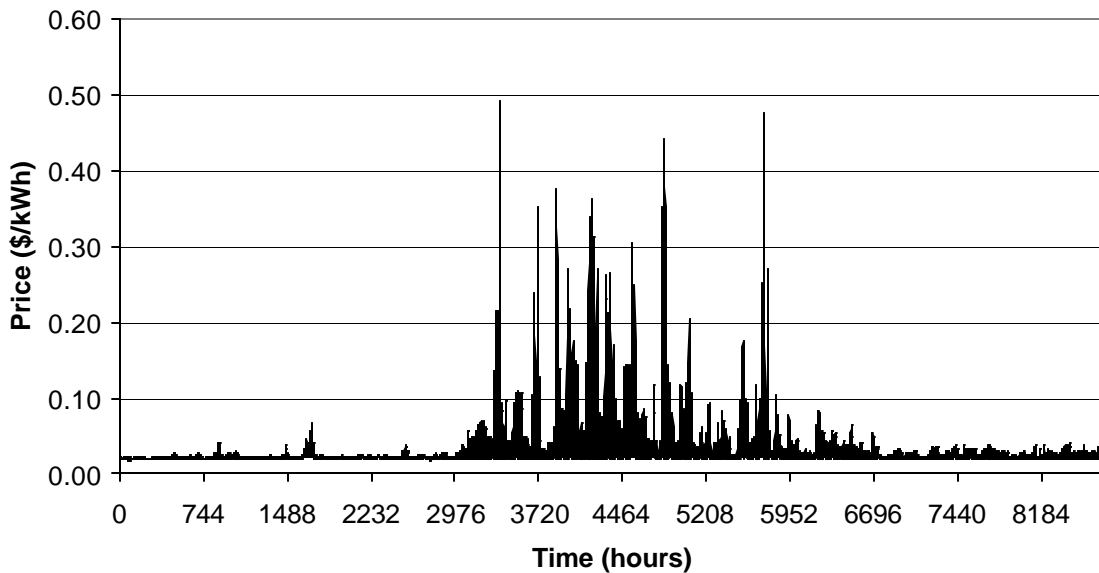
Figure 3.2: Southern Company pricing data for the entire 1998 calendar year

3.A.5   Floating Period Analysis

The full demand-shifting strategy for the purpose of this simulation has been evaluated with the floating window, or the on-peak period, centered around 4 P.M. The annual cost for the demand-shifting simulations, and therefore the annual savings, would depend on the time of the day around which the floating duration has been centered. The "daily price ratio" is defined as the ratio of energy costs during floating periods ("on-peak") to that during operating periods ("off-peak"). This section analyzes the daily price ratios for each month of the year, for two different cases:

- Floating period (on-peak) centered around 4 P.M., and operating period (off-peak) centered around 4 A.M.
- Floating period (on-peak) centered around 2 P.M., and operating period (off-peak) centered around 2 A.M.

The analysis has been done for each day of the month using the PG&E real-time pricing (RTP) structure, where the price of electricity changes every hour of the day. The daily price ratio is expressed as per Equation 3.1.

$$\text{Daily Price Ratio} = \frac{\sum_{i=1}^{\#hourson-peak} C_{on,i}}{\sum_{i=1}^{\#hoursoff-peak} C_{off,i}} \tag{3.1}$$

where, C_{on} and C_{off} denote the hourly electricity prices during the floating period (on-peak) and the operating period (off-peak), respectively, and are averaged over the number of hours, N, to get the daily price ratio for each day of the month. The "Average Ratio" is then defined as the average value of the daily price ratio for the month, and "Maximum Ratio" is defined as the maximum value of the daily price ratio during the month. Equation 3.2 and Equation 3.3, respectively, show the mathematical expressions for the average ratio and the maximum ratio, with D denoting the number of days in the month.

$$\text{Average Ratio} = \frac{\sum_{D}(Daily\ PriceRatio)}{D} \tag{3.2}$$

$$\text{Maximum Ratio} = Max(Daily\ PriceRatio)_{D} \tag{3.3}$$

Table 3.4 shows the average ratio and the maximum ratio for each month of the year for both the floating periods being analyzed for.

Month	Centered around 4 PM		Centered around 2 PM	
	Average ratio	Maximum ratio	Average ratio	Maximum ratio
January	1.20	1.66	1.18	1.51
February	1.27	1.95	1.23	1.67
March	1.24	1.79	1.19	1.59
April	1.31	1.59	1.27	1.58
May	2.78	5.48	2.56	4.47
June	5.67	36.79	4.94	27.81
July	5.49	17.74	5.04	17.48
August	3.24	11.91	3.01	10.61
September	2.31	8.23	2.15	8.03
October	1.66	2.14	1.63	2.04
November	1.42	3.05	1.30	2.23
December	1.64	3.25	1.47	2.58

Table 3.4: Daily price ratio for each month for different floating periods

Figure 3.3 and Figure 3.4 show a plot of the average ratio and the maximum ratio for each month, respectively.
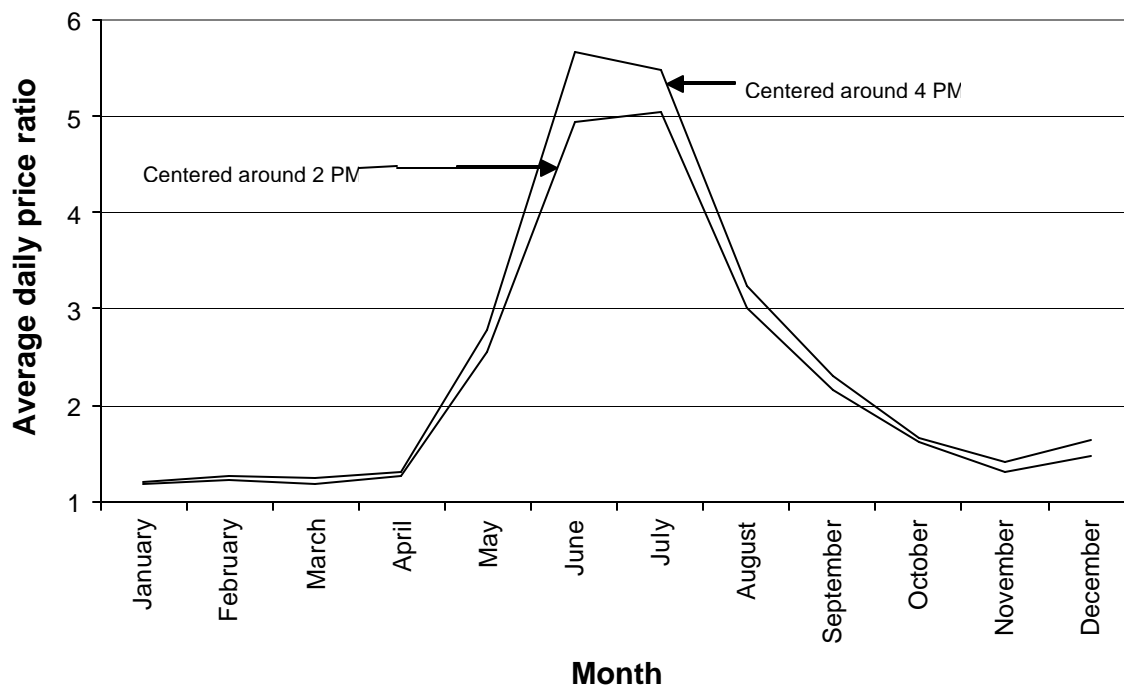
Figure 3.3: Average daily price ratio for each month
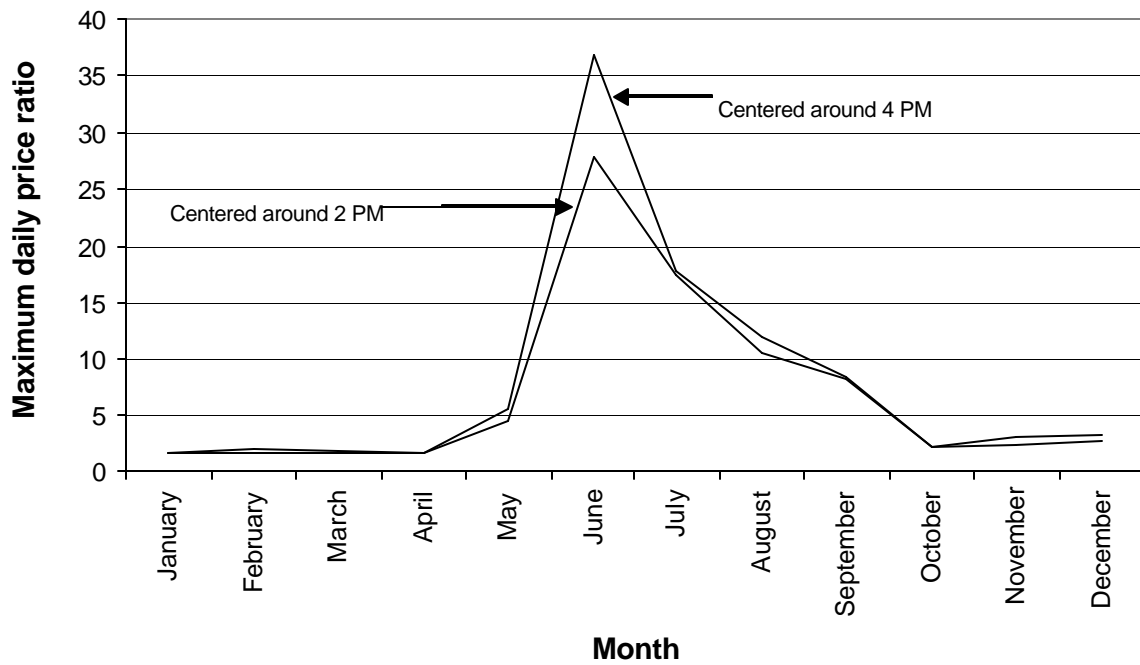
Figure 3.4: Maximum daily price ratio for each month

Figure 3.3 and Figure 3.4 both show that centering the floating period (on-peak) around 4 P.M. gives a greater value of daily price ratio for each month as compared with centering the floating duration around 2 P.M. The potential for maximum savings is in the case which has the higher daily price ratio, and therefore, the floating duration has been centered around 4 P.M. for this study.

3.B   Influence of Product Model Selection

This section is sub-divided into two sections depending on the product model that has been used for the analysis. The methodology used for the analysis is the same for both the first section, which treats the stored product as a lumped capacitance model, and the second section, which discretizes the block of stored product using a three-dimensional finite difference element approach.

The separate treatment for the two different product models is necessitated by the possibility of a difference in the thermal interaction between the stored product and the zone air depending on the model used, and also because of a different range of safe storage temperatures for the two products considered. Separate base cases have been developed for the two product models, and a separate analysis has been done for the demand-shifting strategy.

3.B.1 Lumped Capacitance Product Model

The analysis for the lumped capacitance model has been done assuming milk as the stored product in the warehouse. ASHRAE (1998) recommends a safe storage temperature for milk in the temperature range of 0.6 to 4.4 ^{o}C (33 to 40 ^{o}F). The simulation was run for the entire year using Madison TMY2 weather file. On the basis of the cooler wall construction, three base cases are discussed, and for each base case, sub-cases have been developed using the different electricity pricing structures previously discussed. In addition, varying zone set point temperatures was a parameter in the analysis.

The energy consumption and the costs thereof are for the operation of the cooler refrigeration equipment only. No analysis has been done for different dock wall constructions or the operation of the dock refrigeration equipment under RTP.

The annual integrated cooling load, annual electricity usage, and the annual energy costs under the different utility rate structures are the outputs reported for various base case simulations. Both the annual integrated cooling load and the electrical energy consumption increase as the U-value of the cooler wall is increased. This trend is attributable to the fact that with an increased conductance through the cooler walls, the heat transfer from the ambient into the refrigerated space (i.e. transmission loads) increases. Consequently, the refrigeration equipment has to operate more frequently to meet the higher cooling load and maintain the zone set point temperature. With a higher zone set point temperature,

however, the cooling load reduces irrespective of the wall U-value. Table 3.5 shows the values of the abovementioned variables for each base case simulation.

Base Case Results (no load shifting)							
Zone Set Point Temperature (C)	Wall U-value (W/m^2C)	Cooling Load (kWh)	Electrical Power (kWh)	Case I (Annual Ratio)	Case II ($)	Case III ($)	Case IV ($)
1.0	0.200	1,895,300	506,400	1.271	17,040	37,310	17,390
	0.223	1,917,300	512,800	1.272	17,260	37,780	17,710
	0.261	1,953,500	523,400	1.273	17,620	38,890	18,230
1.5	0.200	1,840,400	487,300	1.271	16,400	35,920	16,720
	0.223	1,860,500	493,100	1.273	16,600	36,380	17,010
	0.261	1,893,300	502,800	1.274	16,930	37,230	17,520
2.0	0.200	1,784,900	468,100	1.271	15,760	34,550	16,050
	0.223	1,802,000	473,000	1.272	15,930	34,990	16,330
	0.261	1,831,800	481,500	1.273	16,220	35,770	16,780
2.5	0.200	1,728,400	449,600	1.271	15,130	33,310	15,400
	0.223	1,742,500	453,400	1.272	15,260	33,530	15,650
	0.261	1,774,600	462,700	1.275	15,600	34,270	16,140
3.0	0.200	1,671,400	431,300	1.271	14,520	31,910	14,790
	0.223	1,684,700	434,700	1.271	14,620	32,290	15,010
	0.261	1,714,600	443,200	1.274	14,930	32,930	15,450
3.5	0.200	1,614,900	413,500	1.270	13,910	30,560	14,150
	0.223	1,627,800	416,800	1.273	14,040	31,010	14,380
	0.261	1,653,200	423,500	1.274	14,260	31,550	14,770
4.0	0.200	1,560,000	396,700	1.273	13,360	29,300	13,580
	0.223	1,570,800	399,100	1.273	13,430	29,630	13,760
	0.261	1,592,300	404,600	1.273	13,610	30,240	14,110

Table 3.5: Yearly base case simulations for product lumped capacitance model

The annual ratios in the column for "Case I" can be used to compute the annual cost for any cost structure based on Table 3.2, knowing the power consumption and the off-peak rate. Equation 3.4 expresses the relationship used to calculate the annual cost.

$$Total\cos t = Power consumption * Offpeak\cos t * Annual ratio \tag{3.4}$$

Figure 3.5 and Figure 3.6 show the annual integrated cooling load and electrical energy consumption results, respectively, for the base case simulations outlined in Table 3.5. Two variables are plotted on the X-axis: a) the zone set point temperature, which is the main division, and b) the wall U-value (W/m^{2}C), which is the sub-division for each set point temperature.
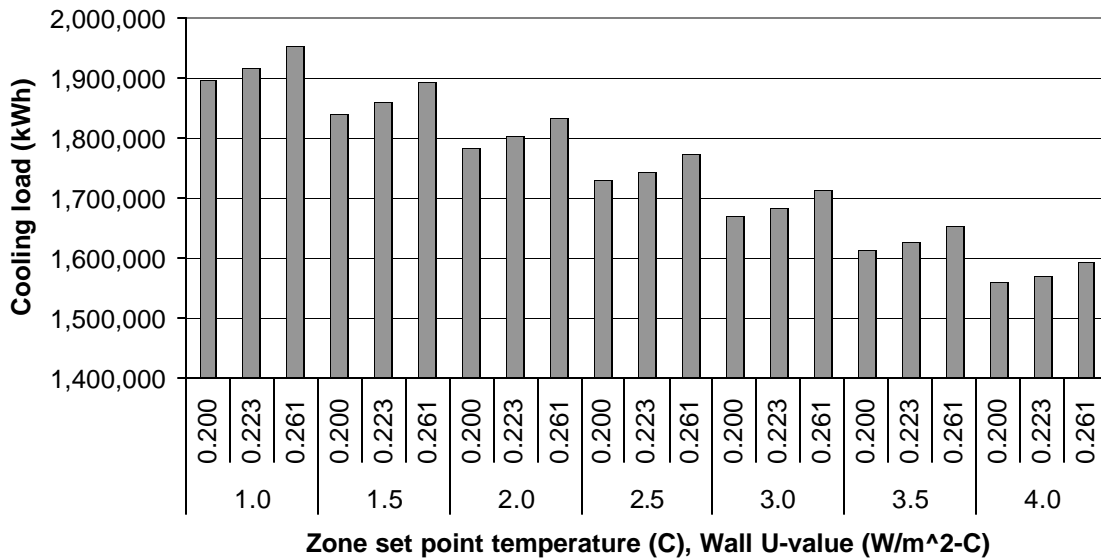
Figure 3.5: Annual base case cooling loads for various set point temperatures and wall constructions
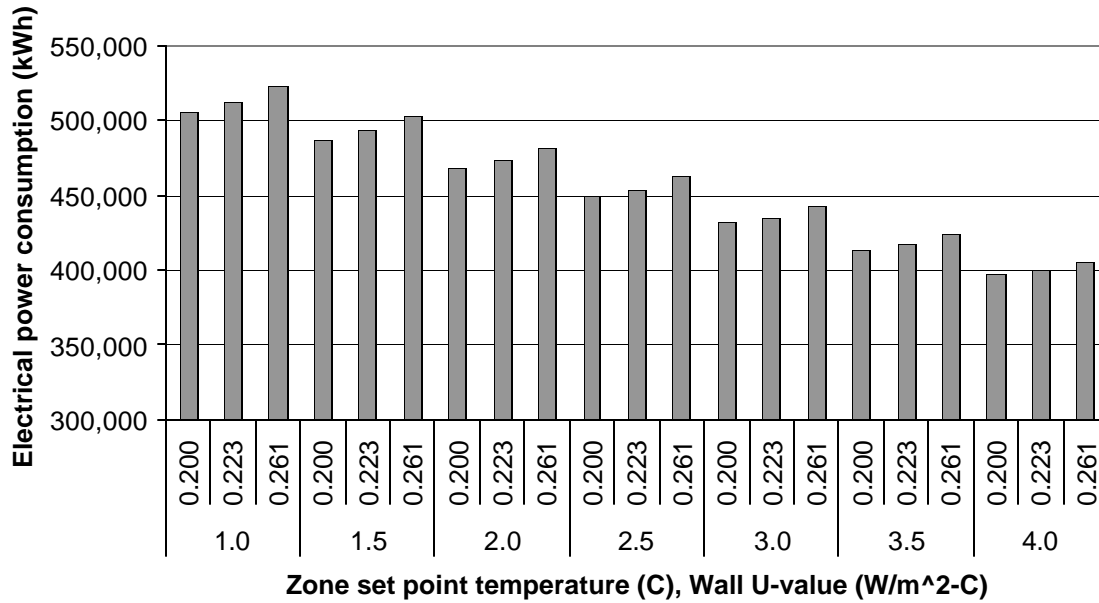
Figure 3.6: Annual base case electrical energy consumption for various zone set point temperatures and wall constructions

For each wall construction considered, varying the zone set point temperature leads to a different average temperature of the product over the entire year. For the seven different set point temperature values explored for each wall construction, the annual electricity cost is plotted as a function of the corresponding product average temperature. The points so obtained have been curve fitted in EES to obtain a linear function between the annual cost and the product average temperature. Figure 3.7, Figure 3.8, and Figure 3.9, respectively, show the Southern Company, PG&E Company, and MG&E annual cost (from Table 3.5) as a function of the product average temperature, for the three different wall constructions. Table 3.6 shows the curve fit functions obtained for the annual cost, along with the R^2 value for each curve fit.
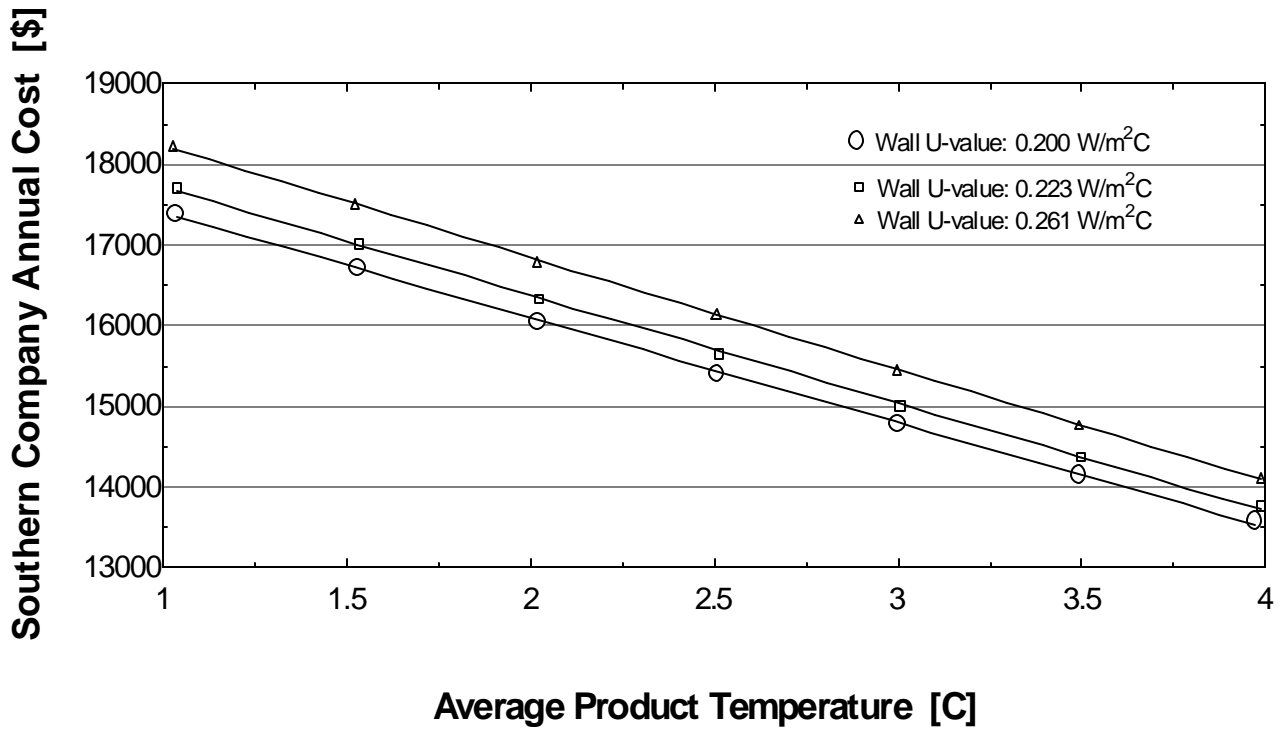
Figure 3.7: Southern Company base case annual cost as a function of product average temperature for different wall U-values
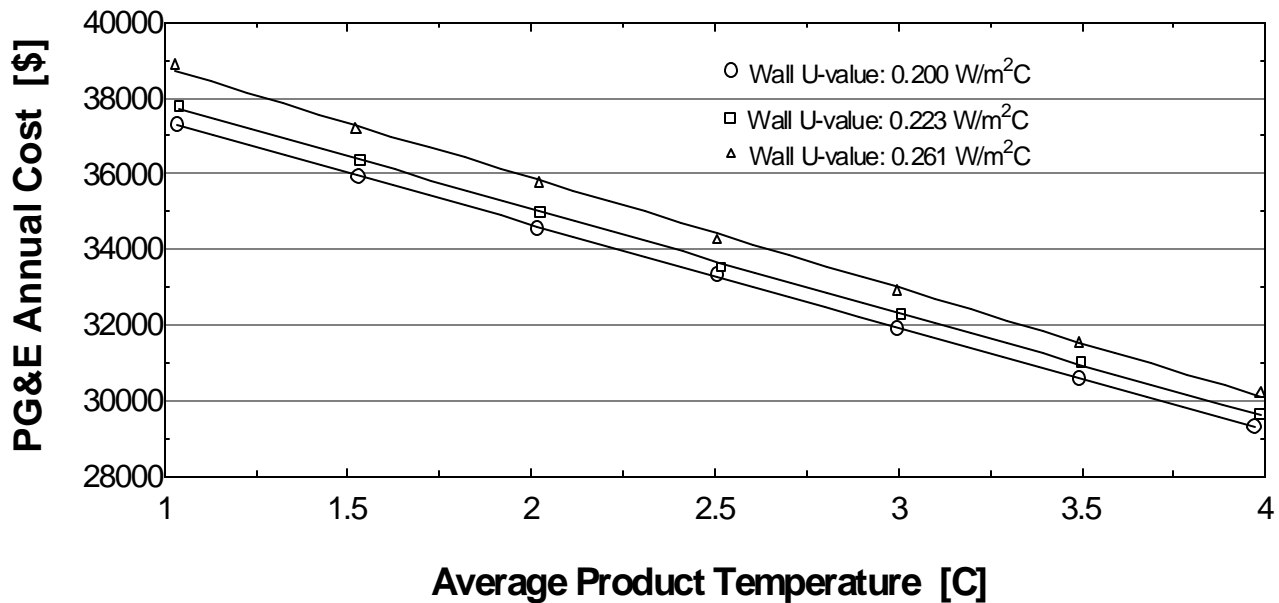
Figure 3.8: PG&E base case annual cost as a function of product average temperature for walls with different U-values
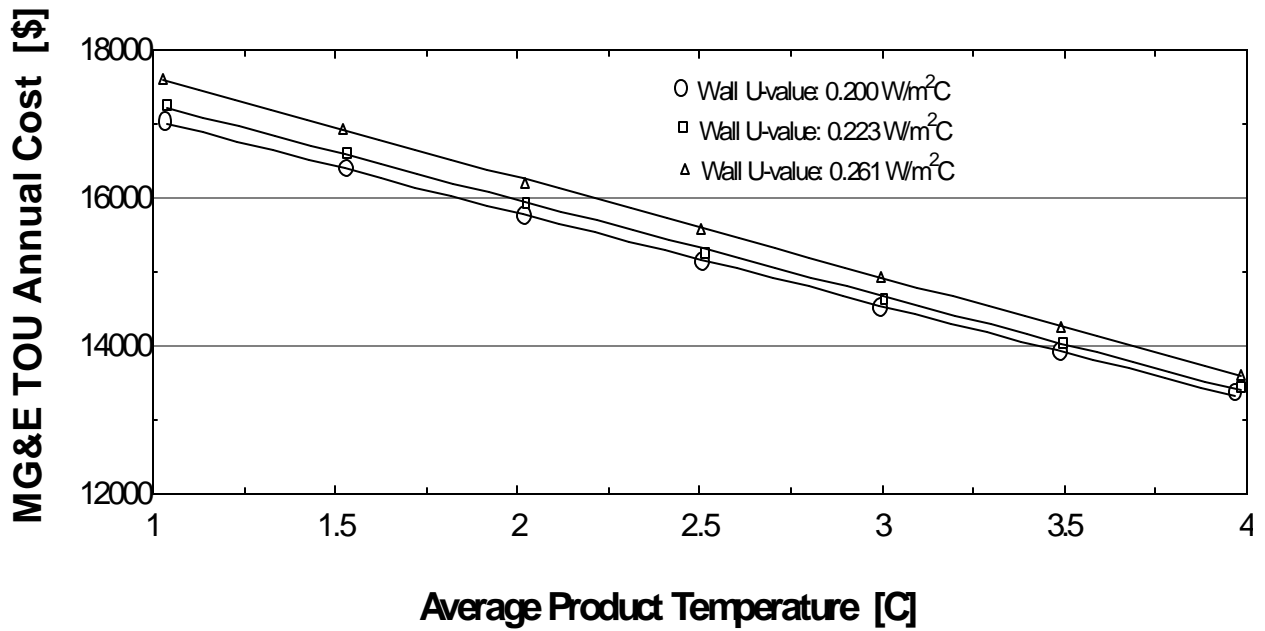
Figure 3.9: MG&E Time-of-Use base case annual cost as a function of product average temperature for walls with different U-values

Base Case Results (no load shifting)			
Wall U-value (W/m^2C)	RTP Structure	Annual Cost - Product Average Temperature Correlation	R^2 Value
0.200	Case II	Annual Cost = 18319.1 - 1260.22*$T_{product,avg}$	99.96%
	Case III	Annual Cost = 40107.8 - 2727.89*$T_{product,avg}$	99.99%
	Case IV	Annual Cost = 18704.6 - 1301.74*$T_{product,avg}$	99.95%
0.223	Case II	Annual Cost = 18578.2 - 1302.07*$T_{product,avg}$	99.94%
	Case III	Annual Cost = 40579.3 - 2753.42*$T_{product,avg}$	99.95%
	Case IV	Annual Cost = 19061.7 - 1340.89*$T_{product,avg}$	99.95%
0.261	Case II	Annual Cost = 18989.4 - 1354.3*$T_{product,avg}$	99.98%
	Case III	Annual Cost = 41710 - 2911.32*$T_{product,avg}$	99.87%
	Case IV	Annual Cost = 19625.7 - 1389.12*$T_{product,avg}$	99.98%

Table 3.6: Base case Annual cost-Product average temperature correlations

The correlations between the annual cost under different utility rate structures and the average product temperature shown in Table 3.6 have been developed using milk as the

stored produc t. In applying the correlations, therefore, it is important to recall that the safe temperature range for milk storage is from 0.6 to 4.4 ^{o}C (33 to 40 ^{o}F). Although, the correlations might correctly predict the cost of electricity consumption even outside this temperature range, the stored milk in the cooler would be spoiled if its temperature goes outside this temperature range at any time, and this cannot be allowed to happen.

Table 3.7 shows the annual integrated cooling load, annual electricity consumption, and the annual costs under different utility rate structures, for the full demand-shifting simulations.

Load Shifting Results							
Zone Set Point Temperature (C)	Wall U-value (W/m^2C)	Cooling Load (kWh)	Electrical Power (kWh)	Case I (Annual Ratio)	Case II ($)	Case III ($)	Case IV ($)
1.0	0.200	1,738,500	463,100	1.04	13,480	20,600	10,270
	0.223	1,757,200	468,200	1.04	13,630	20,750	10,390
	0.261	1,787,500	476,700	1.04	13,870	21,000	10,570
1.5	0.200	1,685,200	445,100	1.04	12,960	19,830	9,860
	0.223	1,702,200	449,700	1.04	13,090	19,960	9,970
	0.261	1,730,100	457,500	1.04	13,310	20,190	10,150
2.0	0.200	1,631,600	427,200	1.04	12,430	19,070	9,470
	0.223	1,647,800	431,500	1.04	12,560	19,180	9,560
	0.261	1,674,500	438,800	1.04	12,770	19,380	9,730
2.5	0.200	1,577,900	410,000	1.04	11,940	18,330	9,080
	0.223	1,593,100	413,900	1.04	12,050	18,430	9,180
	0.261	1,618,500	420,600	1.04	12,240	18,600	9,330
3.0	0.200	1,527,000	393,500	1.04	11,460	17,590	8,710
	0.223	1,540,800	397,100	1.04	11,560	17,690	8,800
	0.261	1,564,100	403,100	1.04	11,730	17,860	8,940
3.5	0.200	1,486,700	380,600	1.07	11,260	17,740	9,240
	0.223	1,501,000	384,400	1.07	11,410	18,320	9,610
	0.261	1,524,900	390,700	1.08	11,680	19,280	10,300
4.0	0.200	1,481,600	377,800	1.16	11,810	24,320	12,270
	0.223	1,494,400	381,300	1.16	11,960	24,930	12,590
	0.261	1,515,300	387,000	1.17	12,200	25,980	13,080

Table 3.7: Results for annual energy consumption and cost when load shifting, using lumped capacitance model for the stored product

Figure 3.10 and Figure 3.11 show the annual integrated cooling load and electrical energy consumption results, respectively, for the demand-shifting simulations outlined in Table 3.7. Two variables are plotted on the X-axis: a) the zone set point temperature, which is the main division, and b) the wall U-value, which is the sub-division for each set point temperature.
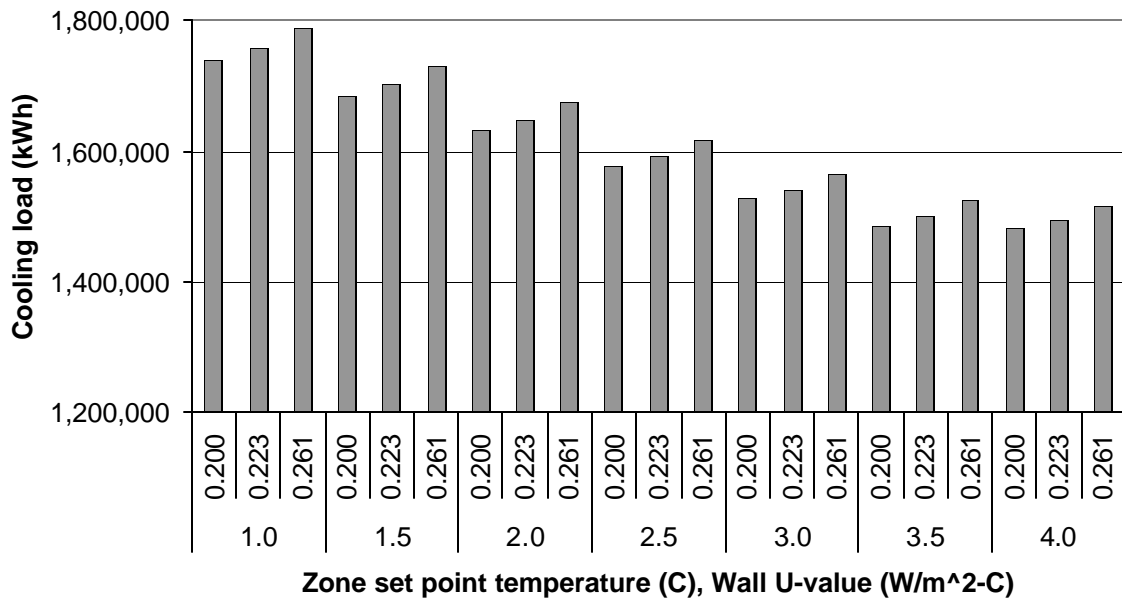
Figure 3.10: Annual integrated cooling loads while demand-shifting for various set point temperatures and wall construction
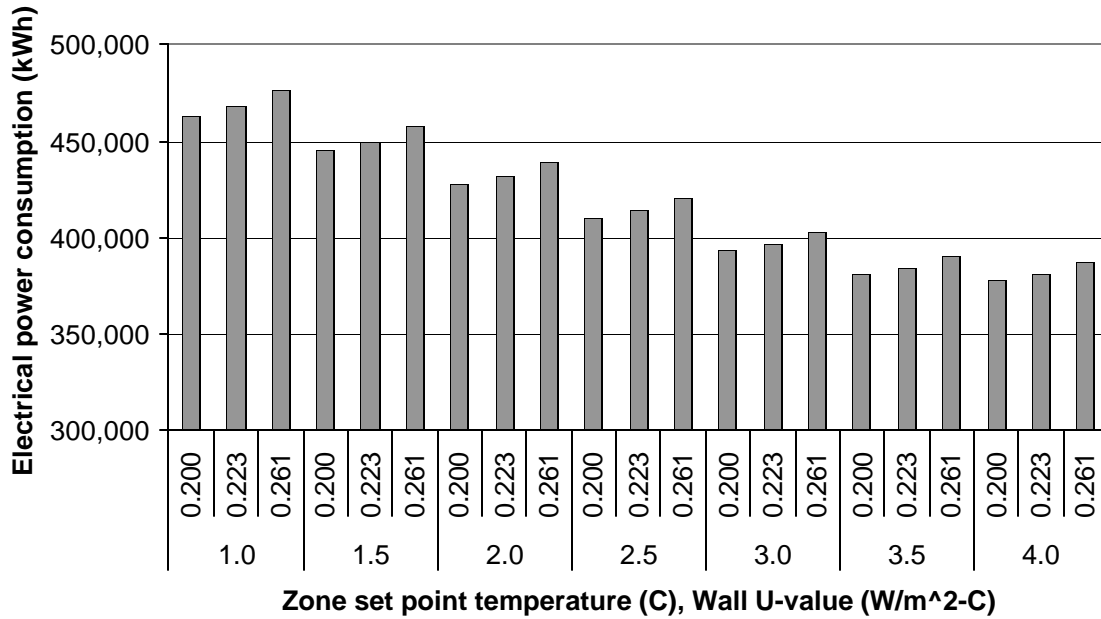
Figure 3.11: Annual electrical energy consumption while operating under demand-shifting for various zone set point temperatures and wall constructions

The annual savings between the demand-shifting and the base case, for each wall construction and zone set point temperature, have been obtained by subtracting each annual cost in Table 3.7 from the corresponding annual cost in Table 3.5. The annual savings are shown in Table 3.8.

Annual Savings				
Zone Set Point Temperature (C)	**Wall U-value (W/m^2C)**	**Savings**		
		Case II ($)	**Case III ($)**	**Case IV ($)**
1.0	0.200	3561	16717	7122
	0.223	3629	17027	7325
	0.261	3748	17886	7656
1.5	0.200	3445	16092	6856
	0.223	3511	16419	7037
	0.261	3619	17038	7370
2.0	0.200	3321	15480	6581
	0.223	3367	15802	6766
	0.261	3446	16387	7049
2.5	0.200	3193	14979	6317
	0.223	3214	15101	6475
	0.261	3352	15668	6812
3.0	0.200	3060	14312	6079
	0.223	3065	14595	6213
	0.261	3192	15071	6509
3.5	0.200	2653	12822	4907
	0.223	2622	12699	4769
	0.261	2584	12270	4472
4.0	0.200	1551	4985	1308
	0.223	1475	4697	1175
	0.261	1407	4256	1027

Table 3.8: Demand-shifting Annual savings for different wall constructions and zone set point temperatures

The annual savings ($), for the three cases shown in Table 3.8, have been plotted as a function of the zone set point temperature (C) and the wall U-value (W/m^{2}C). Regression analysis was performed to obtain second order polynomial representations for the annual savings as a function of the zone set point temperature, T_{set}, and the wall U-value, U_{value}. Equation 3.5 shows the resulting relations for the annual savings for each case. Table 3.9 shows the values of the regression coefficients. Table 3.10 shows the R^2-values for each curve-fit.

$$Savings = C_1 + C_2 * U_{value} + C_3 * U_{value}^2 + C_4 * T_{set} + C_5 * T_{set}^2 + C_6 * U_{value} * T_{set}$$

$$(3.5)$$

Savings	C_1	C_2	C_3	C_4	C_5	C_6
Case II	2.5317171E+03	- 3.027617E+03	1.8661407E+04	1.4039493E+03	- 3.259476E+02	- 1.700748E+03
Case III	5.8075786E+03	1.4810866E+04	4.0827657E+04	9.3711085E+03	- 2.064955E+03	- 1.046617E+04
Case IV	9.8439819E+02	1.2285810E+04	9.9031881E+03	4.8557025E+03	- 1.078392E+03	- 5.125521E+03

Table 3.9: Regression coefficients for annual savings polynomial representations

Cases	R^2 value
Case II: MG&E	94.51%
Case III: PG&E	90.11%
Case IV: Southern	92.91%

Table 3.10: R^2 values for the curve fit for savings in different cases

3.B.1.1 Effect of average product temperature on percentage savings

The investigation for the base case and the demand-shifting case has been done for various set point temperatures for the cooler. Each set point temperature leads to a different average temperature of the product, T_{avg}, over the entire year's simulation, and also a different value for the annual savings. In order to analyze the effect of T_{avg} on the annual savings, it is important to express the annual cost, for both the base cases and demand-shifting cases, as a function of T_{avg}, and compare the savings for different values of the average temperature.

Equation 3.6 and Equation 3.7 express the PG&E annual cost for the base case and demand-shifting case, respectively, as a function of the average product temperature for a wall with U-value of 0.261 W/m²C.

$$Annual\ \cos t = 41710 - 2911.32 * T_{avg} \qquad \underline{\text{Base Case (No load shifting)}} \quad (3.6)$$

$$Annual\ \cos t = 24266.7 - 1669.24 * T_{avg} \qquad \underline{\text{Load Shifting}} \qquad (3.7)$$

Table 3.11 shows the annual costs, yearly savings, and the percentage savings for different product average temperatures.

T_{avg} (C)	Base Cost ($)	Demand-Shifting Cost ($)	Savings ($)	Percentage Savings (%)
1.5	37343.02	21762.84	15580.18	41.72
2.0	35887.36	20928.22	14959.14	41.68
2.5	34431.70	20093.60	14338.10	41.64
3.0	32976.04	19258.98	13717.06	41.60

Table 3.11: PG&E percentage savings as a function T_{avg} for wall U-value 0.261 W/m²C

The percentage savings for different product average temperatures differ only slightly, even though the annual costs for different average temperatures are quite different. It can, therefore, be stated that the percentage savings between the base case and the full demand-shifting case are irrespective of the average product temperature.

Equation 3.8 and Equation 3.9 express the MG&E annual cost for the base case and demand-shifting case, respectively, as a function of the average product temperature for a wall with U-value of 0.261 W/m²C. Table 3.12 presents a similar analysis as Table 3.11 for the MG&E Time-of-Use prices.

$$Annual \cos t = 18989.4 - 1354.3 * T_{avg} \qquad \underline{\text{Base Case (No load shifting)}} \quad (3.8)$$

$$Annual \cos t = 16092.6 - 1135.86 * T_{avg} \qquad \underline{\text{Load Shifting}} \qquad (3.9)$$

T_{avg} (C)	Base Cost ($)	Demand-Shifting Cost ($)	Savings ($)	Percentage Savings (%)
1.5	16957.95	14388.81	2569.14	15.15
2.0	16280.80	13820.88	2459.92	15.11
2.5	15603.65	13252.95	2350.70	15.07
3.0	14926.50	12685.02	2241.48	15.02

Table 3.12: MG&E percentage savings as a function T_{avg} for wall U-value 0.261 W/m^{2}C

3.B.1.2 Effect of wall U-value on percentage savings

The previous section analyzed the effect of average product temperature on the percentage savings, and concluded that the effect is negligible. This section analyzes the effect of the wall U-value on the percentage savings. Table 3.11 and Table 3.12 show the PG&E and MG&E percentage savings, respectively, for a wall with U-value 0.261 W/m^{2}C. Following the same analysis strategy as in the previous section, Table 3.13 has been developed for the PG&E percentage savings, as a function of average product temperatures, for a wall with U-value 0.200 W/m^{2}C. Equation 3.10 and Equation 3.11, respectively, show the PG&E annual base case and demand-shifting cost for the wall U-value in consideration.

$$Annual \cos t = 40107.8 - 2727.89 * T_{avg} \qquad \underline{\text{Base Case (No load shifting)}} \quad (3.10)$$

$$Annual \cos t = 23741.6 - 1603.4 * T_{avg} \qquad \underline{\text{Load Shifting}} \qquad (3.11)$$

T_{avg} (C)	Base Cost ($)	Demand-Shifting Cost ($)	Savings ($)	Percentage Savings (%)
1.5	36015.97	21336.5	14679.47	40.76
2.0	34652.02	20534.8	14117.22	40.74
2.5	33288.08	19733.1	13554.98	40.72
3.0	31924.13	18931.4	12992.73	40.70

Table 3.13: PG&E percentage savings as a function T_{avg} for wall U-value 0.200 W/m^{2}C

Table 3.11 and Table 3.13 both show the PG&E percentage savings for two different wall constructions. Comparing the values in both the tables, it can be stated that the difference in percentage savings for two different wall constructions is negligibly small. Table 3.14 shows the same analysis as Table 3.13, for the MG&E Time-of-Use prices. Equation 3.12 and Equation 3.13, respectively, show the MG&E annual base case and demand-shifting cost for the wall U-value in consideration.

$$Annual \cos t = 18319.1 - 1260.22 * T_{avg} \qquad \underline{\text{Base Case (No load shifting)}} \quad (3.12)$$

$$Annual \cos t = 15597.5 - 1082.65 * T_{avg} \qquad \underline{\text{Load Shifting}} \qquad (3.13)$$

T_{avg} (C)	Base Cost ($)	Demand-Shifting Cost ($)	Savings ($)	Percentage Savings (%)
1.5	16428.77	13973.53	2455.25	14.94
2.0	15798.66	13432.20	2366.46	14.98
2.5	15168.55	12890.88	2277.68	15.01
3.0	14538.44	12349.55	2188.89	15.06

Table 3.14: MG&E percentage savings as a function T_{avg} for wall U-value 0.200 W/m^{2}C

Table 3.12 and Table 3.14 both show the MG&E percentage savings for two different wall constructions. Comparing the values in both the tables, it can be stated that the difference in percentage savings for two different wall constructions is negligibly small, and this reinforces the conclusion obtained from comparing Table 3.11 and Table 3.13.

3.B.2   Three-dimensional Finite Difference Product Model

The analysis for the three-dimensional finite difference model has been done assuming cheddar cheese as the stored product in the warehouse. ASHRAE (1998) recommends an ideal temperature range of storage for cheddar cheese between -1 and 1 ^{o}C (30 and 34 ^{o}F), although the maximum allowable temperature is 15 ^{o}C (59 ^{o}F). The simulation was run for the entire year using Madison TMY2 weather file.

Since it has been shown in Section 3.B.1.2 that the effect of the wall U-value on percentage savings is small, only one type of wall construction has been analyzed for the three-dimensional finite difference product model. The U-value of the cooler wall considered is 0.200 W/m^{2}C. The product block nodal matrix has been fixed at 20*20*20 nodes. No analysis has been done for different dock wall constructions or the operation of the dock refrigeration equipment under RTP.

The simulations were run for different values of the zone set point temperatures in order to obtain a plot of the annual cooling load, electricity consumption and annual cost as a function of the product average temperature. These plots were then curve-fit to obtain annual cost as a function of the product average temperature. The polynomial representation of the annual cost as a function of the average product temperature has been used to determine the annual savings ($) and the percentage savings accruing as a result of following the demand-shifting strategy.

Table 3.15 shows the annual cooling load, annual electricity demand, and the annual costs under different RTP structures, for various base case simulations.

Base Case (no load shifting)						
Zone Set Point Temperature (C)	Cooling Load (kWh)	Electrical Power (kWh)	Case I (ratio)	Case II ($)	Case III ($)	Case IV ($)
-1.00	2,345,400	643,400	1.274	21,690	47,210	22,050
1.00	2,092,000	553,900	1.272	18,650	40,740	19,020
3.00	1,837,400	470,200	1.271	15,820	34,670	16,170
5.00	1,591,600	395,700	1.273	13,320	29,200	13,640

Table 3.15: Yearly base case simulations for 3-D finite difference product model

Figure 3.12 and Figure 3.13 show the annual integrated cooling load and electrical energy consumption results, respectively, for the base case simulations outlined in Table 3.15, using the three-dimensional finite difference model for the stored product.
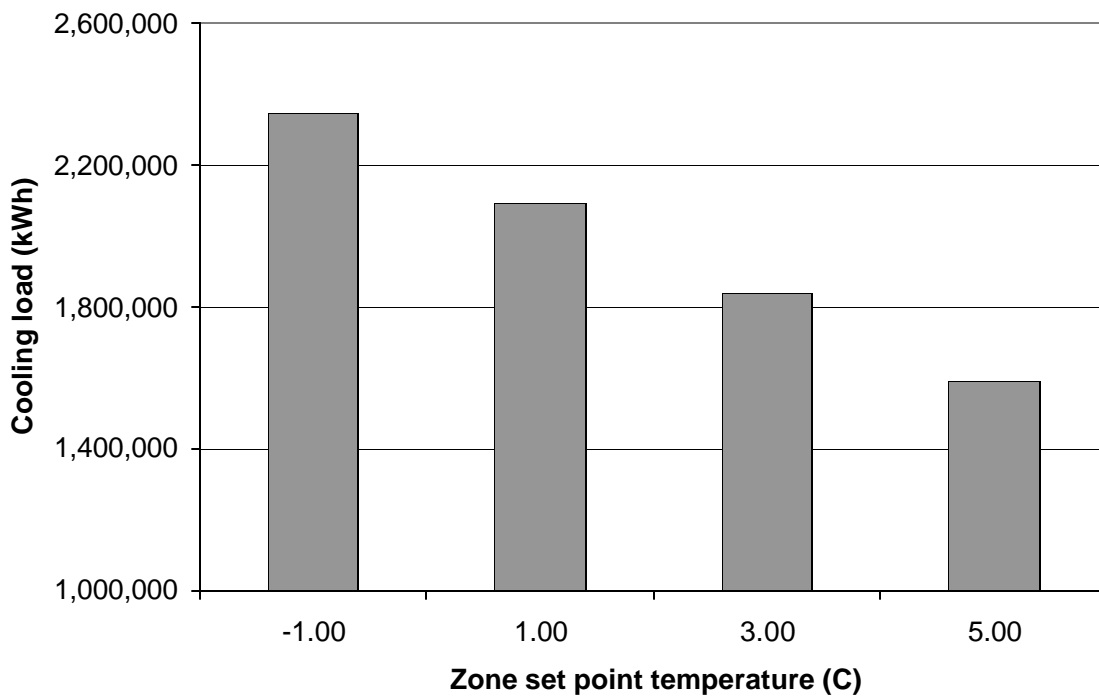
Figure 3.12: Annual base case cooling loads for various zone set point temperatures
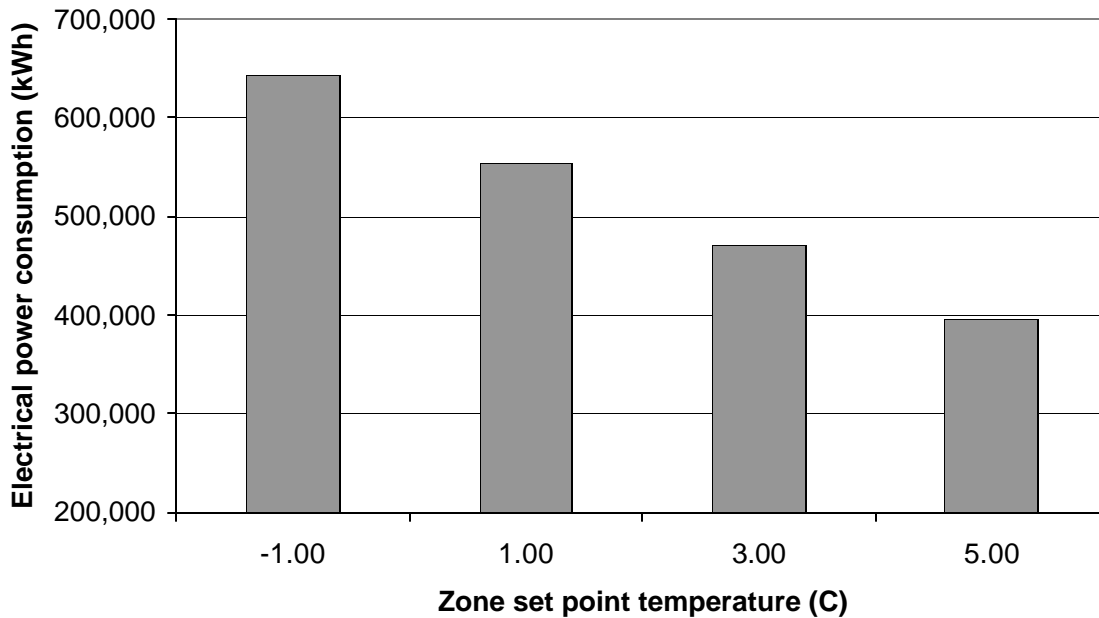
Figure 3.13: Annual base case electrical energy consumption for various zone set point temperatures

The annual costs for various RTP structures shown in Table 3.15 have been plotted against the average product temperature, and the curve-fit of the data points expressing the annual cost as a function of the average product temperature, along with the R^2 values, is shown in Table 3.16.

Base Case Results (no load shifting)		R^2
RTP Structure	**Annual Cost - Product Average Temperature Correlation**	**Value**
Case II: MG&E	Annual Cost = 20199.6 - 1430.48*$T_{product,avg}$	99.81%
Case III: PG&E	Annual Cost = 44044.3 - 3080.09*$T_{product,avg}$	99.86%
Case IV: Southern	Annual Cost = 20566.4 - 1438.6*$T_{product,avg}$	99.84%

Table 3.16: Base case Annual cost-Product average temperature correlations

Table 3.17 shows the annual integrated cooling load, annual electricity consumption, and the annual costs under different utility rate structures, for the full demand-shifting simulations. The simulations were done for different zone pre-cooling set point temperatures with a wall U-value of 0.200 W/m²C. The floating duration was 12 hours, centered around 4 P.M., and the maximum and minimum allowable product corner temperatures were fixed at 10 °C (50 °F) and –1 °C (30 °F), respectively.

Load Shifting Results						
Zone Set Point Temperature (C)	Cooling Load (kWh)	Electrical Power (kWh)	Case I (ratio)	Case II ($)	Case III ($)	Case IV ($)
-1.00	2,383,300	652,400	1.031	17,310	28,850	14,400
1.00	2,118,400	560,300	1.032	14,970	24,800	12,420
3.00	1,865,200	477,100	1.033	12,700	21,180	10,620
5.00	1,621,100	401,700	1.034	10,450	17,730	8,930

Table 3.17: Results for annual energy consumption and cost when load shifting, using three-dimensional finite difference model for the stored product

Figure 3.14 and Figure 3.15 show the annual integrated cooling load and electrical energy consumption results, respectively, for the full demand-shifting simulations outlined in Table 3.17. As the zone set point temperature is increased, both the annual cooling load and the electrical energy consumption decrease as is shown in their respective plots.
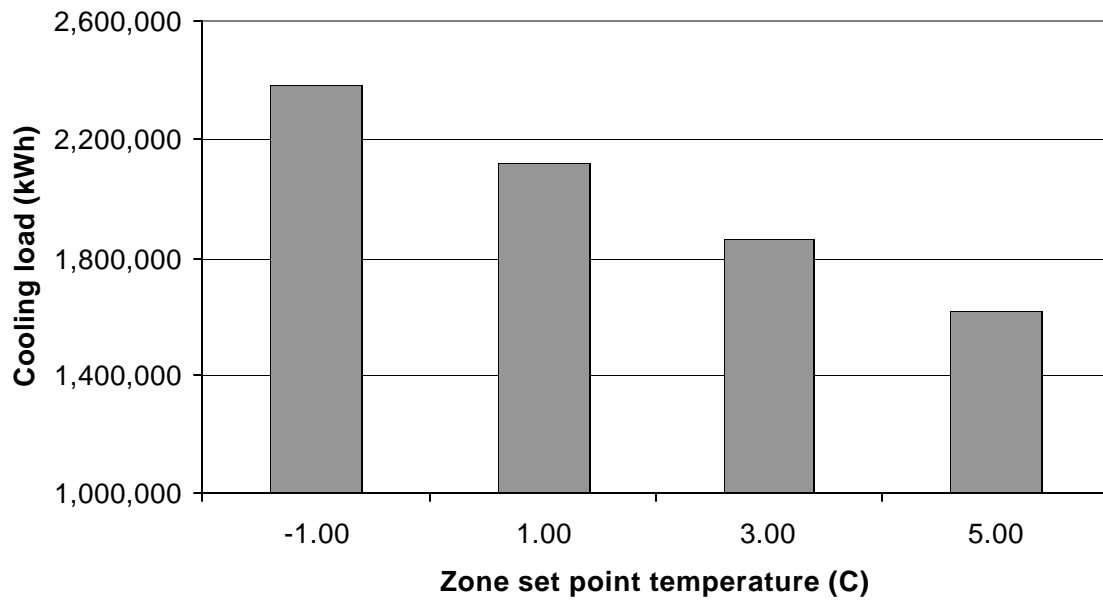
Figure 3.14: Annual integrated cooling loads while demand-shifting for various zone set point temperatures for the three-dimensional finite difference product model
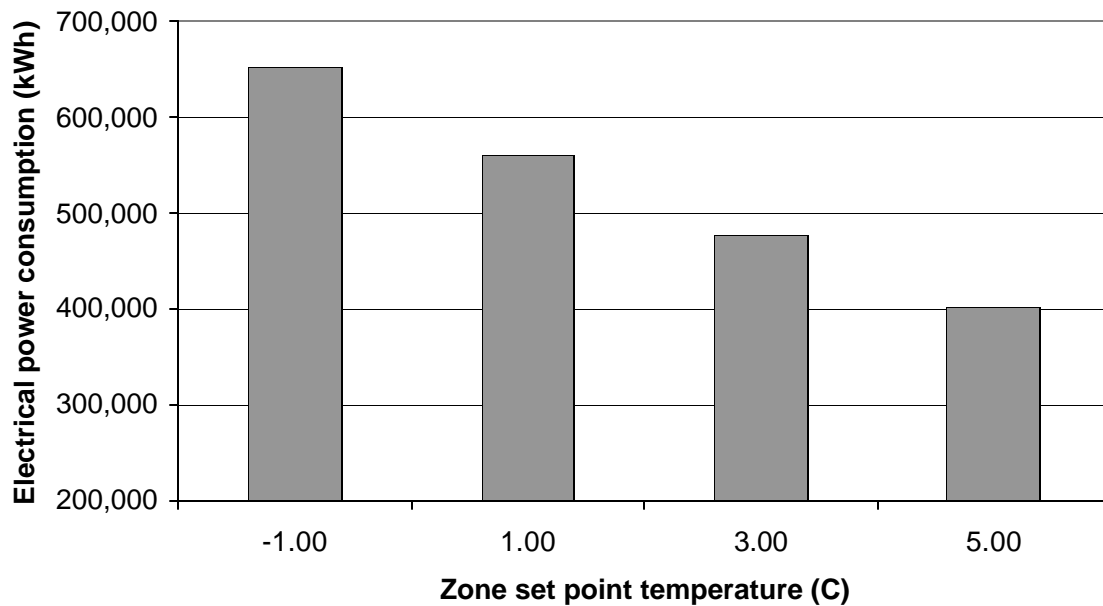
Figure 3.15: Annual electrical energy consumption while demand-shifting for various zone set point temperatures for the three-dimensional finite difference product model

Load Shifting Results		
RTP Structure	Annual Cost - Product Average Temperature Correlation	R^2 Value
Case II: MG&E	Annual Cost = $18223.4 - 1289.04 * T_{product,avg}$	99.88%
Case III: PG&E	Annual Cost = $30202.5 - 2085.92 * T_{product,avg}$	99.92%
Case IV: Southern	Annual Cost = $15075.1 - 1028.3 * T_{product,avg}$	99.93%

Table 3.18: Demand-shifting Annual cost-Product average temperature correlations

The same values of the zone set point temperatures have been used for both the base case simulations and the demand-shifting simulations. Due to a continuous operation of the refrigeration system in the base case simulations, the average product temperature over the entire year is quite close to the set point temperature. However, for the demand-shifting simulations, the average product temperature over the entire year is much higher than the zone pre-cooling set point temperature. Therefore, any comparison in the savings between the demand-shifting case and the base case, for the same value of zone set point temperature, would be inflated on account of a higher average product temperature in the demand-shifting case.

The savings, expressed as a function of the average product temperature, have been obtained by subtracting the annual cost under each individual RTP structure for the demand-shifting case (Table 3.18) from the corresponding annual cost for the base case (Table 3.16). The polynomial expressions are shown in Table 3.19.

Annual Saving	
RTP Structure	Annual Saving - Product Average Temperature Correlation
Case II: MG&E	Annual Saving = 1976.2 – 141.44*$T_{product,avg}$
Case III: PG&E	Annual Saving = 13841.8 - 994.17*$T_{product,avg}$
Case IV: Southern	Annual Saving = 5491.3 - 410.3*$T_{product,avg}$

Table 3.19: Annual saving – product average temperature correlation

Using the results of the simulations for the lumped capacitance product model, it was shown in Section 3.B.1.1 that the percentage savings under any RTP cost structure do not vary significantly with the average product temperature. Using the same analysis approach as in Section 3.B.1.1, Table 3.20 shows the percentage savings for various cases, using the results of the simulations for the three-dimensional finite difference product model.

RTP Structure	$T_{avg,product}$ (C)	Base Cost ($)	Demand Shifting Cost ($)	Savings ($)	Percentage Savings (%)
	1.00	18,770	16,930	1,840	9.80
Case II: MG&E	3.00	15,910	14,370	1,540	9.68
	5.00	13,050	11,790	1,260	9.66
	1.00	40,960	28,120	12,840	31.35
Case III: PG&E	3.00	34,800	23,940	10,860	31.21
	5.00	28,640	19,770	8,870	30.97
	1.00	19,130	14,050	5,080	26.56
Case IV: Southern	3.00	16,250	11,990	4,260	26.22
	5.00	13,370	9,930	3,440	25.73

Table 3.20: Percentage savings for different RTP structures, using the three-dimensional finite difference product model

For each individual RTP structure shown in Table 3.20, though the percentage savings are different for a different value of the average product temperature, the variance is still negligibly small. It can, hence, be stated that the average product temperature does not have a huge effect on the percentage savings even for the three-dimensional finite difference model of the stored product. However, this conclusion is valid only within the safe temperature range of storage that has been investigated for cheddar cheese, and no extrapolation of these results would be applicable outside this temperature range.

3.B.2.1 Break Even Cost Analysis

The economic analysis to calculate the break even cost ratio is performed to establish the viability of cost-effectively demand-shifting refrigeration loads. The analysis considers the annual operating costs for a range of "daily price ratios" where the "daily price ratio" represents the ratio of energy costs during floating periods ("on-peak") to that during operating periods ("off-peak"). For the purpose of this analysis, the "daily price ratio" is a constant value throughout the year. The aim of the analysis is to find the daily price ratio at which following the demand-shifting strategy would yield zero savings as compared to a base case strategy of meeting loads directly as they occur. This "critical daily price ratio" then represents a simple measure to guide daily operation so energy cost savings can be realized.

In cases where the actual ratio of average energy costs during the floating period (on-peak) to average energy costs during the operating period (off-peak) is greater than the break-even or critical cost ratio, there would be positive savings in following the demand-shifting operation strategy. In cases where the actual daily price ratio is less than the break even cost ratio, following the demand-shifting strategy would be more expensive than the base case operation strategy.

Four different cases were analyzed for the daily price ratios, ranging from 1.0 to 3.0. Annual simulations are run both for the base case and the demand-shifting case to calculate

the annual operating costs for each daily price ratio. The four different daily price ratios considered are shown in Table 3.21.

Cases	Daily Price Ratio
Case I	1.0
Case II	2.0
Case III	2.5
Case IV	3.0

Table 3.21: Daily price ratios considered for break even analysis

The results for the base case and demand-shifting simulations are shown for an average product temperature of 3 $^{\circ}$C (37 $^{\circ}$F). The ratio between the annual cost for the demand-shifting strategy and the base case strategy have been determined for each daily price ratio shown in Table 3.21, and is referred to as the "Annual Cost Ratio". The annual cost ratios were then plotted against their corresponding daily price ratio, and curve fit to identify the break-even or critical daily price ratio.
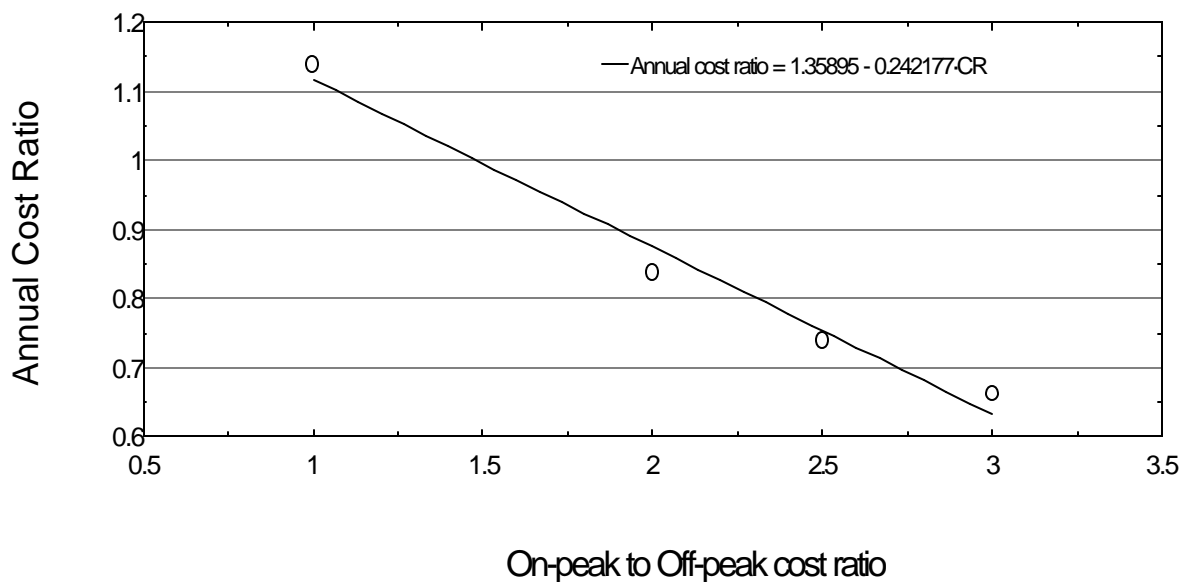
Figure 3.16: Annual cost ratio plotted against daily price ratio

Equation 3.14 expresses the annual cost ratio as a function of the daily price ratio.

Annual Cost Ratio = 1.35895 – 0.242177∗Daily Price Ratio (3.14)

For a break even annual operating cost, the annual cost ratio would be equal to 1.0, as expressed in Equation 3.15.

$$AnnualCostRatio = \frac{(AnnualCost)_{Demandshifting}}{(AnnualCost)_{BaseCase}} = 1.0$$
(3.15)

Solving Equation 3.14 and Equation 3.15 simultaneously, gives a value of 1.48 for the break even daily price ratio, or the "critical price ratio" above which yields operating cost savings and below which nets an operating cost penalty. The critical price ratio of 1.48 in the present analysis is lower than the critical price ratio of 2.2 identified by Stoeckle (2001). The reason for the more favorable critical price ratio in the present analysis is due to the higher operating temperature conditions in the warehouse. As the refrigeration equipment operates at considerably higher suction temperatures to meet the cooling loads, the operating penalty for pre-cooling is not as severe as that in the case of freezers.

3.C   References

American Society of Heating, Refrigerating, and Air-Conditioning Engineers (ASHRAE) (1998), 1998 ASHRAE Handbook – Refrigeration.

Madison Gas & Electric Company (MGE, 2001). Commercial and Industrial Lighting and Power Time-of-Use Rate.
Website: http://www.mge.com/images/PDF/Brochures/ElectricRates/E19.pdf

Madison Gas & Electric Company (MGE, 2001). Oscar Mayer Foods Corporation Time-of-Use Rate.

98

Website: http://www.mge.com/images/PDF/Brochures/ElectricRates/E28.pdf

Stoeckle, R. (2001). Refrigerated Warehouse Operation Under Real-Time Pricing. Solar Energy Laboratory. Madison, WI, University of Wisconsin – Madison.

CHAPTER 4   CONCLUSIONS

4.A   Summary of the Study

The focus of this study has been to model a representative product storage warehouse, where the optimum storage of the food products is above the freezing point. The base case operation in such a warehouse is with the refrigeration equipment operating when required to maintain a constant value of the zone set point temperature throughout the year. The full demand-shifting strategy, which involves pre-cooling the warehouse to a lower temperature during low electricity price periods, and shutting-off the refrigeration equipment during high electricity price periods, has been evaluated against the base case simulations.

Annual operating costs for both operation strategies have been calculated under different utility pricing structures. Different zone set point temperature values have been used to get a curve fit of the annual cost as a function of the product average temperature, for both the base case and demand-shifting strategies. All economic comparisons between the base case and the demand-shifting cases have been done for the same value of product average temperature.

4.A.1   Warehouse Wall Construction

Three different warehouse wall constructions have been analyzed for, each having a different conductance, or U-value. The wall conductance has a major impact on the transmission loads, and therefore, on the warehouse cooling load requirement and also the temperature in the warehouse. The annual integrated cooling load for a warehouse having walls with a high conductance is higher than a warehouse having low conductance walls. As a result, a warehouse with high conductance walls has a higher annual energy bill as compared with a warehouse with low conductance walls. These conclusions hold for both the base case and the demand-shifting cases. However, it has been proved in Section

100

3.B.1.2 that although the actual dollar value of savings would depend on the wall U-value, the percentage savings have almost a negligible variation with the wall U-value.

4.A.2   Product Model Influence

The stored product modeling has been done following two different approaches, the lumped capacitance approach, and a three-dimensional finite difference approach. The former approach assumes an infinite conductance value for the stored product leading to a uniform temperature throughout the entire product. Such an approach is useful for modeling stored fluid products such as milk and juices. The second approach divides the product block into nodes in all three spatial directions and allows heat conduction within the product. The product block in such a model does not have a uniform temperature but a spatial varying temperature at each node in the product block. Such an approach is useful for modeling solid food products, like cheddar cheese.

It is observed that modeling the stored product as a three-dimensional finite difference element leads to a higher annual integrated cooling load for the warehouse as compared with modeling the stored product using the lumped capacitance approach. Consequently, the annual energy bill of the warehouse is higher when the product is modeled as a finite difference element than when the modeling is done assuming the product as a lumped capacitance. These conclusions are valid irrespective of the refrigerating equipment operation strategy followed in the warehouse.

The average product temperature has a major impact on annual integrated load, electric power consumption, and the annual operating cost. A higher value of the average storage temperature of the product leads to a reduced value for the annual integrated cooling load, electric power consumption, and annual cost, for the base cases as well as the demand-shifting cases. It is also observed that the actual dollar value of the savings reduces as the average product temperature is increased. However, it has been established in Section 3.B.1.1 that although the average storage temperature of the product has an effect on the actual dollar value of savings, the effect of the same on percentage savings is negligible.

4.A.3   Utility Pricing Structures

The analysis of the present study has been done for the full demand-shifting scenario, which means that the equipment shut-off, or "floating", duration is for 12 hours every day, and centered around 4 P.M. The refrigeration equipment operates continuously during the pre-cooling duration to maintain the zone set-point temperature, and is operated during the floating duration only if the product temperature exceeds the maximum allowable temperature for safe storage. Different utility pricing structures lead to a different level of savings and a different value for the percentage savings, depending on the ratio of the daily electricity prices during floating (on-peak) and operating (off-peak) periods. The greater the daily price ratio, the greater the savings in following the demand-shifting strategy. However, although a higher value of the daily price ratio would lead to a higher percentage savings, the actual dollar value of savings would be determined by the actual electric rates during floating and operating periods. A higher value of percentage savings does not necessarily imply a substantial benefit in following the demand-shifting strategy unless the actual dollar value of savings is also high.

4.B   Conclusions of the Study

From the various options explored and the simulations carried out, several conclusions have been formulated for the warehouse and product models considered as a part of this study.

- Full demand-shifting during the high cost periods is possible if the pre-cooling set-point temperature in the zone is sufficiently less than the maximum allowable temperature for the safe storage of the product. For the lumped capacitance model of milk as the stored product having an optimum storage temperature between 0.6 ^{o}C (33 ^{o}F) and 4.4 ^{o}C (40 ^{o}F), full demand-shifting is possible only if pre-cooling set-point temperature is less than 3 ^{o}C (37 ^{o}F). For the three-dimensional finite difference model of cheddar cheese as the stored product having a minimum

storage temperature of -1 $^\circ$C (30 $^\circ$F) and a maximum storage temperature of 10 $^\circ$C (50 $^\circ$F), full demand-shifting is possible only if pre-cooling set-point temperature is less than 5 $^\circ$C (41 $^\circ$F).

- The warehouse wall conductance, or U-value, does influence the annual integrated cooling load and the annual energy bill of the warehouse, for both the base case and demand-shifting strategy. Operating cost savings are possible for all three values of wall conductance considered in this study. The maximum percentage savings occurs with walls having the maximum U-value.

- The average temperature at which the product is stored in the warehouse has an effect on the cooling load and on the energy bill. A higher storage temperature translates into a lower annual energy bill for both the base case and the demand-shifting cases. A higher average product temperature has a negligible effect on the percentage savings in following the demand-shifting strategy, but reduces the actual dollar value of savings.

- The utility's pricing structure is directly responsible for determining the energy bill for the warehouse. The utility offering the maximum difference between the rates during floating and operating periods also offers the potential for maximum savings in following the full demand-shifting strategy. To evaluate the monetary benefit of operating under the demand-shifting strategy, it is necessary to consider the dollar value of the difference between the electricity prices during floating and operating periods offered by the utility.

- Two-part pricing structures, like those offered by MG&E, do not offer substantial benefits in following the demand-shifting strategy, as the actual dollars saved is meager in spite of the daily price ratio being 1.5. Under the MG&E pricing structure, although approximately 10% savings are possible in the annual electricity bill if the demand-shifting strategy is followed, the actual value in dollar terms is very small. Two-part pricing, by itself, is not responsible for the low value of actual

dollars saved. The MG&E prices under the two-part pricing scheme are very low, in dollar terms, to offer attractive actual dollar savings.

- Two-part pricing structures, like those offered by MG&E, do not offer substantial benefits in following the demand-shifting strategy, as the actual dollars saved is meager in spite of the daily price ratio being 1.5. Under the MG&E pricing structure, although approximately 10% savings are possible in the annual electricity bill if the demand-shifting strategy is followed, the actual value in dollar terms is very small. Two-part pricing, by itself, is not responsible for the low value of actual dollars saved. The MG&E prices under the two-part pricing scheme are very low, in dollar terms, to offer attractive actual dollar savings.

- Real-Time Price (RTP) structures, like those offered by PG&E, offer the maximum incentive for following the demand-shifting strategy. PG&E pricing structure has the maximum dollar difference between on-peak and off-peak prices, and can lead to approximately 30% savings in the annual electricity bill, equivalent to thousands of dollars in actual savings.

- The break-even price ratio (or critical price ratio) is defined as the daily price ratio at which the annual electricity bill is same for the base case and the demand-shifting strategy. At daily price ratios greater than the critical price ratio, following the demand-shifting strategy yields savings in the annual electricity bill as compared with the base case operation. At daily price ratios less than the critical price ratio, following the demand-shifting strategy leads to a higher annual electricity bill than the base case operation. The break-even cost analysis is presented in Section 3.B.2.1, and the critical daily price ratio for break-even is calculated to be equal to 1.48.

APPENDIX A: TRNSYS non-standard type descriptions

A.1 Type 202 Infiltration Model Component Configuration

This type calculates the infiltration load, and the TRNSYS model is based on the equations outlined in section 2.A.2. The model has 10 parameters, which are component information pieces constant throughout the simulation; 4 input variables, the value of which varies throughout the simulation; and 2 output variables. The parameters, inputs, and outputs are identified below:

PARAMETER NO.	SYMBOL	DESCRIPTION
1	N	Number of doors
2	A	Area of each door (m^2)
3	H	Height of each door (m)
4	g	Acceleration due to gravity (m/s^2)
5	t_p	Door open-close time (s)
6	t_o	Time door stands open (s)
7	t_d	Time period (=1 hr)
8	D_f	Doorway flow factor
9	E	Effectiveness of doorway protective device
10	P	Number of passages per door per hour

INPUT NO.	SYMBOL	DESCRIPTION
1	h_{out}	Enthalpy of outside air (kJ/kg)
2	ρ_{out}	Density of outside air (kg/m^3)
3	h_{zone}	Enthalpy of zone air (kJ/kg)
4	ρ_{zone}	Density of zone air (kg/m^3)

OUTPUT NO.	SYMBOL	DESCRIPTION
1	Q_t	Average infiltration heat gain (kW)
2	$\dot{m}$	Infiltration air mass (kg/s)

A.2 Type 206 Refrigeration System Model Component Configuration

The refrigeration system model developed in TRNSYS is based on the equations outlined in section 2.B. The model has 29 parameters, which are component information pieces constant throughout the simulation; 8 Input variables, the value of which varies throughout the simulation; and 17 Output variables. The parameters, inputs, and outputs are identified below:

PARAMETER NO.	SYMBOL	DESCRIPTION
1	P_{atm}	Atmospheric pressure (atm)
2	N_{comp}	Number of compressors
3	E_{evap}	Evaporator effectiveness
4	E_{cond}	Condenser effectiveness
5-10	$CFACTn$	Cooling capacity regression coefficients
11	$TZone_{c,des}$	Zone design set point temperature (C)
12	SDT_{des}	Design SDT (F)
13	$Q_{cooling,des}$	Design cooling load (kW)
14-19	$PFACTn$	Electrical power regression coefficients
20	$RH_{zone,des}$	Design zone relative humidity
21	$T_{amb,des}$	Design ambient temperature (C)
22	$RH_{amb,des}$	Design ambient relative humidity
23	$w_{cond,max}$	Maximum condenser fan power (kW)
24	power	Condenser fan power exponent
25	steps	SDT step size
26	SDT_{min}	Minimum SDT (F)
27	SDT_{max}	Maximum SDT (F)
28	$TDiff_1$	Lower temperature difference
29	$TDiff_2$	Upper temperature difference
30	$P_{evap,max}$	Maximum evaporator fan power (kW)

INPUT NO.	SYMBOL	DESCRIPTION
1	$T_{air,amb}$	Ambient air temperature (C)
2	$h_{air,amb}$	Ambient air enthalpy (kJ/kg)
3	w_{amb}	Ambient air humidity ratio
4	T_{zone}	Zone air temperature (C)
5	$h_{air,in,evap}$	Zone air enthalpy (kJ/kg)
6	$m_{infil,1}$	Dock-cooler air infiltration rate (kg/s)
7	w_d	Dock air humidity ratio
8	$T_{zone,set}$	Zone set point temperature (C)

OUTPUT NO.	SYMBOL	DESCRIPTION
1	Scale	Design compressor scaling factor
2	$m_{evap,max}$	Maximum evaporator air flow rate (kg/s)
3	$Comp_{kw,des}$	Design compressor power (kW)
4	$m_{cond,max}$	Maximum condenser air flow rate (kg/s)
5	SST_c	Refrigerant SST (C)
6	$w_{air,out,evap}$	Evaporator exit air humidity ratio
7	$T_{air,out,evap}$	Evaporator exit air temperature (C)
8	SDT_{final}	Refrigerant SDT (F)
9	PLR_{final}	Compressor part-load ratio
10	Q_{evap}	Available cooling capacity (kW)
11	$w_{cond,final}$	Condenser fan power requirement (kW)
12	$w_{comp,final}$	Compressor power requirement (kW)
13	$m_{evap,1}$	Evaporator air flow rate (kg/s)
14	$Q_{cond,final}$	Condenser heat rejection (kW)
15	w_f	Cooler air humidity ratio
16	m_{conden}	Condensation rate (kg/s)
17	COP	Coefficient of Performance

A.3   Type 201 Lumped Capacitance Product Model Component Configuration

The lumped capacitance model for the stored product developed in TRNSYS is based on the equations outlined in section 2.C.1. The model has 6 parameters, which are component information pieces constant throughout the simulation; 1 input variable, the value of which varies throughout the simulation; and 3 output variables. The parameters, inputs, and outputs are identified below:

PARAMETER NO.	SYMBOL	DESCRIPTION
1	h	Convection heat transfer coefficient (W/m^2-C)
2	A	Heat transfer surface area (m^2)
3	ρ	Product density (kg/m^3)
4	V	Stored product volume (m^3)
5	c	Product specific heat (J/kg-C)
6	T_{start}	Product initial temperature (C)

INPUT NO.	SYMBOL	DESCRIPTION
1	T_{zone}	Zone air temperature (C)

OUTPUT NO.	SYMBOL	DESCRIPTION
1	T_{final}	Final product temperature (C)
2	Q_{kJhr}	Product-zone heat transfer (kJ/hr)
3	Q_{kW}	Product-zone heat transfer (kW)

A.4 Type 210 Three-Dimensional Finite Difference Product Model Component Configuration

The three-dimensional finite-difference model for the stored product developed in TRNSYS is based on the equations outlined in section 2.C.2. The model has 14 parameters, which are component information pieces constant throughout the simulation; 2 input variables, the value of which varies throughout the simulation; and 5 output variables. The parameters, inputs, and outputs are identified below:

PARAMETER NO.	SYMBOL	DESCRIPTION
1	X_{width}	Half-width of product block in X- direction (m)
2	Y_{height}	Height of product block in Y- direction (m)
3	Z_{depth}	Half-depth of product block in Z- direction (m)
4	Xnodes	Number of nodes in X- direction
5	Ynodes	Number of nodes in Y- direction
6	Znodes	Number of nodes in Z- direction
7	Tinit	Initial product temperature (C)
8	k	Stored product conductivity (W/m-C)
9	C_p	Stored product specific heat (J/kg-C)
10	$Zone_{area}$	Zone floor area (m^2)
11	N	Number of product pallets stored
12	R_{floor}	Wooden palette resistance (m^2-C/W)
13	h	Convective heat transfer coefficient (W/m^2-C)
14	ρ	Product density (kg/m^3)

INPUT NO.	SYMBOL	DESCRIPTION
1	T_{zone}	Zone air temperature (C)
2	T_{floor}	Zone floor temperature (C)

OUTPUT NO.	SYMBOL	DESCRIPTION
1	$Q_{prod,zone}$	Heat flow from product to zone (kJ/hr)
2	$T_{top,corner}$	Product block top corner temperature (C)
3	$T_{bottom,corner}$	Product block bottom corner temperature (C)
4	$T_{front,middle}$	Product block front-middle temperature (C)
5	deltaU	Change in product internal energy (kJ)

A.5   Type 208 Zone Temperature Set-point Controller Component Configuration

The zone set point temperature controller developed in TRNSYS is based on the equations outlined in section 2.D. The model has 6 parameters, which are component information pieces constant throughout the simulation; 1 input variable, the value of which varies throughout the simulation; and 1 output variable. The parameters, inputs, and outputs are identified below:

PARAMETER NO.	SYMBOL	DESCRIPTION
1	$T_{precool}$	Pre-cooling set point temperature (C)
2	T_{normal}	Normal set point temperature(C)
3	T_{float}	Floating set point temperature (C)
4	$deltat_{precool}$	Half-duration of pre-cooling (hours)
5	$deltat_{float}$	Half-duration of floating (hours)
6	T_{max}	Maximum allowable zone temperature (C)

INPUT NO.	SYMBOL	DESCRIPTION
1	T_{zone}	Zone air temperature (C)

OUTPUT NO.	SYMBOL	DESCRIPTION
1	T_{set}	Zone set point temperature (C)

APPENDIX B: TRNSYS Input File

VERSION 15
```
*******************************************************************************
******
*** TRNSYS input file (deck) generated by IISiBat 3
*** on Wednesday, January 01, 2003 at 19:46
*** from IISiBat project: C:\Trnsys15\Nitin\Projects\warehouse11.TPF
***
*** If you edit this file, use the File/Import TRNSYS Input File function in
*** IISiBat 3 to update the project.
***
*** If you have problems, questions or suggestions please contact your local
*** TRNSYS distributor or mailto:iisibat@cstb.fr
***
*******************************************************************************
******

ASSIGN "Project11.LST" 6

*******************************************************************************
******
*** Control cards
*******************************************************************************
******
* START, STOP and STEP
CONSTANTS 3
START=1
STOP=8760
STEP=0.1
*SIMULATION Start time    End time      Time step
SIMULATION          START         STOP  STEP


* User defined CONSTANTS

*                          Integration    Convergence
TOLERANCES 0.001 0.001
*                          Max iterations  Max warnings Trace limit
LIMITS 30 30 30
*                          TRNSYS numerical integration solver method
DFQ 1
*                          TRNSYS output file width, number of characters
WIDTH 80
*                          NOLIST statement
```

114

LIST
*   MAP statement
MAP
*   Solver statement
SOLVER 0

****
******
*** Units
****
******

* Model "TYPE89d" (Type 89)

UNIT 1 TYPE 89   TYPE89d
*$UNIT_NAME TYPE89d
*$MODEL .\Utility\Weather and Other Data Readers\Standard Weather File
Types\Tmy2\Skip N Lines before starting\TYPE89d.tmf
*$POSITION 62 296
*$LAYER Main

PARAMETERS 2
* 1 Mode
-2
* 2 Logical unit
13
*** External files
ASSIGN "C:\Trnsys15\Weather\TMY2\madisn.tm2" 13
*|? Which file contains the TMY2 weather information? |1000
*---

* Model "TYPE16g" (Type 16)

UNIT 2 TYPE 16   TYPE16g
*$UNIT_NAME TYPE16g
*$MODEL .\Physical Phenomena\Radiation Processors\Total Horiz, Direct Normal
Known (Mode=4)\No Radiation Smoothing\TYPE16g.tmf
*$POSITION 94 435
*$LAYER Weather / Data Files

PARAMETERS 9
* 1 Horiz. radiation mode
4
* 2 Tracking mode
1
* 3 Tilted surface mode

3
* 4 Starting day
1
* 5 Latitude
43.13
* 6 Solar constant
4871.0
* 7 Shift in solar time
0.67
* 8 Not used
2
* 9 Solar time?
1
INPUTS 13
* TYPE89d:Global horizontal radiation ->Total radiation on horizontal surface
1,4
* TYPE89d:Direct normal radiation ->Direct normal beam radiation on horizontal
1,3
* TYPE89d:Time of last read ->Time of last data read
1,99
* TYPE89d:Time of next read ->Time of next data read
1,100
* [unconnected] Ground reflectance
0,0
* [unconnected] Slope of surface-1
0,0
* [unconnected] Azimuth of surface-1
0,0
* [unconnected] Slope of surface-2
0,0
* [unconnected] Azimuth of surface-2
0,0
* [unconnected] Slope of surface-3
0,0
* [unconnected] Azimuth of surface-3
0,0
* [unconnected] Slope of surface-4
0,0
* [unconnected] Azimuth of surface-4
0,0
*** INITIAL INPUT VALUES
0.0 0 0.0 1.0 0.2 90 -180 90 0 90 -90 90 90
*--

* Model "TYPE69b" (Type 69)

UNIT 3 TYPE 69   TYPE69b
*$UNIT_NAME TYPE69b
*$MODEL .\Physical Phenomena\Sky Temperature\calculate cloudiness
factor\TYPE69b.tmf
*$POSITION 275 413
*$LAYER Main

PARAMETERS 2
* 1 mode for cloudiness factor
0
* 2 height over sea level
0
INPUTS 5
* TYPE89d:Dry bulb temperature ->Ambient temperature
1,5
* Ambient:Dew point temperature. ->Dew point temperature at ambient conditions
4,8
* TYPE16g:Beam radiation on horizontal ->Beam radiation on the horizontal
2,5
* TYPE16g:Horizontal diffuse radiation ->Diffuse radiation on the horizontal
2,6
* [unconnected] not used with this mode
0,0
*** INITIAL INPUT VALUES
0 20 0 0 0
*--

* Model "Ambient Psychrometrics" (Type 33)

UNIT 4 TYPE 33   Ambient
*$UNIT_NAME Ambient
*$MODEL .\Physical Phenomena\Thermodynamic Properties\Psychrometrics\Dry Bulb
and Relative Humidity Known\TYPE33e.tmf
*$POSITION 223 252
*$LAYER Main

PARAMETERS 4
* 1 Psychrometrics mode
2
* 2 Pressure
1.0
* 3 Wet bulb mode
1
* 4 Error mode
2
INPUTS 2

* TYPE89d:Dry bulb temperature ->Dry bulb temp.
1,5
* TYPE89d:Percent relative humidity ->Percent relative humidity
1,10
*** INITIAL INPUT VALUES
22.0 60.0
*---

* Model "Freezer Psychrometrics" (Type 33)

UNIT 5 TYPE 33   Freezer
*$UNIT_NAME Freezer
*$MODEL .\Physical Phenomena\Thermodynamic Properties\Psychrometrics\Dry Bulb
and Humidity Ratio Known\TYPE33c.tmf
*$POSITION 89 72
*$LAYER Main

PARAMETERS 4
* 1 Psychrometrics mode
4
* 2 Pressure
1.0
* 3 Wet bulb mode
1
* 4 Error mode
2
INPUTS 2
* type56:   1- (air temperature of zone) TAIR   1 ->Dry bulb temp.
9,1
* Freezerequip:Freezer humidity ratio ->Absolute humidity ratio
8,16
*** INITIAL INPUT VALUES
-10 0.006
*---

* Model "Dock Refrigeration Equipment" (Type 204)

UNIT 6 TYPE 204   Dockequip
*$UNIT_NAME Dockequip
*$MODEL .\Nitin\Type204.tmf
*$POSITION 637 68
*$LAYER Main

*$# This Type models the Condenser and gives the condensing temperature of the refrigerant as the output.
*$# It also gives the air and refrigerant temperatures at the evaporator exit.
PARAMETERS 32
* 1 Atmospheric Pressure
1
* 2 Number of compressors
1
* 3 Evaporator effectiveness
0.6
* 4 Condenser effectiveness
0.4
* 5 Cooling capacity regression factors
135.07
* 6 Cooling capacity regression factors
3.4549
* 7 Cooling capacity regression factors
0.025544
* 8 Cooling capacity regression factors
-0.19667
* 9 Cooling capacity regression factor
-0.0014444
* 10 Cooling capacity regression factor
-0.006755
* 11 Design temperature of zone
10
* 12 Design SDT
95
* 13 Design cooling load
200
* 14 Electrical power regression factors
-7.1422
* 15 Electrical power regression factors
-1.2347
* 16 Electrical power regression factors
-0.0075143
* 17 Electrical power regression factors
1.7382
* 18 Electrical power regression factors
0.00058333
* 19 Electrical power regression factors
0.024345
* 20 Design zone RH
0.8
* 21 Design ambient temperature
30

* 22 Design ambient RH
0.90
* 23 Max condenser fan power
10
* 24 Condenser fan power exponent
0.76
* 25 SDT step size
2
* 26 Maximum zone temperature
10
* 27 Zone Volume
6700
* 28 Minimum zone temperature
5
* 29 Minimum SDT
75
* 30 Maximum SDT
100
* 31 Temperature difference 1
1
* 32 Temperature Difference 2
2
INPUTS 9
* Ambient:Dry bulb temperature ->Ambient temperature
4,7
* Ambient:Enthalpy ->Ambient air enthalpy
4,3
* Ambient:Humidity ratio ->Ambient air humidity ratio
4,1
* type56:   2- (air temperature of zone) TAIR   2 ->Zone temperature
9,2
* Dock Psychrometrics:Enthalpy ->Zone air enthalpy
12,3
* Dock Freezer:Mass Infiltration Rate ->Mass infiltration
14,2
* Dock Ambient:Mass Infiltration Rate ->Mass Infiltration
13,2
* Dock Psychrometrics:Density of dry air ->Dock air density
12,5
* Freezer:Humidity ratio ->Freezer humidity ratio
5,1
*** INITIAL INPUT VALUES
0 0 0 0 0 0 0 0 0
*---

* Model "Set-point Temperature Controller" (Type 208)

UNIT 7 TYPE 208   Controller
*$UNIT_NAME Controller
*$MODEL .\Nitin\Type208.tmf
*$POSITION 160 15
*$LAYER Main
*$# This is the controller for precooling and floating duration temperature setpoints.

PARAMETERS 4
* 1 Precool setpoint
1
* 2 Floating temperature
7
* 3 Floating duration
6
* 4 Maximum product temperature
10
INPUTS 1
* Product:Top corner temp ->Zone temperature
10,2
*** INITIAL INPUT VALUES
0
*--

* Model "Freezer Refrigeration Equipment" (Type 206)

UNIT 8 TYPE 206   Freezerequip
*$UNIT_NAME Freezerequip
*$MODEL .\Nitin\Type206.tmf
*$POSITION 339 15
*$LAYER Main
*$# This Type models the refrigeration equipment in the freezer, namely, evaporator,
compressor, and condenser.
*$# The model designs for the appropriate equipment sizes to be used based on the design
parameters.
*$# For operating conditions, it uses a controller based on the zone temperature to
determine the level of
*$# operation of the equipment.

PARAMETERS 38
* 1 Atmospheric Pressure
1
* 2 Number of compressors
1
* 3 Evaporator effectiveness
0.6

* 4 Condenser effectiveness
0.4
* 5 Cooling capacity regression factor
135.07
* 6 Cooling capacity regression factor
3.4549
* 7 Cooling capacity regression factor
0.025544
* 8 Cooling capacity regression factor
-0.19667
* 9 Cooling capacity regression factor
-0.0014444
* 10 Cooling capacity regression factor
-0.006755
* 11 Design zone temperature
1
* 12 Design SDT
95
* 13 Design zone cooling load
700
* 14 Electrical power regression factor
-7.1422
* 15 Electrical power regression factor
-1.2347
* 16 Electrical power regression factor
-0.0075143
* 17 Electrical power regression factor
1.7382
* 18 Electrical power regression factor
0.00058333
* 19 Electrical power regression factor
0.024345
* 20 Design zone RH
0.7
* 21 Design ambient temperature
30
* 22 Design ambient RH
0.9
* 23 Maximum condenser fan power
10
* 24 Cond fan power exponent
3
* 25 SDT step size
2
* 26 Minimum SDT
75

* 27 Maximum SDT
100
* 28 Temperature Difference 1
0.05
* 29 Temperature Difference 2
0.1
* 30 Temperature Difference 3
0.15
* 31 Temperature Difference 4
0.2
* 32 Temperature Difference 5
0.25
* 33 Temperature Difference 6
0.3
* 34 Temperature Difference 7
0.35
* 35 Temperature Difference 8
0.4
* 36 Temperature Difference 9
0.45
* 37 Temperature difference 10
0.5
* 38 Max evaporator fan power
5.86
INPUTS 8
* Ambient:Dry bulb temperature ->Ambient air temperature
4,7
* Ambient:Enthalpy ->Ambient air enthalpy
4,3
* Ambient:Humidity ratio ->Ambient humidity ratio
4,1
* type56:   1- (air temperature of zone) TAIR   1 ->Zone temperature
9,1
* Freezer:Enthalpy ->Zone air enthalpy
5,3
* Dock Freezer:Mass Infiltration Rate ->Mass infiltration
14,2
* Dockequip:Dock humidity ratio ->Dock humidity ratio
6,16
* Controller:Equipment operating temperature ->Zone setpoint temperature
7,1
*** INITIAL INPUT VALUES
0 0 0 0 0 0 0 0
*--

* Model "Type56 Warehouse Model" (Type 56)

UNIT 9 TYPE 56   type56
*$UNIT_NAME type56
*$MODEL .\Loads and Structures\Multi-Zone Building\type56.tmf
*$POSITION 590 243
*$LAYER Main

PARAMETERS 5
* 1 Logical unit for description file
26
* 2 Logical unit for transfer function file
27
* 3 Logical unit for window library
28
* 4 Star network calculation switch
0
* 5 Weighting factor for operative temperature
0.50
INPUTS 30
* TYPE89d:Dry bulb temperature ->   1- TAMB (AMBIENT TEMPERATURE)
1,5
* TYPE89d:Percent relative humidity ->   2- ARELHUM (RELATIVE AMBIENT
HUMIDITY)
1,10
* TYPE69b:Fictive sky temperature ->   3- TSKY (FIKTIVE SKY TEMPERATURE)
3,1
* TYPE16g:Total radiation on surface 1 ->   4- ITNORTH (INCIDENT RADIATION
FOR ORIENTATION NORTH)
2,7
* TYPE16g:Total radiation on surface 2 ->   5- ITSOUTH (INCIDENT RADIATION
FOR ORIENTATION SOUTH)
2,12
* TYPE16g:Total radiation on surface 3 ->   6- ITEAST (INCIDENT RADIATION FOR
ORIENTATION EAST)
2,17
* TYPE16g:Total radiation on surface 4 ->   7- ITWEST (INCIDENT RADIATION FOR
ORIENTATION WEST)
2,22
* TYPE16g:Total horizontal radiation ->   8- ITHORIZONT (INCIDENT RADIATION
FOR ORIENTATION HORIZONTAL)
2,4
* TYPE16g:Beam radiation on surface 1 ->   9- IBNORTH (INCIDENT BEAM
RADIATION FOR ORIENTATION NORTH)
2,8
* TYPE16g:Beam radiation on surface 2 ->   10- IBSOUTH (INCIDENT BEAM
RADIATION FOR ORIENTATION SOUTH)

2,13
* TYPE16g:Beam radiation on surface 3 ->   11- IBEAST (INCIDENT BEAM RADIATION FOR ORIENTATION EAST)
2,18
* TYPE16g:Beam radiation on surface 4 ->   12- IBWEST (INCIDENT BEAM RADIATION FOR ORIENTATION WEST)
2,23
* TYPE16g:Beam radiation on horizontal ->   13- IBHORIZONT (INCIDENT BEAM RADIATION FOR ORIENTATION HORIZONTAL)
2,5
* TYPE16g:Incidence angle for surface 1 ->   14- AINORTH (ANGLE OF INCIDENCE FOR ORIENTATION NORTH)
2,10
* TYPE16g:Incidence angle of surface 2 ->   15- AISOUTH (ANGLE OF INCIDENCE FOR ORIENTATION SOUTH)
2,15
* TYPE16g:Incidence angle of surface 3 ->   16- AIEAST (ANGLE OF INCIDENCE FOR ORIENTATION EAST)
2,20
* TYPE16g:Incidence angle of surface 4 ->   17- AIWEST (ANGLE OF INCIDENCE FOR ORIENTATION WEST)
2,25
* TYPE16g:Solar zenith angle ->   18- AIHORIZONT (ANGLE OF INCIDENCE FOR ORIENTATION HORIZONTAL)
2,2
* [unconnected]   19- SFREEZER (INPUT)
0,0
* [unconnected]   20- SDOCK (INPUT)
0,0
* [unconnected]   21- WIND (INPUT)
0,0
* [unconnected]   22- ABLFREEZER (INPUT)
0,0
* [unconnected]   23- ABLDOCK (INPUT)
0,0
* [unconnected]   24- BRIGHT (INPUT)
0,0
* Product:Heat flow ->   25- QPROD (INPUT)
10,1
* Dock Ambient:Average heat gain for 24 hr period ->   26- INFIL (INPUT)
13,1
* Dock Freezer:Average heat gain for 24 hr period ->   27- INFILDF (INPUT)
14,1
* Dockequip:Cooling power ->   28- QAVAILD (INPUT)
6,10
* Freezerequip:Cooling load ->   29- QAVAILF (INPUT)

8,10
* Freezerequip:Condenser fan power ->   30- FANPOWER (INPUT)
8,11
*** INITIAL INPUT VALUES
0 0 0 0 0 0 0 0 0 0 0 0 0 0 0 0 0 0 0 0 1 1 1 1 1 1 0 0 0 0 0 0

*** External files
ASSIGN "C:\Trnsys15\Nitin\Projects\STOECKLE1.bld" 26
|? Which file contains the building description (.BLD)? |1000
ASSIGN "C:\Trnsys15\Nitin\Projects\STOECKLE1.trn" 27
|? Which file contains the transfer function iformation (.TRN)? |1000
ASSIGN "C:\Trnsys15\prebid\Lib\American\W4-lib.dat" 28
*|? Which file contains the window library for TYPE 56? |1000
*---

* Model "3-D Finite Difference Product Model" (Type 210)

UNIT 10 TYPE 210   Product
*$UNIT_NAME Product
*$MODEL .\Nitin\Type210.tmf
*$POSITION 518 15
*$LAYER Main
*$# This type models the stored product as a 3-D finite difference model.

PARAMETERS 14
* 1 X-halflength
0.44775
* 2 Y-length
1.0668
* 3 Z-halflength
0.5667
* 4 X nodes
20
* 5 Y nodes
20
* 6 Z nodes
20
* 7 Initial temperature
1
* 8 Thermal conductivity
0.31
* 9 Specific heat
2.102
* 10 Zone area
9204
* 11 Number of product blocks

50000
* 12 Floor Resistance
0.1656
* 13 Air-product convection coefficient
4.26
* 14 Density
1090
INPUTS 2
* type56:   1- (air temperature of zone) TAIR   1 ->Zone temperature
9,1
* type56:   1- (air temperature of zone) TAIR   1 ->Floor temperature
9,1
*** INITIAL INPUT VALUES
0 0
*--

* EQUATIONS "Equa-3"
*
EQUATIONS 1
QkW = [10,1]/3600
*$UNIT_NAME Equa-3
*$LAYER Main
*$POSITION 685 207

*--

* Model "Dock Psychrometrics" (Type 33)

UNIT 12 TYPE 33   Dock Psychrometrics
*$UNIT_NAME Dock Psychrometrics
*$MODEL .\Physical Phenomena\Thermodynamic Properties\Psychrometrics\Dry Bulb
and Humidity Ratio Known\TYPE33c.tmf
*$POSITION 691 520
*$LAYER Main

PARAMETERS 4
* 1 Psychrometrics mode
4
* 2 Pressure
1.0
* 3 Wet bulb mode
1
* 4 Error mode
2
INPUTS 2

* type56:   2- (air temperature of zone) TAIR   2 ->Dry bulb temp.
9,2
* Dockequip:Dock humidity ratio ->Absolute humidity ratio
6,16
*** INITIAL INPUT VALUES
22.0 0.0001
*---

* Model "Dock-Ambient Infiltration" (Type 202)

UNIT 13 TYPE 202   Dock Ambient
*$UNIT_NAME Dock Ambient
*$MODEL .\Nitin\Type202.tmf
*$POSITION 108 186
*$LAYER Main
*$# This model calculates the infiltration load due to air exchange between the dock and
the surroundings

PARAMETERS 10
* 1 Number of Doors
30
* 2 Area of each door
6.6856
* 3 Height of each door
2.44
* 4 Acceleration due to gravity
9.81
* 5 Door open-close time
30
* 6 Time door stands open
30
* 7 Daily Time period
1
* 8 Doorway Flow factor
0.8
* 9 effectiveness of doorway protective device
0.8
* 10 Number of passages per door per hour
1
INPUTS 4
* Ambient:Enthalpy ->Enthalpy of outside air
4,3
* Ambient:Density of mixture ->Density of outside air
4,4
* Dock Psychrometrics:Enthalpy ->Enthalpy of dock air
12,3

* Dock Psychrometrics:Density of mixture ->Density of dock air
12,4
*** INITIAL INPUT VALUES
100 1.25 100 1.25
*---

* Model "Dock-Freezer Infiltration" (Type 202)

UNIT 14 TYPE 202   Dock Freezer
*$UNIT_NAME Dock Freezer
*$MODEL .\Nitin\Type202.tmf
*$POSITION 435 463
*$LAYER Main
*$# This model calculates the infiltration load due to air exchange between the dock and
the surroundings

PARAMETERS 10
* 1 Number of Doors
5
* 2 Area of each door
13.0235
* 3 Height of each door
3.05
* 4 Acceleration due to gravity
9.81
* 5 Door open-close time
1800
* 6 Time door stands open
1800
* 7 Daily Time period
1
* 8 Doorway Flow factor
0.8
* 9 effectiveness of doorway protective device
0.8
* 10 Number of passages per door per hour
1
INPUTS 4
* Dock Psychrometrics:Enthalpy ->Enthalpy of outside air
12,3
* Dock Psychrometrics:Density of mixture ->Density of outside air
12,4
* Freezer:Enthalpy ->Enthalpy of dock air
5,3
* Freezer:Density of mixture ->Density of dock air
5,4

*** INITIAL INPUT VALUES
100 1.25 100 1.25
*--

* Model "Temperatures: Online Plotter" (Type 65)

UNIT 15 TYPE 65   Temperatures
*$UNIT_NAME Temperatures
*$MODEL .\Output\Online Plotter\Online Plotter w_ file\TYPE65b.tmf
*$POSITION 245 595
*$LAYER Outputs

PARAMETERS 10
* 1 Nb. of left-axis variables
6
* 2 Nb. of right-axis variables
3
* 3 Left axis minimum
-2
* 4 Left axis maximum
1
* 5 Right axis minimum
0.0
* 6 Right axis maximum
10
* 7 Number of plots per simulation
1
* 8 X-axis gridpoints
7
* 9 Shut off Online w/o removing
0
* 10 Logical Unit for ouput file
19
INPUTS 9
* TYPE89d:Dry bulb temperature ->Left axis variable-1
1,5
* type56:   1- (air temperature of zone) TAIR   1 ->Left axis variable-2
9,1
* Product:Top corner temp ->Left axis variable-3
10,2
* Product:Bottom corner temp ->Left axis variable-4
10,3
* Product:Front middle temp ->Left axis variable-5
10,4
* Controller:Equipment operating temperature ->Left axis variable-6
7,1

* Freezerequip:Evap exit air temp ->Right axis variable-1
8,7
* type56:   2- (air temperature of zone) TAIR   2 ->Right axis variable-2
9,2
* Freezerequip:Refrigerant SST ->Right axis variable-3
8,5
*** INITIAL INPUT VALUES
ambient freezer Top Bottom Front Equipment evapexit Dock SST
LABELS 5
C C
Temperature
Temperature
Temperatures
*** External files
ASSIGN "C:\Trnsys15\Nitin\Outputs\Temperature.xls" 19
*|? What file should the ONLINE write to ? |1000
*---

* Model "Infiltration Loads: Online Plotter" (Type 65)

UNIT 16 TYPE 65   Infiltration Loads
*$UNIT_NAME Infiltration Loads
*$MODEL .\Output\Online Plotter\Online Plotter w_ file\TYPE65b.tmf
*$POSITION 73 563
*$LAYER Outputs

PARAMETERS 10
* 1 Nb. of left-axis variables
4
* 2 Nb. of right-axis variables
2
* 3 Left axis minimum
0
* 4 Left axis maximum
300
* 5 Right axis minimum
0
* 6 Right axis maximum
10
* 7 Number of plots per simulation
1
* 8 X-axis gridpoints
7
* 9 Shut off Online w/o removing
0
* 10 Logical Unit for ouput file

22
INPUTS 6
* Dock Ambient:Average heat gain for 24 hr period ->Left axis variable-1
13,1
* Dock Freezer:Average heat gain for 24 hr period ->Left axis variable-2
14,1
* Freezerequip:Maximum evap flow rate ->Left axis variable-3
8,2
* Freezerequip:Condenser air flow rate ->Left axis variable-4
8,13
* Freezerequip:Equipment COP ->Right axis variable-1
8,18
* Freezerequip:Condenser fan power ->Right axis variable-2
8,11
*** INITIAL INPUT VALUES
InfilS-D InfilD-F Maxevapmass Evapmass COP Condfanpower
LABELS 5
kW kW
Power (kW)
Power (kW)
Infiltration loads
*** External files
ASSIGN "C:\Trnsys15\Nitin\Outputs\Infilloads.xls" 22
*|? What file should the ONLINE write to ? |1000
*--

* Model " Infiltration Mass: Online Plotter" (Type 65)

UNIT 17 TYPE 65   Infiltration mass
*$UNIT_NAME Infiltration mass
*$MODEL .\Output\Online Plotter\TYPE65.tmf
*$POSITION 541 563
*$LAYER Outputs

PARAMETERS 10
* 1 Nb. of left-axis variables
2
* 2 Nb. of right-axis variables
3
* 3 Left axis minimum
0
* 4 Left axis maximum
0.0015
* 5 Right axis minimum
0
* 6 Right axis maximum

1
* 7 Number of plots per simulation
1
* 8 X-axis gridpoints
7
* 9 Shut off Online w/o removing
0
* 10 Logical Unit for ouput file
-1
INPUTS 5
* Freezerequip:Condensation rate ->Left axis variable-1
8,17
* [unconnected] Left axis variable-2
0,0
* Dock Ambient:Mass Infiltration Rate ->Right axis variable-1
13,2
* Dock Freezer:Mass Infiltration Rate ->Right axis variable-2
14,2
* Freezerequip:Compressor PLR ->Right axis variable-3
8,9
*** INITIAL INPUT VALUES
Condensation zilch Infildockambient Infildockfreezer PLR
LABELS 5
kg/s kg/s
Zone Moisture (kg/s)
Infiltration mass (kg/s)
TYPE205 and Infiltration Mass
*--

* Model "Psychrometrics: Online Plotter" (Type 65)

UNIT 18 TYPE 65   Zone Psychrometrics
*$UNIT_NAME Zone Psychrometrics
*$MODEL .\Output\Online Plotter\TYPE65.tmf
*$POSITION 489 126
*$LAYER Outputs

PARAMETERS 10
* 1 Nb. of left-axis variables
3
* 2 Nb. of right-axis variables
3
* 3 Left axis minimum
0
* 4 Left axis maximum
100

* 5 Right axis minimum
0
* 6 Right axis maximum
0.005
* 7 Number of plots per simulation
1
* 8 X-axis gridpoints
7
* 9 Shut off Online w/o removing
0
* 10 Logical Unit for ouput file
-1
INPUTS 6
* Freezer:Percent relative humidity ->Left axis variable-1
5,6
* Dock Psychrometrics:Percent relative humidity ->Left axis variable-2
12,6
* Ambient:Percent relative humidity ->Left axis variable-3
4,6
* Freezer:Humidity ratio ->Right axis variable-1
5,1
* Dock Psychrometrics:Humidity ratio ->Right axis variable-2
12,1
* Ambient:Humidity ratio ->Right axis variable-3
4,1
*** INITIAL INPUT VALUES
FreezerRH DockRH AmbientRH Freezerhumrat Dockhumrat Ambienthumrat

LABELS 5
% kg/kg
Percent Relative Humidity
Humidity Ratio
ZonePsychrometrics
*--

* Model "TYPE9c: RTP Data Reader" (Type 9)

UNIT 19 TYPE 9   TYPE9c
*$UNIT_NAME TYPE9c
*$MODEL .\Utility\Weather and Other Data Readers\All Other Data Files\Skip Lines to
Start\Free Format Read\TYPE9c.tmf
*$POSITION 304 744
*$LAYER Weather / Data Files

PARAMETERS 21
* 1 Mode

134

-1
* 2 Header Lines to Skip
1
* 3 No. of values to read
5
* 4 Time interval of data
1.0
* 5 Interpolate or not?-1
-1
* 6 Multiplication factor-1
1.0
* 7 Addition factor-1
0
* 8 Interpolate or not?-2
-2
* 9 Multiplication factor-2
1.0
* 10 Addition factor-2
0
* 11 Interpolate or not?-3
-3
* 12 Multiplication factor-3
1.0
* 13 Addition factor-3
0
* 14 Interpolate or not?-4
-4
* 15 Multiplication factor-4
1.0
* 16 Addition factor-4
0
* 17 Interpolate or not?-5
-5
* 18 Multiplication factor-5
1.0
* 19 Addition factor-5
0
* 20 Logical unit
14
* 21 Not used
-1
*** External files
ASSIGN "C:\Trnsys15\Nitin\RTPdata\breakeven1.txt" 14
*|? Which file contains the data to be read by this component? |1000
*---

* EQUATIONS "Equa-4"

EQUATIONS 4
Costgen = [19,2]*[8,12]
Costoscar = [19,3]*[8,12]
Costpge = [19,4]*[8,12]
Costsou = [19,5]*[8,12]
*$UNIT_NAME Equa-4
*$LAYER Main
*$POSITION 77 729

*--
* Model "TYPE55: Annual Energy Cost Integrator" (Type 55)

UNIT 21 TYPE 55   TYPE55
*$UNIT_NAME TYPE55
*$MODEL .\Utility\Integrators\Periodic Integrator\TYPE55.tmf
*$POSITION 486 648
*$LAYER Main

PARAMETERS 42
* 1 Integrate or sum input-1
1
* 2 Relative starting hour for input-1
0
* 3 Duration for input-1
8760
* 4 Cycle repeat time for input-1
8760
* 5 Reset time for input-1
8760
* 6 Absolute starting hour for input-1
0
* 7 Absolute stopping hour for input -1
8760
* 8 Integrate or sum input-2
2
* 9 Relative starting hour for input-2
0
* 10 Duration for input-2
8760
* 11 Cycle repeat time for input-2
8760
* 12 Reset time for input-2
8760
* 13 Absolute starting hour for input-2

0
* 14 Absolute stopping hour for input -2
8760
* 15 Integrate or sum input-3
3
* 16 Relative starting hour for input-3
0
* 17 Duration for input-3
8760
* 18 Cycle repeat time for input-3
8760
* 19 Reset time for input-3
8760
* 20 Absolute starting hour for input-3
0
* 21 Absolute stopping hour for input -3
8760
* 22 Integrate or sum input-4
4
* 23 Relative starting hour for input-4
0
* 24 Duration for input-4
8760
* 25 Cycle repeat time for input-4
8760
* 26 Reset time for input-4
8760
* 27 Absolute starting hour for input-4
0
* 28 Absolute stopping hour for input -4
8760
* 29 Integrate or sum input-5
5
* 30 Relative starting hour for input-5
0
* 31 Duration for input-5
8760
* 32 Cycle repeat time for input-5
8760
* 33 Reset time for input-5
8760
* 34 Absolute starting hour for input-5
0
* 35 Absolute stopping hour for input -5
8760
* 36 Integrate or sum input-6

6
* 37 Relative starting hour for input-6
0
* 38 Duration for input-6
8760
* 39 Cycle repeat time for input-6
8760
* 40 Reset time for input-6
8760
* 41 Absolute starting hour for input-6
0
* 42 Absolute stopping hour for input -6
8760
INPUTS 6
* Freezerequip:Cooling load ->Input-1
8,10
* Freezerequip:Compressor power requirement ->Input-2
8,12
* Equa-4:Costgen ->Input-3
Costgen
* Equa-4:Costoscar ->Input-4
Costoscar
* Equa-4:Costpge ->Input-5
Costpge
* Equa-4:Costsou ->Input-6
Costsou
*** INITIAL INPUT VALUES
0. 0. 0. 0. 0. 0.
*---

* Model "TYPE55-2: Energy Stored in Product" (Type 55)

UNIT 22 TYPE 55   TYPE55-2
*$UNIT_NAME TYPE55-2
*$MODEL .\Utility\Integrators\Periodic Integrator\TYPE55.tmf
*$POSITION 597 819
*$LAYER Main

PARAMETERS 14
* 1 Integrate or sum input-1
1
* 2 Relative starting hour for input-1
0
* 3 Duration for input-1
8760
* 4 Cycle repeat time for input-1

8760
* 5 Reset time for input-1
8760
* 6 Absolute starting hour for input-1
0
* 7 Absolute stopping hour for input -1
8760
* 8 Integrate or sum input-2
-2
* 9 Relative starting hour for input-2
0
* 10 Duration for input-2
8760
* 11 Cycle repeat time for input-2
8760
* 12 Reset time for input-2
8760
* 13 Absolute starting hour for input-2
0
* 14 Absolute stopping hour for input -2
8760
INPUTS 2
* Product:Heat flow ->Input-1
10,1
* Product:Internal energy change ->Input-2
10,5
*** INITIAL INPUT VALUES
0. 0.
*--

* Model "TYPE25c: Temperature Printer" (Type 25)

UNIT 23 TYPE 25   TYPE25c
*$UNIT_NAME TYPE25c
*$MODEL .\Output\Printer\Don't Print Units to File\TYPE25c.tmf
*$POSITION 179 659
*$LAYER Outputs

PARAMETERS 4
* 1 Printing interval
1
* 2 Start time
1
* 3 Stop time
8760
* 4 Logical unit

17
INPUTS 10
* TYPE89d:Dry bulb temperature ->Input to be printed-1
1,5
* type56:   1- (air temperature of zone) TAIR   1 ->Input to be printed-2
9,1
* Product:Top corner temp ->Input to be printed-3
10,2
* Product:Bottom corner temp ->Input to be printed-4
10,3
* Product:Front middle temp ->Input to be printed-5
10,4
* Controller:Equipment operating temperature ->Input to be printed-6
7,1
* type56:   2- (air temperature of zone) TAIR   2 ->Input to be printed-7
9,2
* Freezerequip:Refrigerant SST ->Input to be printed-8
8,5
* TYPE55-3:Mean value of input-1 ->Input to be printed-9
27,3
* TYPE55-3:Mean value of input-2 ->Input to be printed-10
27,13
*** INITIAL INPUT VALUES
Ambient Freezer Top Bottom Front Equipment Dock Refrigerant Zoneavg Prodavg

*** External files
ASSIGN "C:\Trnsys15\Nitin\Outputs\Temp25.xls" 17
*|? Which file should contain the printed results? |1000
*--

* Model "TYPE25c-2: Printer" (Type 25)

UNIT 24 TYPE 25   TYPE25c-2
*$UNIT_NAME TYPE25c-2
*$MODEL .\Output\Printer\Don't Print Units to File\TYPE25c.tmf
*$POSITION 707 691
*$LAYER Outputs

PARAMETERS 4
* 1 Printing interval
1
* 2 Start time
1
* 3 Stop time
8760
* 4 Logical unit

18
INPUTS 11
* Freezerequip:Cooling load ->Input to be printed-1
8,10
* Freezerequip:Refrigerant SDT ->Input to be printed-2
8,8
* Equa-3:QkW ->Input to be printed-3
QkW
* TYPE55:Integral of input-1 ->Input to be printed-4
21,1
* TYPE55:Integral of input-2 ->Input to be printed-5
21,11
* TYPE55:Integral of input-3 ->Input to be printed-6
21,21
* TYPE55:Integral of input-4 ->Input to be printed-7
21,31
* TYPE55:Integral of input-5 ->Input to be printed-8
21,41
* TYPE55:Integral of input-6 ->Input to be printed-9
21,51
* TYPE55-2:Integral of input-1 ->Input to be printed-10
22,1
* TYPE55-2:Integral of input-2 ->Input to be printed-11
22,11
*** INITIAL INPUT VALUES
Coolingload SDT QkW LoadkWhr PowerkWhr Costgen Costoscar CostPGE CostSou
ProductQkJ deltaUkJ
*** External files
ASSIGN "C:\Trnsys15\Nitin\Outputs\Coolingload25.xls" 18
*|? Which file should contain the printed results? |1000
*---

* Model "Cooling Loads: Online Plotter" (Type 65)

UNIT 25 TYPE 65   Cooling Loads
*$UNIT_NAME Cooling Loads
*$MODEL .\Output\Online Plotter\Online Plotter w_ file\TYPE65b.tmf
*$POSITION 781 915
*$LAYER Outputs

PARAMETERS 10
* 1 Nb. of left-axis variables
4
* 2 Nb. of right-axis variables
8
* 3 Left axis minimum

0
* 4 Left axis maximum
1000
* 5 Right axis minimum
0
* 6 Right axis maximum
4000000
* 7 Number of plots per simulation
1
* 8 X-axis gridpoints
7
* 9 Shut off Online w/o removing
0
* 10 Logical Unit for ouput file
20
INPUTS 12
* Freezerequip:Cooling load ->Left axis variable-1
8,10
* Freezerequip:Refrigerant SDT ->Left axis variable-2
8,8
* Equa-3:QkW ->Left axis variable-3
QkW
* Freezerequip:Compressor power requirement ->Left axis variable-4
8,12
* TYPE55:Integral of input-1 ->Right axis variable-1
21,1
* TYPE55:Integral of input-2 ->Right axis variable-2
21,11
* TYPE55:Integral of input-3 ->Right axis variable-3
21,21
* TYPE55:Integral of input-4 ->Right axis variable-4
21,31
* TYPE55:Integral of input-5 ->Right axis variable-5
21,41
* TYPE55:Integral of input-6 ->Right axis variable-6
21,51
* TYPE55-2:Integral of input-1 ->Right axis variable-7
22,1
* TYPE55-2:Integral of input-2 ->Right axis variable-8
22,11
*** INITIAL INPUT VALUES
Coolingload SDT Productload Totalpower Load(kWhr) Power(kWhr) Costgen
Costoscar CostPGE CostSou ProductQkJ deltaUkJ
LABELS 5
kW kWhr
Freezer Load (kW)

Dock Load (kW)
Cooling Loads
*** External files
ASSIGN "C:\Trnsys15\Nitin\Outputs\Coolingloads.xls" 20
*|? What file should the ONLINE write to ? |1000
*--

END